Department of Physics
Université de Fribourg (Suisse)

Study of ^{110}Cd using the (n,n$'\gamma$) reaction and ^{114}Te using the (α,2n) reaction

THESE

Frédéric Corminboeuf

de Ménières (FR)

Acceptée par la Faculté des Sciences Naturelles de l'Université de Fribourg (Suisse) sur la proposition :

Prof. Dr. Lukas Schaller, Université de Fribourg, Président du Jury,

Prof. Dr. Jan Jolie, Université de Fribourg, Directeur de Thèse,

Prof. Dr. Jean-Claude Dousse, Université de Fribourg, Rapporteur,

Prof. Dr. Ulrich Kneissl, Universität Stuttgart, Rapporteur.

Fribourg, le 27 novembre 2000

Le Directeur de thèse: Le Doyen:

Prof. Dr. Jan Jolie   Prof. Dr. Alexander Von Zelewski

A mon épouse, Stéphanie, et mon fils, Hugo.

Contents

Résumé en Français.

L'étude de la structure nucléaire est un des domaines de recherche en physique nucléaire qui a connu un important développement. Il a demandé un grand effort tant de la part des expérimentateurs que des théoriciens, pour mieux comprendre le problème à N-corps posé par le noyau atomique.

Dans le cadre de cette thèse, nous avons testé plusieurs modèles nucléaires pour deux noyaux : le ^{110}Cd et le ^{114}Te. Ce choix ne s'est pas fait au hasard. En effet le ^{110}Cd est considéré comme l'un des meilleurs exemples de noyaux vibrationnels. De plus, la présence d'une deuxième structure, appelée deux particules - deux trous, fut clairement établie il y a quelques années. Le ^{114}Te est supposé exhiber lui aussi une structure deux particules - deux trous comme le ^{110}Cd. C'est pourquoi un des buts de l'étude de cet isotope est de déterminer la présence d'états intrus à basse énergie.

Il existe plusieurs façons expérimentales d'étudier la structure du noyau atomique. Dans ce travail, nous avons utilisé deux techniques différentes. La première méthode consite à extraire les temps de vie des états nucléaires du ^{110}Cd peuplés par une réaction induite par des neutrons rapides. En utilisant la méthode de l'atténuation du décalage Doppler, il est alors possible d'obtenir le temps de vie des niveaux nucléaires d'intêret. La détermination du temps de vie est importante car elle permet d'avoir directement accès à la connaissance des taux de transitions réduites et par conséquent de savoir si un état excité a un caractère collectif ou non. Les résultats obtenus ont été comparés à différents modèles tels le modèle collectif, le modèle U(5)-O(6) et le modèle des bosons en interactions (IBM).

La deuxième méthode pour explorer la structure nucléaire d'un noyau est de construire son schéma de niveaux. Nous pouvons ensuite le comparer à différentes prédictions théoriques. C'est pourquoi, nous avons étudié le ^{114}Te en utilisant la réaction (α, 2n). A l'aide d'un ensemble de mesures effectuées à l'Institut Paul Scherrer (PSI) de Villigen (CH), nous avons pu montrer que le ^{114}Te était un bon candidat pour la symmétrie dynamique U(5), mais malheureusement nous n'avons pu établir la présence d'états intrus à basse énergie.

Abstract in English.

The study of nuclear structure is one of the research domains in nuclear physics which have known an important development. It has asked a great effort for the experimenters as well as the theoreticians to study in detail the nuclear many-body problem.

In the framework of this thesis, we have tested several nuclear models for two nuclei : ^{110}Cd and ^{114}Te. This choice has not been made at random. Actually, ^{110}Cd is considered as one of the best example of a vibrational nucleus. Moreover, the presence of a second structure, so called two particles - two holes, has been clearly established some years ago. ^{114}Te is also supposed to exhibit a two particles - two holes structure as ^{110}Cd. It is why one of the aim of the study of this isotope is to determine the presence of low-lying intruder states.

There exist several experimental manners to study the nuclear structure of the atomic nucleus. In this work, we have used two different techniques. The first one consists to extract lifetimes of the nuclear states in ^{110}Cd populate by induced neutron reaction. Using the Doppler shift method, we can then obtain the lifetimes of the levels of interest. The determination of lifetimes is important because it allows to have direct access to the reduced transition rates and so to know if a state has a collective character or not. The obtained results have been compared to different models such as the collective model, the U(5)- O(6) model and the Interacting Boson Model (IBM).

The second method to investigate the nuclear structure of a nucleus consist to build his level scheme. We can next compare it with different theoretical predictions. Consequently, we have studied ^{114}Te by using the $(\alpha,2n)$ reaction. A set of experiments were made at the Paul Scherrer Institute (PSI) of Villigen (CH). We have shown that ^{114}Te was a good candidate for nuclei exhibiting the U(5) dynamical symmetry, but no evidence of the presence of intruder states at low-lying energy was found.

Part I

INTRODUCTION

Chapter 1
Short description of models.

1.1 Introduction.

Many models have been developed to explore the structure of nuclei. In this section, we will discuss two classes of approximation schemes. The first one is based on a multipole expansion. We will discuss more particularly the electric quadrupole expansion. The second one used the concept of symmetries in the Interacting Boson Model. This two descriptions allowed us to introduce and explain the concept of multiphonon states. Finally, we will discuss the shape-coexistence structure observed for example in ^{110}Cd.

1.2 Standard harmonic vibrator

This model is based on a multipole expansion of the density variation of a liquid drop. It was originally developed by Bohr and Mottelson [1]. They considered a nuclear shape where the radius of this surface is described by the polar angles θ and ϕ :

$$R(\theta, \phi) = R_0(1 + \sum_{\lambda,\mu} \alpha_{\lambda,\mu} Y^*_{\lambda,\mu}(\theta, \phi)), \qquad (1.1)$$

where λ describes the multipolarity of the shape, R_0 is the radius of the spherical nucleus with same volume as the considered nucleus, $\alpha_{\lambda,\mu}$ are expansion coefficients and $Y^*_{\lambda,\mu}$ are the spherical functions.

The use of the second quantification formalism permits to obtain the Hamiltonian :

$$H_{vibr} = \sum_{\lambda} \hbar\omega_\lambda \sum_{\mu} (b^\dagger_{\lambda\mu} b_{\lambda\mu} + \frac{1}{2}), \qquad (1.2)$$

where $b^\dagger_{\lambda\mu}$ and $b_{\lambda\mu}$ represent the creation respectively the annihilation operator.

In our case, we consider the mode λ=2 also named the quadrupole vibration. Using a multipole expansion the Hamiltonian from Equ. 1.2 can be rewritten as :

$$H = E_0 + \hbar\omega \sum_{\mu} (b^\dagger_{2\mu} b_{2\mu} + \frac{1}{2}) + C \sum_{\mu} [((b^\dagger_{2\mu} b^\dagger_{2\mu})^L (b_{2\mu} b_{2\mu})^L]^{(0)}, \qquad (1.3)$$

We can observe that the second term is the energy in a purely harmonic vibrational spectrum of an N-phonon state which also can be written as $E_x = \hbar\omega(N_{ph} + 5/2)$. The coupling of quadrupole phonons implies a set of possible spins due to the Pauli principle. Coupling two quadrupole phonons give a triplet of levels $J^\pi = 0^+, 2^+, 4^+$. The construction of the triplet is given in Table 1.1. The other multiplets can be built on the same example. The

Table 1.1: Possible spins by coupling two quadrupole phonons.

$J_1=2$	$J_2 = 2$		
m_1	m_2	M	J
2	2	4	
2	1	3	
2	0	2	4
2	-1	1	
2	-2	0	
1	1	2	
1	0	1	2
1	-1	0	
0	0	0	0

energies of the 2-phonon states are calculated using Equ. 1.4:

$$E_I^{(2)} = 2E_0 + \epsilon_I (I = 0, 2, 4), \tag{1.4}$$

whereas the energies of 3-phonon states, according to Brink et al. [2], are given by:

$$E_I^{(3)} = 3E_0 + \sum_{J=0,2,4} A_{IJ}\epsilon_J (I = 0, 2, 3, 4, 6), \tag{1.5}$$

where the A_{IJ} are coefficients of fractional parentage needed to fulfill rotational invariance and the Pauli principle. They can be found for example in Ref. [3]. An example of level scheme using the formula 1.4 and 1.5 can also be found in Ref. [3].

The collectivity of a state is defined by the magnitude of the reduced transition probabilities. We have also the selection rule for this model which is $\Delta N_{ph} = \pm 1$ because the transition operator is the boson annihilation operator. Finally, we can calculate the B(E2) values for the harmonic vibrator model. They are given by:

$$B(E2; J_{N_{ph}} \rightarrow J'_{N_{ph}-1}) = A_{IJ}^2. \tag{1.6}$$

where A_{IJ} are the coefficients of fractional parentage. This equation is correct only by setting B(E2;$2_1^+ \rightarrow 0_1^+$)=1. Moreover, we can remark that the sum of the B(E2) from the transitions decaying a N-phonon state are equal to $N_{ph} \times$B(E2;$2_{1ph}^+ \rightarrow 0_1^+$).

If we take as example the 3-phonon state in ^{110}Cd, we remark that this rule is right for the 3^+, 4^+ and 6^+, whereas the 2^+ decay is in disagreement. It is why we will introduce the coexistence of two structures which are called normal and intruder. The latter is formed by 2p-2h excitation across the Z=50 shell. In the present case they both exhibit dynamical symmetries (see 1.3). That this occurs in a single nucleus can be shown by the influence of the common O(5) subgroup will be pointed out in the second publication of this work.

1.3 IBM and dynamical symmetry.

The concept of dynamical symmetries has been introduced in 1974 by Arima and Iachello [4] in the Interacting Boson Model (IBM). The aim of this model is to describe, as for the harmonic vibrator model, the collective motion in the nucleus. The dynamical symmetries allow us to construct Hamiltonians which are analytically solvable. In general, the valence nucleons are coupled pairwise to a total angular momentum of J=0, which can be considered as a s boson, or J=2 (d boson). These combinations are favoured because they are energetically the lowest. The IBM uses the second quantification formalism and group theory; in particular the U(6) group structure. The second quantification is constructed by the use of creation and annihilation operators. Consequently state vectors can be written as a combination of the six boson creation operators and the annihilation operators $b_{LM}^{\dagger}$:

$$s^{\dagger}, d_{\mu}^{\dagger}$$
$$\tilde{s}^{\dagger}, \tilde{d}_{\mu}^{\dagger}.$$

with $-2 \leq \mu \leq 2$. In IBM-1, no distinction is made between neutron and proton bosons so the excitation of the nucleus is described by N bosons, given by:

$$N = \frac{n_{\nu} + n_{\pi}}{2}, \tag{1.7}$$

with n_{ν} the number of valence neutrons and n_{π} the number of valence protons. The 36 bilinear combinations form the generators G_i^j of the U(6) group. This group can be reduced in three dynamical symmetries called U(5), SU(3) and O(6). They form three chains of subgroup reduction :

$$
\begin{array}{llllllllll}
U(6) & \supset & U(5) & \supset & O(5) & \supset & O(3) & \supset & O(2) & U(5) \; chain \\
U(6) & \supset & SU(3) & \supset & O(3) & \supset & O(2) & & & SU(3) \; chain \\
U(6) & \supset & O(6) & \supset & O(5) & \supset & O(3) & \supset & O(2) & O(6) \; chain
\end{array}
$$

Each of the dynamical symmetries are related to a type of nucleus described by the collective model, the U(5) limit describes the vibrational nuclei, the O(6) limit describes the γ-unstable nuclei, and the SU(3) limit describes the rotational nuclei. We will now focused on the U(5) dynamical symmetry because this work concerns principally this class of nuclei.

1.3.1 U(5) dynamical symmetry.

In the IBM the Hamiltonian can be written in terms of so called Casimir operators. The definition of a Casimir operator depends of the type of group. For the unitary groups U(n) the first order Casimir operators are given by :

$$C_1[U(n)] = \sum_i G_i^i, \tag{1.8}$$

where G_i^i are the diagonal generators of the considered group U(n). To see if this operator is a Casimir operator it must commute with all generators of the group. There are no equivalent operators for the orthogonal groups O(n).

The second order Casimir operators for the U(n) group are given by :

$$C_2[U(n)] = \sum_{ij} G_i^j G_j^i \tag{1.9}$$

and for O(n) by:

$$C_2[O(n)] = \sum_{ij} H_{ij} H_{ji}. \tag{1.10}$$

Having defined the Casimir operator we can now construct a general Hamiltonian containing Casimir operators of all subgroups. It takes the form :

$$H = \epsilon C_{1U5} + \alpha C_{2U5} + \beta C_{2O5} + \gamma C_{2O3} + \delta C_{SU3} + \eta C_{2O6}. \tag{1.11}$$

For the particular U(5) dynamical symmetry we taken $\delta = \eta = 0$. In this case the eigenvalues of the Casimir operators give the energy of a level in the U(5) dynamical symmetry.

$$E_{U(5)} = \epsilon n_d + \alpha n_d(n_d + 4) + \beta \nu(\nu + 3) + \gamma L(L + 1), \tag{1.12}$$

where n_d is the number of d-bosons, ν is the boson seniority and L the angular momentum. The calculated energies for ^{114}Te are presented in Fig. 1.1. We see a good agreement between the experimental and theoretical energies. As for the harmonic vibrator model, we have to calculate the relative E2 reduced transition probabilities. There is a direct relation between the harmonic vibrator B(E2) values and the U(5) limit, which incorporates the finite-N effect, due to the restricted number of bosons available:

$$\frac{N}{N - n_d + 1} B(E2; n_d \to n_d - 1)_{IBM} = B(E2; N_{ph} \to N_{ph} - 1)_{HV} \tag{1.13}$$

where n_d is the number of d-bosons in the IBM and N the total number of bosons [8]. A more detailed description of the model can be found in Ref. [4].
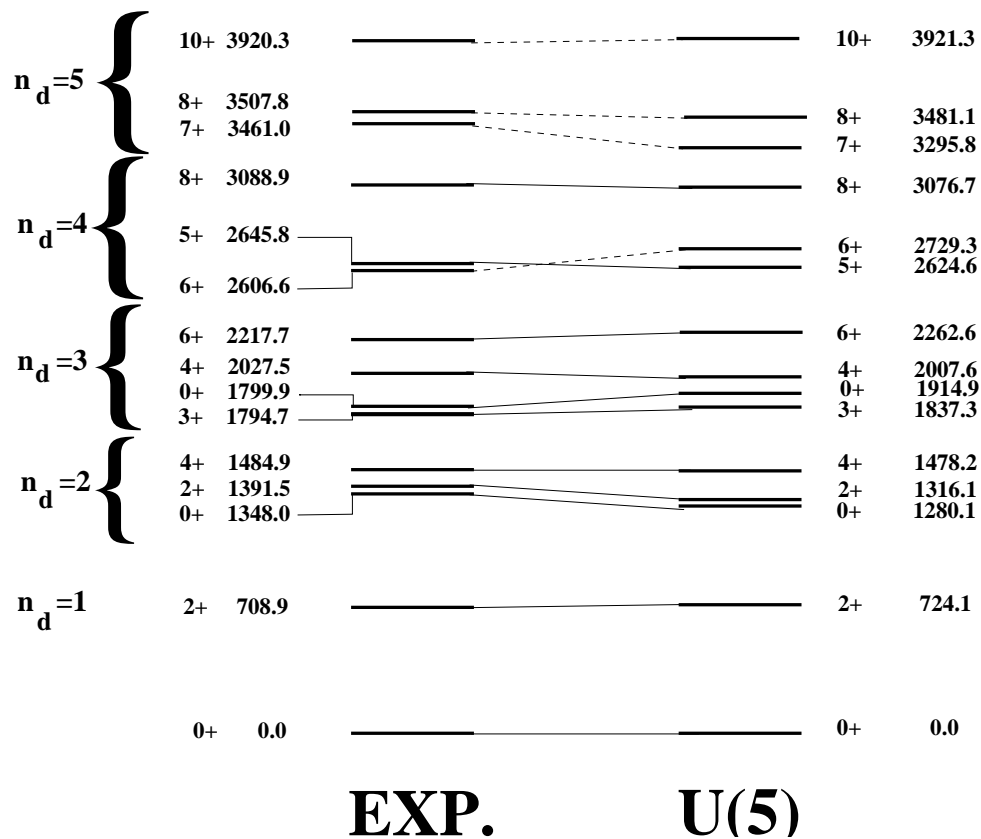
Figure 1.1: Comparison of experimental and theoretical energies [keV] of multiphonon levels for ^{114}Te. On the left side is given the number of d-bosons. Levels connected with solid lines were used for the fit.

1.4 Shape-coexistence.

Shape-coexistence in nuclei was first time observed in 1956 by Morinaga [6] in the double magic nucleus of ^{16}O. This observed structure are understood by the coexistence of two different shapes in the same nucleus. It is why we speak of shape-coexistence. This shape-coexistence configuration is explained by the excitation of protons or neutrons across the shell gap to the next shell (see Fig. 1.2).

Since this work, shape-coexistence has been observed in a variety of nuclei. Due to the large number of valence neutrons and the small number of valence protons , the Cadmium isotopes are particularly good examples for exhibiting a shape-coexistence structure. The shape-coexistence in heavy nuclei was formulated in terms of intruder states and was explained by theoretical work of Heyde et al. [7].

Moreover Heyde et al. [9] suggested in 1992 the possibility of a classification of nuclei in term of intruder analogue multiplets. The idea was to connect nuclei in multiplets with the same number of valence protons or neutrons independent of whether they are particles or holes. It was one of the motivation to study ^{114}Te because the multiplet for this nucleus is composed by :

$$^{106}\text{Ru} \quad ^{110}\text{Cd}_{intr} \quad ^{114}\text{Te}_{intr} \quad ^{118}\text{Ba}$$
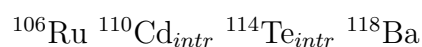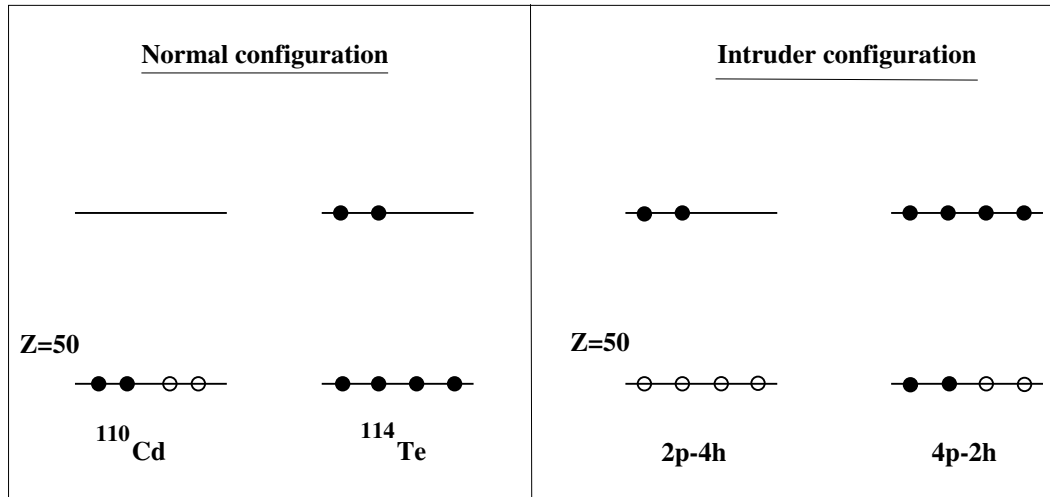
Figure 1.2: Illustration of intruder excitations and normal states in Cd and Te.

The main indication is that the level spacing of the intruder band resembles to the one of the low-lying excitation states of the other nuclei belonging to the multiplets.

More recently, the U(5)-O(6) model was proposed to explain the details of the shape coexistence. This model is based on the U(5) dynamical symmetry to describe the normal states and on the O(6) dynamical symmetry to describe the intruder states. In this model, only states with the same spin and belonging to the same O(5) irreducible representation are mixed. These conditions allowed to reduce the number of parameters. A more detailed description concerning the Hamiltonian and the model description can be found in Ref. [27].

Chapter 2
Study of ^{110}Cd using (n,n′γ) reaction.

2.1   Introduction.

Since many years, ^{110}Cd is considered as a classic example of a vibrational nucleus. Important and intensive experimental works were made these last years to resolve the structure of ^{110}Cd and to extend the knowledge of the level scheme. A lot of techniques were used in the aim to extend the level scheme of ^{110}Cd : transfer reactions [10, 11], inelastic proton scattering [12, 13], β decay measurements [13, 14, 15, 16], inelastic neutron scattering [17, 18], and in-beam gamma-ray spectroscopy using the (α, 2n) reaction [13, 19]. As a vibrational nucleus, ^{110}Cd exhibits so-called multiphonon states. These states were identified some years ago by Kern et al. [19] in their study of ^{110}Cd by the (α,2n) reaction and Bertschy et al. in their β decay measurements. Moreover in the Z=50 mass region additional levels were observed and were interpreted as evidence of shape coexistence. This type of excitation allows to build a band of the so-called intruder states. In ^{110}Cd, an intruder band up to spin 8^+ was identified. However, a clear characterization of these states was lacking. A way to access directly to the structure of these states is to determine the absolute electromagnetic transition rates, but this value depends on the lifetime of the level of interest. Only a few lifetimes of excited states were measured in ^{110}Cd [17, 20]. It is why an experiment to determine the lifetimes of the levels in ^{110}Cd was performed using the Doppler Shift Attenuation Method (DSAM). The obtained lifetimes have allowed us to answer partially an important question of Iachello [21] concerning the survival of collectivity at high excitation energies. Moreover, we also were able to characterize the intruder states proposed by Bertschy et al. [16].

2.2   DSAM/INS : experimental method.

Many methods for lifetimes measurements have been developed [22]. In general each one has a field of application depending on the lifetime range, which can be measured and depending on the type of nuclear excitation, which we want to study. In order to observe the persistence of symmetries in ^{110}Cd, lifetime determination of 3-phonon levels was necessary in this nucleus. In this aim a measurement using the Doppler Shift Attenuation Method (DSAM) following Inelastic Neutron Scattering (INS) was performed at the University of Kentucky Van de Graaff accelerator facility. We have chosen the DSAM/INS measurement principally for the following advantages :

- Contrary to other method using charged particles there is no Coulomb barrier. Consequently, levels of interest can be populated close to the energy threshold.

- As the (n,n′γ) reaction is non-selective, we populate any level with low spin (J < 7).

- The use of accelerator-produced neutrons allow to change the neutron energy and so the excitation energy of the studied nucleus. Therefore, there are no feeding problems unlike to other lifetime methods measurements as for example GRID method.

However, there are also some disadvantages:

- A huge amount of separated isotopes is necessary for the target. In general, it is in the order of ten grams.

- Only stable isotopes can be studied with this method.

- It is very hard to obtain tritium gas.

The fast neutrons were produced using the $^{3}H(p,n)^{3}He$ reaction. The gas cell contains approximately one atmosphere of tritium gas. The tritium gas is insulated from the vacuum by a thin molybdenum foil of 8μm thickness. The neutrons obtained have a well defined energy in the range from 1 to 5 MeV. But the combination of the spread of the monoenergetic proton beam and the thickness of the molybdenum foil induced an energy width of the neutron beam of about 50 – 100 keV. Gamma rays following the (n,n'γ) reaction are detected by the use of a high purity Ge detector located 125 cm from the center of the scattering sample. It was placed inside a BGO anti-Compton shield and heavy shield of lead, tungsten, polyethylene and copper. The experimental arrangement is presented in Fig. 2.1.

Three types of measurements can be performed at the University of Kentucky Van de Graaff accelerator facility :

- a γ-ray excitation functions measurement,

- a γ-ray angular distributions measurement,

- a γ-γ coincidences measurement.

In our study of ^{110}Cd the two first of three possible measurements were performed.

The γ-ray excitation function measurement consisted in varying the neutron energy by steps of 0.1 MeV. The main advantages of this measurement are a clear determination of γ rays belonging to the studied nucleus and the determination of the threshold of the levels of interest. Moreover using the γ-ray excitation functions, it is possible to extract spins by comparing the relative shape of experimental excitation functions with the theoretical ones calculated using the program CINDY [24]. However, it is clear that this method does not permit to distinguish the parity of a state and in general, it gives only a set of possible spins.

The γ-ray angular distribution consists to measure γ lines at different angles in the range from 40° to 153°. The experimental arrangement is the same as for the γ-ray excitation function measurement but the detector turns around a pivot coinciding with the symmetry axes of the sample. This measurement allowed to extract the lifetimes of the levels of interest using DSAM. The angular distribution can be fitted with a Legendre expansion, which allowed us to extract the multipole mixing-ratios for the γ-ray transitions.
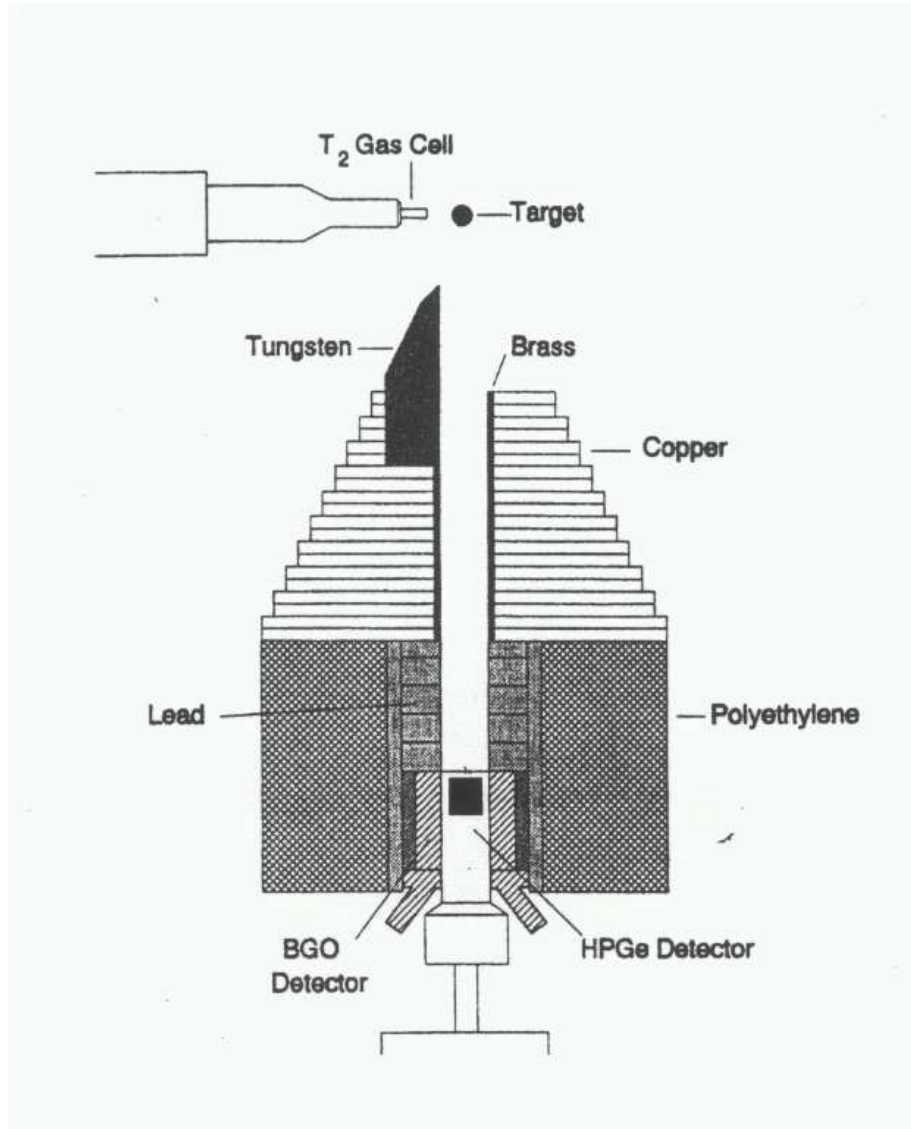
Figure 2.1: Experimental arrangement used for our measurements. Taken from Ref. [23].

The DSAM is based on the fact that the energy of an observed γ-ray change with respect of the angle following the basic equation :

$$E_\gamma(\theta) = E_0[1 + \beta F(\tau)cos\theta_\gamma], \qquad (2.1)$$

where E_0 is the unshifted γ-ray energy determined at the angle of 90° and $\beta = v/c$, with v the recoil velocity of the nucleus in the center-of-mass frame.

To determine lifetimes two values have to be known : the initial velocity β and the theoretical F(τ) value. The value of β is given by:

$$\beta = 0.04635 \frac{A_n}{A_n + A_A} \sqrt{\frac{E_n}{A_n}}, \qquad (2.2)$$

3-phonon states   **intruder states**   **octupole states**

^{110}Cd

U(5)-O(6)

IBM(2)

Figure 2.2: Comparison of experimental B(E2) and theoretical calculations used in this work. The widths of the arrows correspond to the B(E2) values.

where A_n=1, A_A is the number of nucleons of the studied isotope and E_n is the energy of the neutrons in MeV. In the present method the theoretical F(τ) value is calculated using the Winterbon formalism [25]. This formalism describes the movement of the recoiling nucleus in a homogeneous, isotropic and infinite medium with binary collisions. This slowing down is due to two physical processes. Firstly, the excitation and exchange of electrons as the ionised atom of the recoil nucleus moves through the stopping material. This part of slowing down is called electronic stopping. Secondly, the scattering between the moving nucleus and the nuclei of the medium. This part of slowing down is called nuclear stopping.

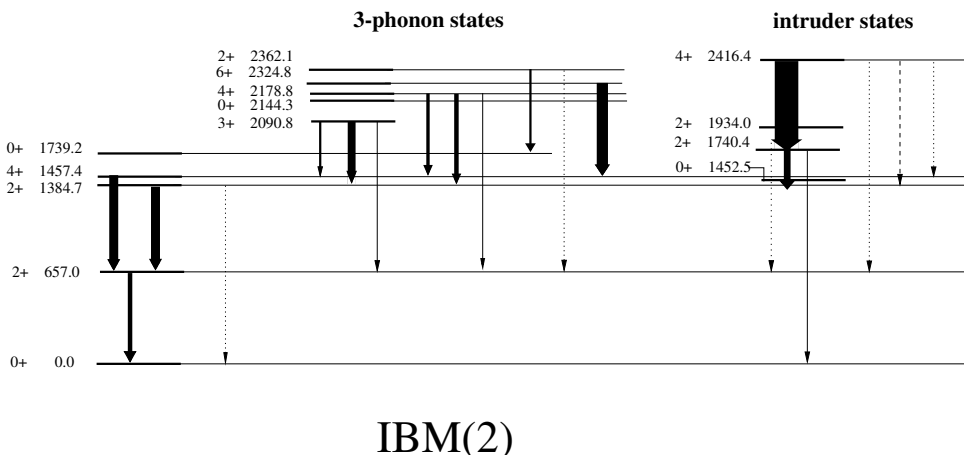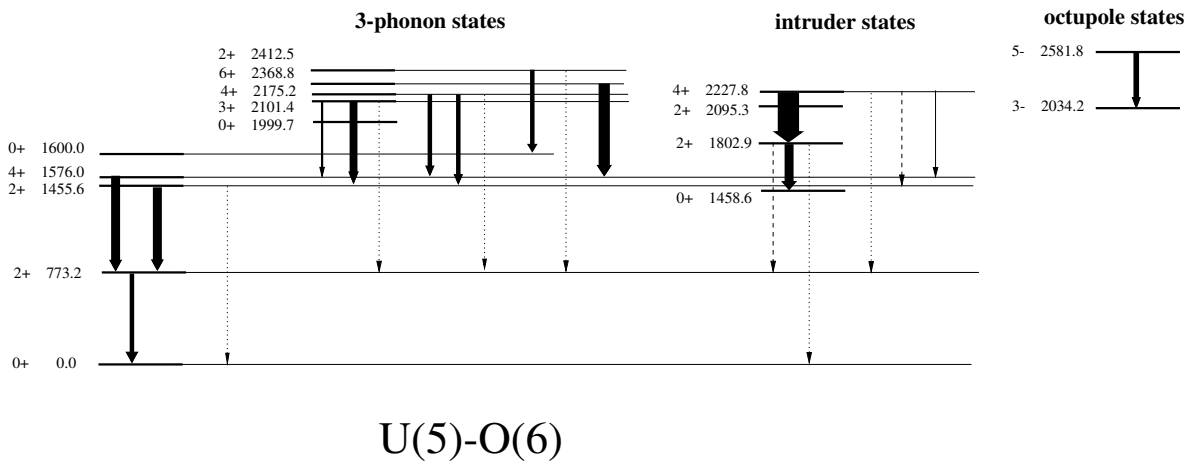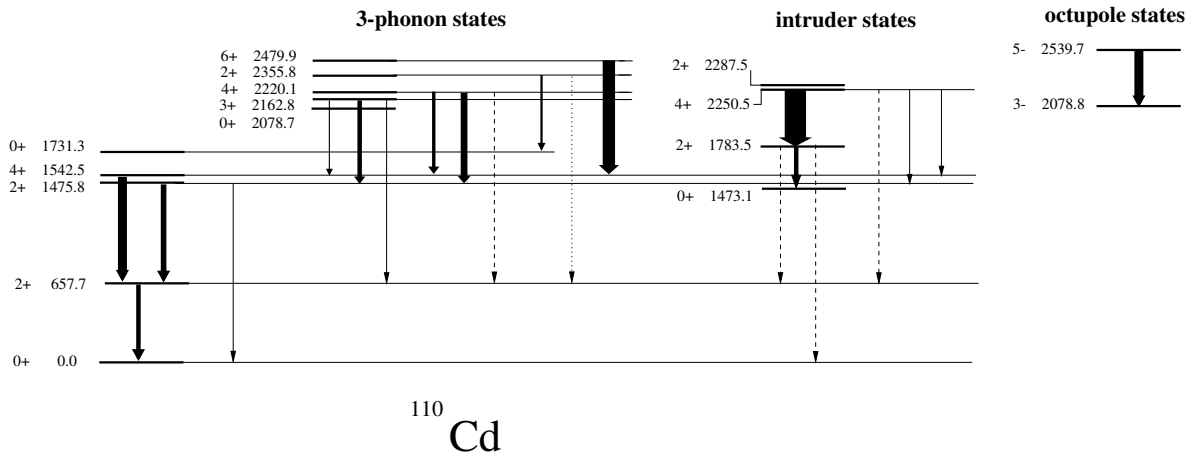The stopping process and the calculation of the initial velocity distributions are well described in Ref. [26].

Experimentally it is possible to determine quite small shifts (<0.1 keV). This is done by measuring simultaneously γ rays from the (n,n$'\gamma$) reaction with the ones of radioactive sources. Consequently the energy shifts of the in-beam γ rays are determined relatively to the internal calibration lines and these ones determine largely the precision with which lifetimes can be measured.

2.3   Results.

The measurements, which we performed, allowed us to obtain two main results. The first one is the characterization of the three-phonon states in ^{110}Cd. By comparing the experimental B(E2) to different theoretical descriptions we have shown that the collectivity of such states survives despite their high energies. Fig. 2.2 shows a partial level scheme of the experimental B(E2) compare to the different theoretical predictions used in this work. As we can see, we have a good agreement between the experimental and theoretical results.

This first part of results allowed us to give a partial answer to Iachello's question [21]. This part of results are presented in the first publication of the second part. Moreover, we also obtained lifetimes of some intruder states. This result allowed us to show a relatively good agreement between the U(5)-O(6) model [27] and the experimental results showing that ^{110}Cd is also a good example for this model. We extracted also lifetimes of the 5^- and 3^- octupole states which permitted us to clearly characterize the 5^- as the quadrupole-octupole coupled state. These last results are all presented in the second publication.

Chapter 3
Study of ^{114}Te using (α,2nγ) reaction.

3.1   Introduction.

Because ^{114}Te is the intruder analogue of ^{110}Cd, it is supposed to exhibit a quite similar structure. An high spin study of ^{114}Te [28] has found a positive parity intruder band. But the scarce of experimental data did not allow to clearly resolve the structure of ^{114}Te at low energy. In order to improve the knowledge on this level scheme, a set of in-beam measurements were done. It consisted of excitation function, angular distribution and γ – γ coincidences measurements. Each of this ones have a specific utility to increase our experimental knowledge of a nucleus.

3.2   In-beam experiments.

3.2.1 γ-ray excitation functions.

The cross-section for the formation of a compound nucleus is greatly dependent on the energy of the incident particle. Other (α,xn) channels can be populated depending on the α-beam energy as we can see in Fig. 3.1. It is why an excitation functions measurement is performed in order to obtain (α,2n) maximum strength to populate ^{114}Te. The excitation functions are obtained by the use of a Compton-suppression spectrometer [29] at several α-particle energies. The excitation functions shape can also be used to assign the γ rays to particular isotopes and it has been shown in Ref. [19], that the slope of the excitation function can be used to determine the spin of a level depopulated by the transition.

3.2.2 γ-ray angular distributions.

One of the most complicated things in γ spectroscopy is to determine the spin and parity of states. In a first step, the γ-ray angular distribution allows to determine if γ rays are pure E2 or mixed transitions. So we can restrict the possible spins for levels and when more than one transition depopulates a level, it is often possible to determine the exact spin and parity. Using a χ^2 analysis of the angular distribution, one can extract the multipole mixing ratio δ for mixed transitions and also determine the spin and parity of a level. This measurement is performed by the same Compton-suppression spectrometer used for excitation functions. In angular distributions the spectrometer is moved at different angle varying from 25° to 90 ° with respect to the beam direction.
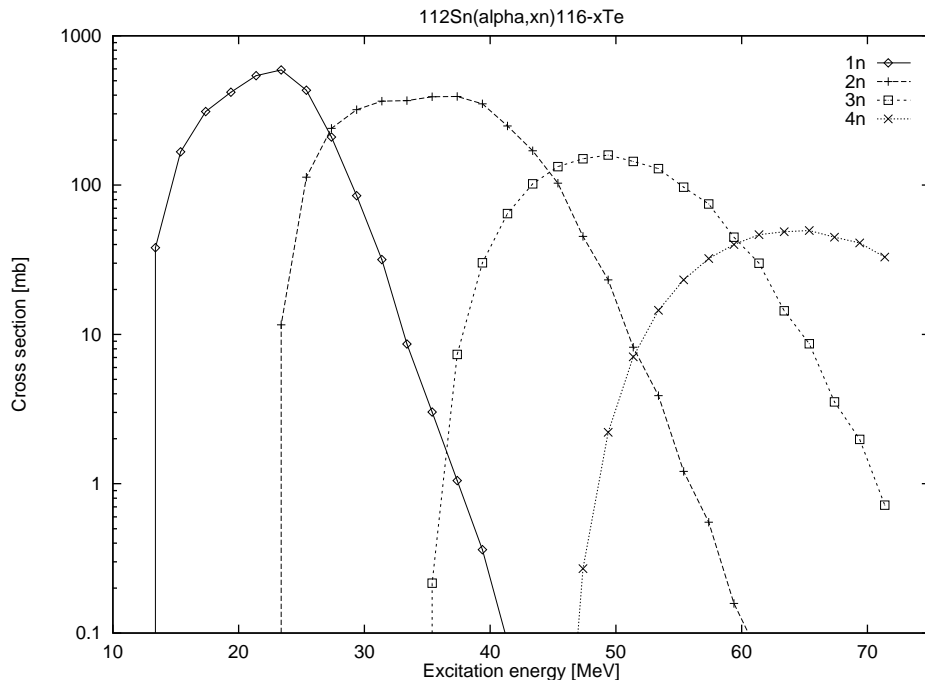
Figure 3.1: Cross section calculated with the program SPIT for the different (α,xn) channels as function of the α-beam energy.

3.2.3 $\gamma-\gamma$ coincidences experiment.

A system of five HPGe detectors with anti-Compton shield has been used for the coincidences measurement. The experimental arrangement is shown in Fig. 3.2. In γ-γ
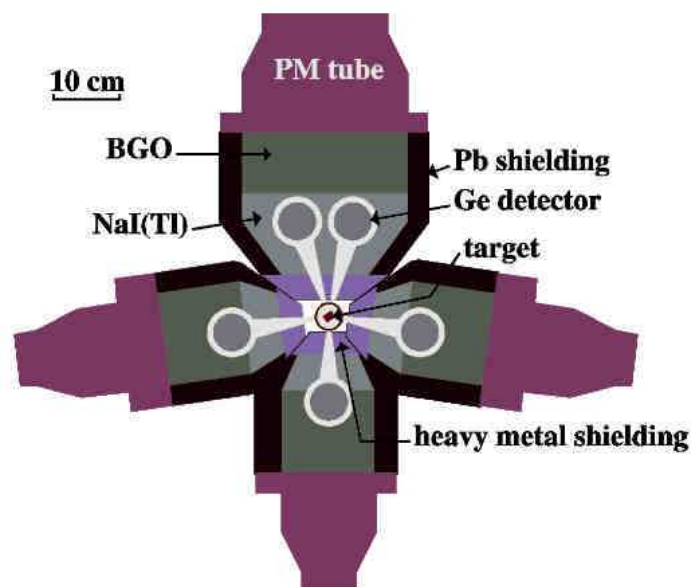
Figure 3.2: Multidetectors system used for $\gamma\gamma$ coincidences measurement.
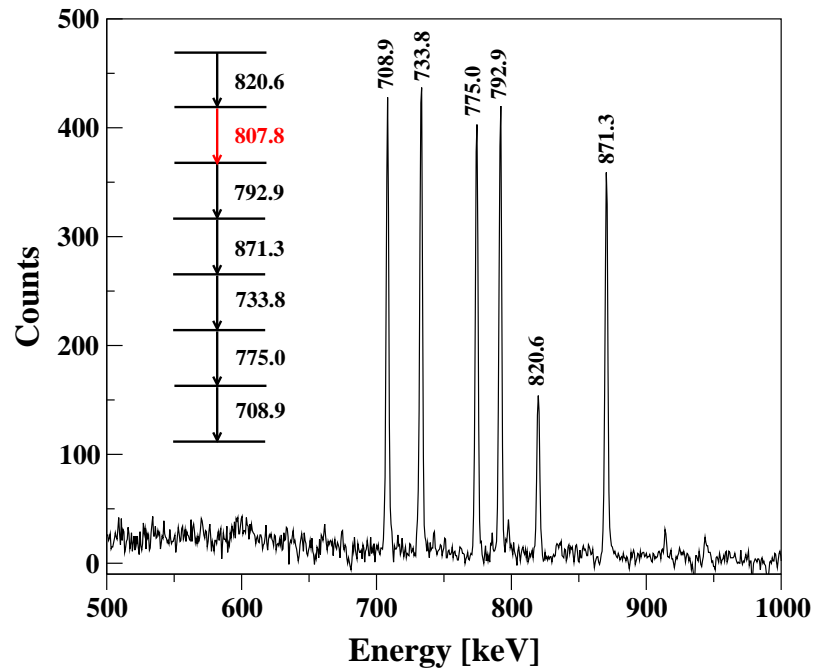
Figure 3.3: Example of coincident γ rays with the proposed level scheme built on the coincidence relation. Red arrow is the γ-ray energy used as gate.

coincidences, one measures two or more γ rays which arrive each in a different detector at the same time. This measurement allows us to say that the observed γ rays are connecting each particular states in cascade. We can so build a level scheme based on the coincidences measurement. An example of γ-rays in coincidences is shown in Fig. 3.3 with the proposed partial level scheme based on the coincidence relation. This experiment allows to construct the level scheme of the studied nucleus and also to determine transitions which do not belong to the isotope of interest. All the experiments described above give a powerful instrument to obtain informations about the experimental level scheme.

3.3   Results.

As exposed in the last publication of the present work, we have increased the level scheme of ^{114}Te by 16 new levels and tried to explain the observed structure. Using a U(5) dynamical symmetry calculation, we were able to extend the observed band structure. The ground-state band was extended up to the spin I=12, the quasi-γ band was extended up to spin I=9. Moreover, this U(5) calculation allowed us to show that ^{114}Te is a good candidate of nucleus exhibiting vibrational character. However, severe problems persist with the obtained B(E2) ratios because they are in disagreement with the theoretical values. No convincing explanation was found for this fact. It will be necessary to obtain lifetimes of excited levels of ^{114}Te in order to clarify the situation and to clearly characterize these states.

Bibliography of Part I.

[1] A. Bohr and B. Mottelson, K. Danske,
Vidensk. Selsk. Mat-Fys. Medd. **27** No.16 (1953).

[2] D.M. Brink, R. de Toledo Piza and A.K. Kerman, Phys. Lett. **19**, 413 (1965).

[3] R.F. Casten, *Nuclear Structure From a Simple Perspective*,
(Oxford, New York), 1990.

[4] A. Arima and F. Iachello, Ann. of Phys. **99**, 253 (1976); **111**, 201 (1978);
123, 468 (1979).

[5] H. Lehmann and J. Jolie, Nucl. Phys. **A588**, 623 (1995).

[6] H. Morinaga, Phys. rev. 101, 254 (1956).

[7] K. Heyde, J. Jolie, J. Moreau, J. Ryckebush, M. Waroquier, P. Van Puppen,
M. Huyse, and J.L. Wood, Nucl. Phys. **A466**, 189 (1987).

[8] H. Lehmann, P.E. Garrett, J. Jolie, C.A. McGrath, Minfang Yeh,and S.W. Yates,
Phys. Lett. **B387**, 259 (1996).

[9] K. Heyde, C. De Coster, J. Jolie, J.L. Wood, Phys. Rev. **C46**, 541 (1992).

[10] N. Blasi, S. Micheletti, M. Pignanelli, R. De Leo, R. Hertenberger, M. Bisemberger,
D. Hofer, H. Kader, P. Schiemenz, and G. Graw, Nucl. Phys. **A536**, 1 (1992).

[11] B.L. Cohen, R. Patell, A. Prakash, E.J. Schneid, Phys. Rev. **135**, B383 (1964).

[12] M. Pignanelli, N. Blasi, S. Micheletti, R. De Leo, M.A. Hofstee, J.M. Schippers,
S.Y. van der Werf, M.N. Harakeh, Nucl. Phys. **A519**, 567, (1990).

[13] J. Kumpulainen, R. Julin, J. Kantele, A. Passoja, W.H. Trzaska, E. Verho,
J. Väärämäki, C. Cutoiu, and M. Ivascu, Phys.Rev. **C45**, 640 (1992).

[14] Y. Kawase, K. Okano, S. Uehara, T. Hayashi, Nucl. Phys. **A193**, 204 (1972).

[15] L.L. Kiang, P.K. Teng, G.C. Kiang, W.S. Chang, P.J. Tu , J.
Phys. Soc. Jpn. **62**, 888 (1993).

[16] M. Bertschy, S. Drissi, P.E. Garrett, J. Jolie, J. Kern, S.J. Mannanal, J.P. Vorlet,
N. Warr, and J. Suhonen, Phys. Rev. **C51**, 103 (1995),**C52**, 1148 (1995).

[17] S.Yu. Araddad, A.M. Demidov, M.M. Dyufani, S.M. Zlitni, V.A. Kurkin, I.V. Mikhailov, D.M. Rateb, and S.M. Sergiwa, Yad. Fiz. **52**, 3 (1990); Sov. J. Nucl. Phys. **52**, 1 (1990).

[18] A.M. Demidov, S.M. Zlitni, V.A. Kurkin, J.M. Rateb, S.M. Sergiva, A.M. Shermit, Bull. Rus. Acad. Sci. Phys. **56**, 8 (1992).

[19] J. Kern, A. Bruder, S. Drissi, V.A. Ionescu, and D. Kusnezov, Nucl. Phys. **A512**, 1 (1990).

[20] M. Piiparinen *et al.*, Nucl. Phys. **A565**, 671 (1993).

[21] F. Iachello, J. Phys. G. **25**, 655 (1999).

[22] Experimental Techniques in Nuclear Physics, Ed. by Dorin N. Poenaru and Walter Greiner, Berlin;New-York : de Gruyter (1997).

[23] S.W. Yates, C.A. McGrath, P.E. Garrett, Minfang Yeh, T. Belgya, in Proc. of the 9th. Int. Symp. on Capture Gamma-Ray Spectroscopy and related topics, Ed. G.L. Molnàr, T. Belgya, Zs. Révay, 211 (1996).

[24] E. Sheldon and V.C. Rogers, Comput. Phys. Commun. **6**, 99 (1973).

[25] K.B. Winterbon, Nucl. Phys. **A246**, 293 (1975).

[26] T. Belgya, G. Molnár, S.W. Yates, Nucl. Phys. **A607**, 43 (1996).

[27] H. Lehmann and J. Jolie, Nucl. Phys. **A588**, 623 (1995).

[28] C.B. Moon, J.U. Kwon, S. J. Chae, J.C. Kim, S.H. Bhatti, C.S. Lee, T. Komatsubara, J. Mukai, T. Hayakawa, H. Kimura, J. Lu, M. Matsuda, T. Wanabe, and K. Furuno, Phys. Rev. **C51**, 2222 (1995).

[29] V.A. Ionescu, J. Kern, C. Nordmann, S. Olbrich and W. Reichart, Nucl. Instr. Meth. **190** (1981) 19.

Part II

PUBLICATION

Characterization of Three-Phonon States in ^{110}Cd

F. Corminboeuf,[1,*] T. B. Brown,[2] L. Genilloud,[1] C. D. Hannant,[2] J. Jolie,[1] J. Kern,[1]
N. Warr,[2] and S. W. Yates[2]

[1]*Institut de Physique, Université de Fribourg, Pérolles, CH-1700 Fribourg, Switzerland*
[2]*University of Kentucky, Lexington, Kentucky 40506-0055*
(Received 23 December 1999)

The three-phonon structure of ^{110}Cd has been studied with the $(n, n'\gamma)$ reaction. The measurements consisted of γ-ray excitation functions and angular distributions, and lifetimes of proposed three-phonon quadrupole states in ^{110}Cd have been measured using the Doppler-shift attenuation method. Moreover, decay of the three-phonon 2^+ state in ^{110}Cd at 2356 keV to a two-phonon state is observed for the first time. The experimental results allow the determination of transition rates of decays from the three-phonon excitations, and the collectivity of these states is established. The experimental $B(E2)$ values are compared to different theoretical descriptions.

Since Bohr and Mottelson [1] proposed their existence, low-lying collective states in nuclei have been the subject of intense study. An important step in this field was the application of symmetry concepts within the interacting boson model (IBM) [2] to describe these states in a variety of nuclei. In this context, Iachello has formulated several fundamental questions concerning symmetries in nuclei [3]. One of the most important is how far the symmetries extend in excitation energy. This question can be answered only by the measurement of absolute transition rates between proposed multiphonon states at higher ($1-3$ MeV) excitation energy. The simplest collective excitations are described by quadrupole phonons in the collective model and by the U(5) dynamical symmetry in the IBM. The classic example of a vibrational nucleus in both models is ^{110}Cd [4]. In this nucleus, situated just below the $Z = 50$ shell closure, candidates for three-phonon states were identified some years ago in the $1-3$ MeV energy region; however, stringent tests of their three-phonon character were lacking due to the absence of measured lifetimes.

The primary aim of the present work was to improve our understanding of the proposed three-phonon states in ^{110}Cd. For this purpose, a set of measurements consisting of γ-ray excitation functions and angular distributions has been performed using the $(n, n'\gamma)$ reaction at the University of Kentucky Van de Graaff accelerator facility. The scattering sample consisted of 23.5 g of metallic ^{110}Cd (97.25% isotopically enriched). The excitation functions allowed us to characterize the decay of the proposed three-phonon 2^+ state (2^+_{3ph}) and, from the angular distributions, the lifetimes of the proposed three-phonon candidates could be extracted using the Doppler-shift attenuation method (DSAM) following inelastic neutron scattering [5].

To search for a decay branch from the proposed [6,7] three-phonon 2^+ state to the two-phonon multiplet, a detailed γ-ray excitation function was performed. The measurement consisted of varying the energy of the incident neutrons produced with the ^{3}H$(p, n)^3$He reaction from 2.1 to 3.4 MeV in 0.1 MeV steps. A 624.3 keV γ ray from the

decay of the three-phonon 2^+ state to the two-phonon 0^+ state ($2^+_{3ph} \rightarrow 0^+_{2ph}$) was found. Figure 1 shows the excitation function supporting the new placement of the 624 keV transition. For comparison, that of the 1697 keV transition, which was known to deexcite the three-phonon 2^+ state, is also shown. An alternate placement of the 624 keV transition depopulating another lower-lying level is not possible because of the observed relative excitation energies yielding this difference. Table I lists the transitions deexciting the 2356 keV level and their measured intensities.

For the γ-ray angular distribution measurement, a neutron energy of 2.9 MeV was selected to avoid the population of higher-lying levels which could feed the three-phonon states perturbing the measured lifetimes. The measured energy of a γ ray emitted at an angle θ by a recoiling nucleus is given by

$$E_\gamma(\theta) = E_0[1 + \beta F(\tau) \cos\theta_\gamma], \qquad (1)$$

where E_γ is the observed γ-ray energy at an angle θ_γ
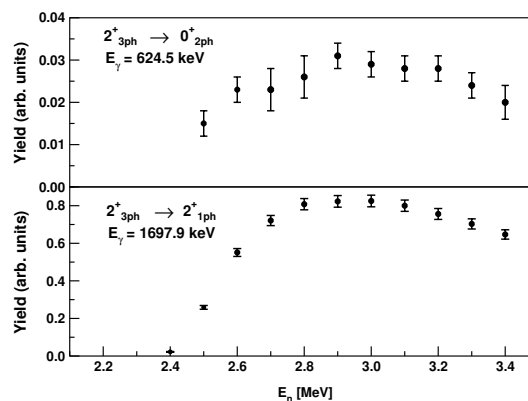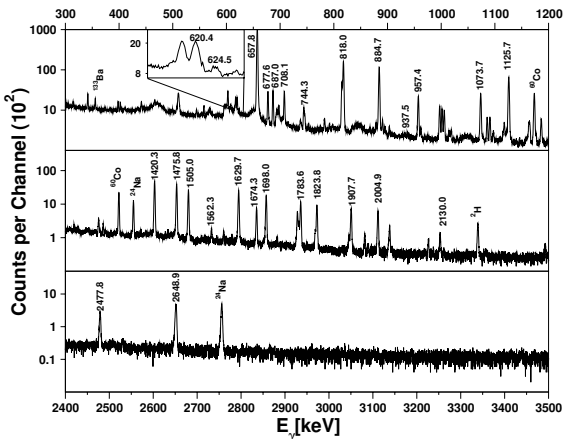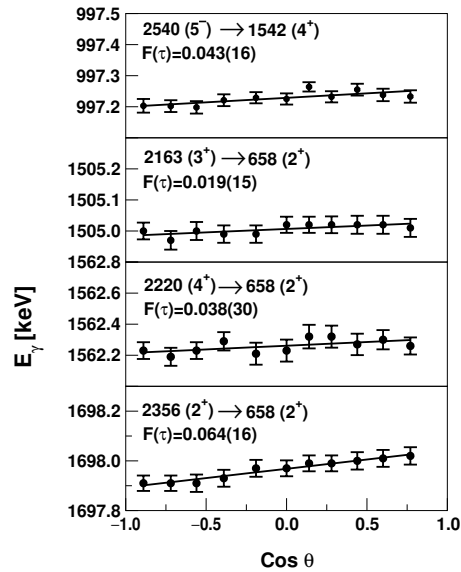

FIG. 1. Excitation functions of the two transitions depopulating the 2^+_{3ph} at 2356 keV.

TABLE I.   Observed transitions from the 2355.8 keV 2^+_{3ph} level.

E_x (keV)	E_γ (keV)	Rel. intensity	E_f (keV)	J^π_f	λL
2355.7	624.466(91)	0.030(2)	1731.5	0^+	$E2$
	1697.933(67)	0.970(2)	657.8	2^+	$M1 + E2$

with respect to the recoil direction, E_0 is the unshifted γ-ray energy, and $\beta = v/c$, with v the recoil velocity of the nucleus in the center-of-mass frame. The lifetimes of the states can be determined [5] by a comparison of the measured $F(\tau)$ values with those calculated using the Winterbon formalism [8]. In order to get precise values for $F(\tau)_{\exp}$, the experiment was performed with spectra recorded at 11 angles using a ~50% (relative) efficient HPGe detector located 125 cm from the scattering sample. The detector was placed inside a bismuth germanium oxide anti-Compton shield. The energy calibration of the detector was continuously monitored through the use of radioactive sources of ^{24}Na, ^{60}Co, and ^{133}Ba during the acquisition of the in-beam spectra. Because γ rays from the $(n, n'\gamma)$ reaction and those from the radioactive sources are recorded simultaneously, reliable Doppler shifts are possible even when these shifts are quite small, i.e., <0.1 keV. In fact, the energy shifts of the in-beam γ rays relative to these internal calibration lines or to other γ rays from long-lived (>2 ps) states largely determine the precision with which the $F(\tau)$ values can be measured. In order to take account of all transitions decaying from a level, we have combined the results of all $F(\tau)$ determinations and have obtained a weighted average value of $F(\tau)$ for each level. Figure 2 shows the γ-ray spectrum acquired at 90°. In Fig. 3, the measured γ-ray energies are plotted as a function of angle for selected transitions at $E_n = 2.9$ MeV. We have compared

FIG. 3.   Measured γ-ray energies as a function of $\cos\theta$ for selected transitions at $E_n = 2.9$ MeV.

(see Table II) our measured lifetimes with previous determinations using other methods. Clearly, our results are in good agreement with these values. The fitted $F(\tau)$ values and their errors, together with the deduced lifetimes for the three-phonon states, are presented in Table III. As a result of the large uncertainty of the lifetime for the three-phonon 6^+ state in our measurement, we adopted the value from Ref. [9] which, while in good agreement with our value, is more precise (see Table II). The results used to extract the $B(E2)$ values are summarized in Table III. The δ values have been deduced from the angular distribution data. When two δ values were possible, we chose the one which was in better agreement with the tabulated values in Ref. [10]. Figure 4 shows the partial level scheme of the three-phonon states.

In Table IV, the experimental $B(E2)$ values for transitions depopulating the proposed three-phonon states [6,7] are compared to theoretical predictions. No attempt is made to fit the theory to the experimental results; for instance, all calculations have effective charges which

FIG. 2.   Observed γ-ray spectrum at 90°. The prominent peaks from ^{110}Cd are labeled with their energies.

TABLE II.   Comparison of the present lifetime results with values from previous publications.

E_x (keV)	J^π	$\tau_{(n,n'\gamma)}$ (ps)	τ_{previous} (ps)
1783.5	2^+	$1.19^{+1.19}_{-0.4}$	$1.44(20)^a$
2078.9	3^-	$0.7(2)$	$1.05^{+0.50}_{-0.35}{}^b$
2480.0	6^+	$0.23^{+1.11}_{-0.12}$	$0.58^{+0.22}_{-0.13}{}^b$
2539.7	5^-	$0.8^{+0.5}_{-0.2}$	$0.90^{+0.40}_{-0.25}{}^b$

^{a}From Ref. [16].
^{b}From Ref. [9].

TABLE III.   Results for three-phonon states.

E_x (keV)	J^π	$F(\tau)$	$\tau_{adopted}$ (ps)[a]	E_γ (keV)	I_{rel} [b]	δ [c]
2162.8	3^+_{3ph}	0.030(12)	$1.20^{+0.83}_{-0.35}$	620.4	0.165(5)	$-0.46^{+0.07}_{-0.06}$ $(-1.61^{+0.21}_{-0.19})$
				687.0	0.247(6)	$-1.66^{+0.09}_{-0.08}$
				1505.0	0.587(9)	$-1.52^{+0.11}_{-0.14}$ $(-0.39^{+0.04}_{-0.05})$
2220.1	4^+_{3ph}	0.037(11)	$0.97^{+0.43}_{-0.23}$	677.6	0.639(8)	$-0.41(2)$
				744.3	0.281(7)	$E2$
				1562.3	0.081(3)	$E2$[d]
2355.7	2^+_{3ph}	0.068(16)	$0.51^{+0.14}_{-0.10}$	624.5	0.030(2)[e]	$E2$
				1697.9	0.970(2)	$-0.07(2)$ $(2.86^{+0.21}_{-0.22})$
2480.0	6^+_{3ph}	0.141(114)	$0.58^{+0.22}_{-0.13}$[f]	937.5	1.000	$E2$

[a]Average including all observed deexciting transitions.
[b]From this experiment. Where values are available in Ref. [16], the agreement is good.
[c]From the angular distribution (see text).
[d]This transition was listed as $E2 + M3$ in Ref. [16], but from our experiment it has an $E2$ multipolarity.
[e]Transition placed for the first time.
[f]Adopted from Ref. [9].

reproduce exactly the $B(E2; 2^+_1 \to 0^+_1)$. Instead, we compare several theoretical predictions for three-phonon states available in the literature to our data. Each successive model used is of increasing sophistication. The first uses the predictions of the standard harmonic vibrator [1]. The second uses a pure U(5) dynamical symmetry description in the IBM. The relation between the harmonic vibrator $B(E2)$ values and the U(5) limit, which incorporates finite-N effects, is given by

$$\frac{N}{N - n_d + 1} B(E2; n_d \to n_d - 1)_{IBM}$$
$$= B(E2; N_{ph} \to N_{ph} - 1)_{HV}, \quad (2)$$

where n_d is the number of d bosons in the IBM and N is the total number of bosons [4,11]. Two-particle, four-hole intruder excitations lead to a second collective structure, which manifests itself around an excitation energy of 1.5 MeV in ^{110}Cd [10]. In order to account for these coexisting structures, models incorporating these features are also considered [12]. The results in the third column of Table IV correspond to the U(5)-O(6) model [13], where the normal states are described by the U(5) limit and the intruders by the O(6) symmetry. The last column presents a more sophisticated configuration mixing IBM-2 calculation using the parameters from Ref. [14]. The U(5)-O(6) calculations were performed using the computer code OCTUPOLE [15] and thus involve mixing between all states. One sees that the proposed three-phonon states 2^+, 3^+, 4^+, and 6^+ decay to the next multiplet by collective transitions. Because of the presence of a 3^- state at 2078.9 keV, which has almost the same excitation energy as the 0^+_{3ph} excitation at 2078.7 keV, no lifetime could be extracted for the 0^+_{3ph} state. Inspection of Table IV reveals some general tendencies. The pure harmonic vibrator clearly overpredicts the $B(E2)$ values in a systematic way. The U(5) limit, which incorporates finite-N effects, does a much better job, but is unable to describe the small branchings. The more sophisticated models, in particular, the IBM-2 with configuration mixing [12,14], do better in explaining the weak branches and the $2^+_{3ph} \to 0^+_{2ph}$ transition. The latter is reduced due to selective mixing of the 0^+ two-phonon state with the intruder state [11].

TABLE IV.   Comparison of experimental and theoretical $B(E2)$ values from three-phonon states in ^{110}Cd.

Transition	E_γ (keV)	Exp. (W.u.)	Theory (W.u.)			
			HV	U(5)	U(5)-O(6)	IBM-2
$3^+_{3ph} \to 4^+_{2ph}$	620.4	7^{+6}_{-4}	24	17	16	15
$3^+_{3ph} \to 2^+_{2ph}$	687.0	25^{+13}_{-11}	59	42	39	43
$3^+_{3ph} \to 2^+_{1ph}$	1505.0	$1.1^{+0.6}_{-0.5}$	0.0	0.0	0.002	0.4
$4^+_{3ph} \to 4^+_{2ph}$	677.6	17^{+8}_{-6}	39	28	26	23
$4^+_{3ph} \to 2^+_{2ph}$	744.3	33(11)	43	31	29	32
$4^+_{3ph} \to 2^+_{1ph}$	1562.3	0.23(8)	0.0	0.0	0.002	0.100
$2^+_{3ph} \to 0^+_{2ph}$	624.5	16(5)	38	27	18	19
$2^+_{3ph} \to 2^+_{1ph}$	1697.9	$0.02^{+0.02}_{-0.01}$	0.0	0.0	0.02	0.08
$6^+_{3ph} \to 4^+_{2ph}$	937.5	62^{+18}_{-17}	82	59	56	59
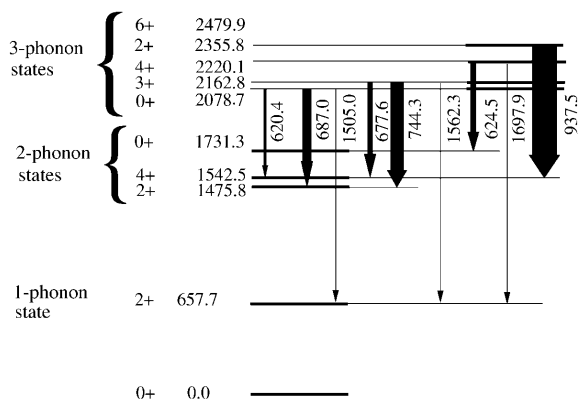
FIG. 4. Partial level scheme of ^{110}Cd. The widths of the arrows correspond to the experimental $B(E2)$ values.

In conclusion, the $(n, n'\gamma)$ reaction and DSAM have been used to characterize the three-phonon states in ^{110}Cd. Specifically, the results of the excitation function measurements allowed us to improve our knowledge of the decay of the three-phonon 2^+ state. The angular distributions enabled us to extract the lifetimes of the three-phonon states as well as the multipolarities of the depopulating transitions. These results clearly demonstrate that these states are collective. Irrespective of the agreement or disagreement with the different nuclear models, this study provides new information in answer to the question of how far up in energy symmetries extend [3]. Questions remain concerning higher multiphonon multiplets and, in particular, the four-phonon multiplets as discussed in Ref. [9].

*Email address: frederic.corminboeuf@unifr.ch

[1] A. Bohr and B. Mottelson, K. Dan. Vidensk. Selsk. Mat. Fys. Medd. **27**, 16 (1953).
[2] F. Iachello and A. Arima, *The Interacting Boson Model* (Cambridge University Press, Cambridge, England, 1987).
[3] F. Iachello, J. Phys. G **25**, 655 (1999).
[4] A. Arima and F. Iachello, Ann. Phys. (N.Y.) **99**, 253 (1976).
[5] T. Belgya, G. Molnár, and S. W. Yates, Nucl. Phys **A607**, 43 (1996).
[6] M. Bertschy, S. Drissi, P. E. Garrett, J. Jolie, J. Kern, S. J. Mannanal, J. P. Vorlet, N. Warr, and J. Suhonen, Phys. Rev. C **51**, 103 (1995); **52**, 1148 (1995).
[7] J. Kern, P. E. Garrett, J. Jolie, and H. Lehmann, Nucl. Phys. **A593**, 21 (1995).
[8] K. B. Winterbon, Nucl. Phys. **A246**, 293 (1975).
[9] Yu. N. Lobach, A. D. Efimov, and A. A. Pasternak, Eur. Phys. J. A **6**, 131 (1999).
[10] J. Kern, A. Bruder, S. Drissi, V. A. Ionescu, and D. Kusnezov, Nucl. Phys. **A512**, 1 (1990).
[11] H. Lehmann, P. E. Garrett, J. Jolie, C. A. McGrath, Minfang Yeh, and S. W. Yates, Phys. Lett. B **387**, 259 (1996).
[12] J. L. Wood, K. Heyde, W. Nazarewiecz, M. Huyse, and P. Van Duppen, Phys. Rep. **102**, 291 (1983), and references therein.
[13] H. Lehmann and J. Jolie, Nucl. Phys. **A588**, 623 (1995).
[14] M. Délèze, S. Drissi, J. Kern, P. A. Tercier, J. P. Vorlet, J. Rikovska, T. Otsuka, S. Judge, and A. Williams, Nucl. Phys. **A551**, 269 (1993).
[15] D. Kusnezov, computer code OCTUPOLE (unpublished).
[16] D. De Frenne, Nucl. Data Sheets **67**, 809 (1992).

Structures and lifetimes of states in ^{110}Cd

F. Corminboeuf[1]*, T.B. Brown[2], L. Genilloud[1], C.D. Hannant[2], J. Jolie[1], J. Kern[1][†], N. Warr[2] and S.W. Yates[2]

[1] *Institut de Physique, Université de Fribourg, Pérolles, CH-1700 Fribourg, Switzerland*

[2] *University of Kentucky, Lexington, KY 40506-0055 USA*

(September 28, 2000)

A set of measurements consisting of γ-ray excitation functions and angular distributions has been performed using the (n,n'γ) reaction on ^{110}Cd. Gamma-ray excitation functions allowed us to clarify the level scheme by placing 10 new transitions and to establish one new level. From γ-ray angular distributions, the lifetimes for 16 excited states were extracted using the Doppler shift attenuation method. The experimental B(E2), B(M1) and B(E1) values of transitions from intruder, octupole and three-phonon states are compared to different theoretical models.

I. INTRODUCTION

The Z=50 mass region is very favorable for nuclear structure studies due to the large abundance of stable isotopes combined with the interesting feature of neutrons at mid-shell and protons near the Z=50 shell closure. In this region, ^{110}Cd emerged early as a classic example of a vibrational nucleus [1,2]. However, although the excited nucleus showed the two-phonon states expected for a vibrator, additional levels were observed forming a deformed band up to $J^{\pi} = 6^{+}$ [3]. These states were interpreted as evidence of shape coexistence, where 2-particle 2-hole excitations across the Z=50 closed proton shell drive the nucleus into deformation [4]. Both types of excitations have been studied up to higher spin by Kern et al. [5].

Numerous experiments have been performed to develop the ^{110}Cd level scheme, utilizing a wide variety of techniques, including transfer reactions [6,7], inelastic proton scatering [8,9], beta-decay measurements [9–12], inelastic neutron scattering [13,14], and the (α,2n) reaction [5,9]. An extensive level scheme has been developed, including lifetimes for the excited states with high spins [15,16]. Some years ago, the nature of low-spin states was studied state-by-state through in-beam techniques and many multiphonon states were proposed [12]. However, due to the absence of measured lifetimes, complete characterization of these states was not possible.

With the aim of extending the knowledge of lifetimes of low-spin states, measurements at the University of Kentucky Van de Graaff facility have been performed using the Doppler-shift attenuation method (DSAM) following inelastic neutron scattering. The experiments consisted of γ-ray excitation functions and angular distributions. The former allowed us to extend the level scheme by 10 new transitions and add one new level. The latter

yielded lifetimes of 16 excited states in ^{110}Cd, in particular for the three-phonon, intruder and octupole states. In addition, multipole mixing ratios were measured. The complete data set is compared with different theoretical descriptions incorporating shape coexistence. A portion of these results has been presented in Ref. [17] in the context of the collectivity of the 3-phonon states.

II. EXPERIMENTAL RESULTS

Gamma rays were observed following the ^{110}Cd(n,n'γ) reaction with the facilities at the University of Kentucky accelerator laboratory [18]. For the excitation function measurements, γ-ray spectra were recorded in 0.1-MeV increments of incident neutron energy, and angular distribution measurements were performed at two neutron energies. The approximately monoenergetic neutrons ($\Delta E_n \sim 100$ keV) for these measurements were produced with the ^{3}H(p,n) reaction. Protons from the University of Kentucky Van de Graaff accelerator were pulsed at a 1.875 MHz rate with a pulse width of < 2 ns. The pulsed proton beam with an average current of 1.8 μA was focussed through an 8 μm molybdenum entrance foil into a 1-cm x 3-cm tantalum-lined stainless steel gas cell containing approximately one atmosphere of tritium gas. The scattering sample consisted of three ingots of cadmium metal, enriched to 97.25% in ^{110}Cd, arranged in a nearly cylindrical geometry with a diameter of 1.2 cm and a height of 2.4 cm. This scattering sample was suspended 3.0 cm from the end of the gas cell.

---

*email: frederic.corminboeuf@unifr.ch

[†]Deceased
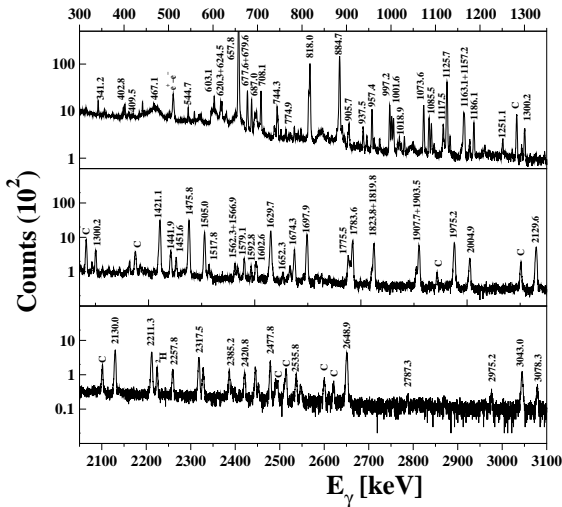
FIG. 1. Gamma-ray spectrum acquired at E_n=3.4 MeV. The prominent peaks from ^{110}Cd are labelled with their energies in keV. Peaks marked with C are contaminants.

A. γ-ray excitation functions

A γ-ray excitation function measurement was performed with the aim of clarifying the decay scheme of low-spin states. It consisted of varying the energy of the

incident neutrons from 2.1 to 3.4 MeV in 0.1-MeV steps. The experiment was performed using a ~50% (relative) efficient HPGe detector located 125 cm from the scattering sample. The detector was placed inside a BGO anti-Compton shield and had an energy resolution of 2.0 keV at 1.33 MeV. Time-of-flight gating was used to reduce extraneous background events. Fig. 1 shows the γ-ray spectrum acquired at E_n=3.4 MeV. Fig. 2 shows excitations functions for selected γ rays. In all cases the branching ratios of the used transitions were considered in order to extract the experimental excitation function yields. The theoretical excitation functions were calculated with the program CINDY [19], and the data were normalized to the calculated values using levels with known spins. The relative shapes of the excitation functions also proved helpful in assessing the possible spin values; however it is not possible to determine the parities of the states. Therefore, we adopt, in general, the same parities as given in Ref. [20].

B. γ-ray angular distribution

Gamma-ray angular distributions measurements were performed at neutron energies of 3.2 and 2.9 MeV. The latter energy was chosen to avoid the population of higher-lying levels which could feed the states of interest and perturb the measured lifetimes and to maximize the population of the levels of interest.

FIG. 2. Excitation functions for γ rays from levels with known spins [4^+ (2561), 0^+ (2662)], the 403-keV and 1824-keV γ rays from the 2482-keV level, the 1157-keV γ rays from the 2633-keV level, and the 1674-keV γ rays from the 2332-keV level compared with calculations from the program CINDY [19].

658 (2⁺)→0 (0⁺)

$F(\tau)=0.002(2)$

2433 (3⁺)→1475 (2⁺)

$F(\tau)=0.011(15)$

2433 (3⁺) →658 (2⁺)

$F(\tau)=0.008(21)$

FIG. 3. Measured γ-ray energies as a function of cos θ for transitions with lifetimes too long to be determined with the DSAM.

The Doppler-shift attenuation measurement consisted of determining the energy of a γ ray emitted at various angles. The energy of the observed γ ray, E_γ at an angle θ_γ with respect to the recoil direction is given by :

$$E_\gamma(\theta) = E_0[1 + \beta F(\tau)cos\theta_\gamma], \qquad (1)$$

where E_0 is the unshifted γ-ray energy and $\beta = v/c$, with v the recoil velocity of the nucleus in the center-of-mass frame. The lifetimes of the states can be determined by comparison of the measured $F(\tau)$ values with those calcu-

lated using the Winterbon formalism [21]. A description of the method can be found in Ref. [22].

The 2.9-MeV measurement was performed with spectra recorded at 11 angles using the same detector placed inside a BGO anti-Compton shield and the same geometry as for the γ-ray excitation function measurement. Th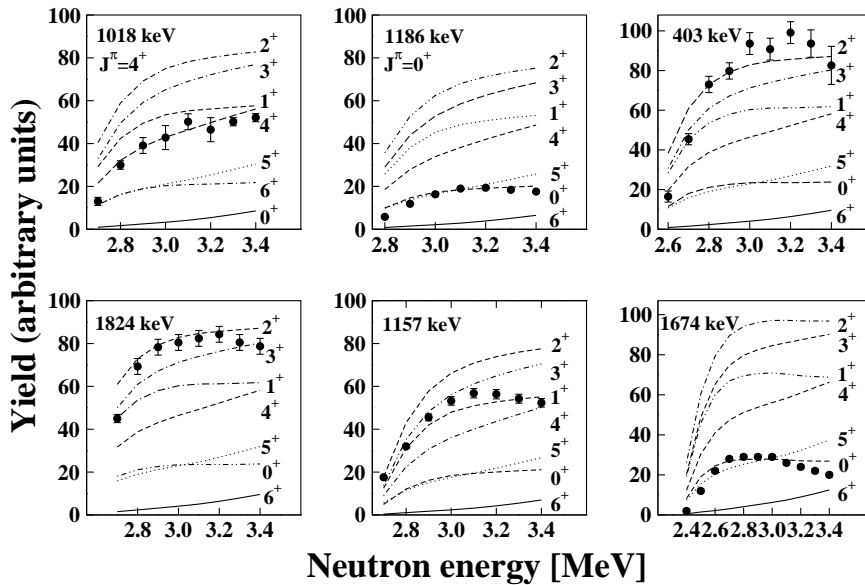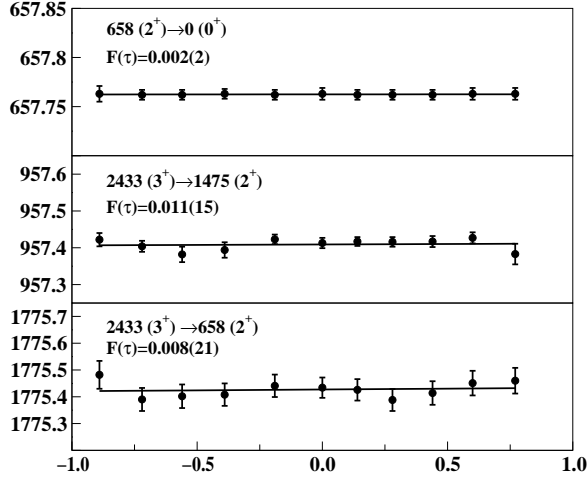e energy resolution was 2.2 keV at 1.33 MeV. The experiment at 3.2 MeV was performed with spectra recorded at 7 angles using a ~50% (relative) efficient HPGe detector located at 112.5 cm from the scattering sample. The 2.9-MeV measurement was used for the lower-lying states, in order to minimize the effects of feeding.

The energy calibration of the detectors was simultaneously monitored through the use of radioactive sources of ^{24}Na, ^{60}Co, and ^{133}Ba during the acquisition of the in-beam spectra. Because γ rays from the (n,n'γ) reaction and those from the radioactive sources are recorded simultaneously, reliable Doppler shifts can be measured even when these shifts are quite small, i.e., <0.1 keV. In fact, the energy shifts of the in-beam γ rays relative to the internal calibration lines or to other γ rays from long lived (> 2 ps) states largely determine the precision with which lifetimes can be measured. In order to take into account all transitions depopulating a level, we have combined the results from these transitions to obtain a weighted average value of $F(\tau)$ for each level. Examples of levels with lifetimes too long to be determined by DSAM are presented in Fig. 3. In Figs. 4 and 5, the γ-ray energies, measured at E_n=2.9 MeV, are plotted as a function of angle for the most intense transitions from levels of interest.

TABLE I. Measured lifetimes and comparisons with values from previous work [16,20].

E_x [keV]	$J^\pi_{adopted}$	τ[ps]	
		Literature	present
1783.5	$2^+_{1,intr}$	$1.44^{+2.00}_{-0.60}$	$1.16^{+0.49\,a)}_{-0.27}$
2078.8	3^-_{oct}	$1.05^{+0.50}_{-0.35}$	$0.67^{+0.21\,a)}_{-0.13}$
2162.8	3^+_{3ph}		$1.20^{+0.83\,a)}_{-0.35}$
2220.1	4^+_{3ph}		$0.97^{+0.43\,a)}_{-0.23}$
2250.6	4^+_{intr}		$0.87^{+0.71\,a)}_{-0.28}$
2287.4	$2^+_{2,intr}$		$0.42^{+0.10\,a)}_{-0.07}$
2355.7	2^+_{3ph}		$0.51^{+0.17\,a)}_{-0.10}$
2480.0	6^+_{3ph}	$0.58^{+0.22}_{-0.13}$	$0.23^{+1.11\,a)}_{-0.12}$
2481.6	2^+		$0.67^{+0.33\,a)}_{-0.17}$
2539.7	5^-_{oct}	$0.90^{+0.40}_{-0.25}$	$0.83^{+0.51\,a)}_{-0.23}$
2561.3	4^+		$1.25^{+1.20\,a)}_{-0.42}$
2633.1	$(2^+, 3^+)$		$0.20^{+0.03\,a)}_{-0.02}$
2649.5	(1^-)		$0.04(1)^{b)}$
2758.2	$(1^+, 2^+, 3^+)$		$0.33^{+0.13\,a)}_{-0.08}$
2787.4	(2^+)		$0.04(1)^{b)}$
2984.5	5^-		$0.16^{+0.29\,b)}_{-0.07}$

[a] From the γ-ray angular distribution performed at E_n=2.9 MeV
[b] From the γ-ray angular distribution performed at E_n=3.2 MeV
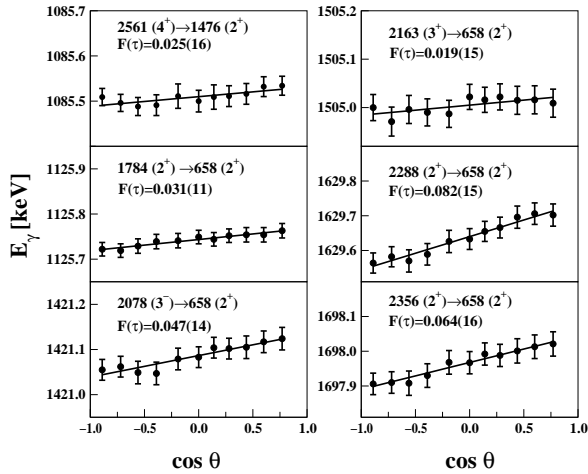
FIG. 4. Measured γ-ray energies as a function of $\cos \theta$ for transitions from several levels of interest. $F(\tau)$ values are indicated.
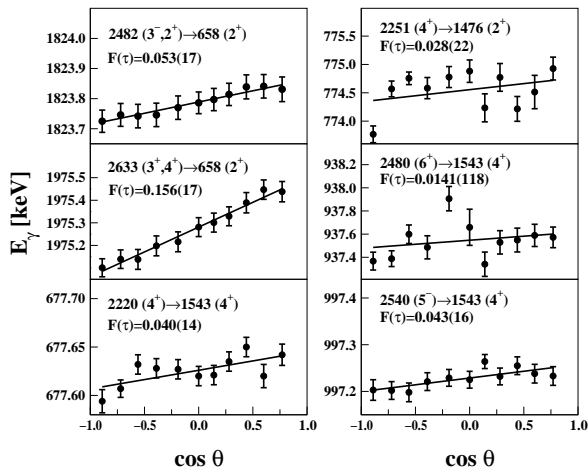
FIG. 5. Same caption as Fig 4, but for additionnal γ rays.

In order to test the lifetimes obtained, we have compared our values with previously published results from Ref. [15,16]. As Table I shows, the results are in agreement with the literature values. Because of the large uncertainty of the lifetime for the 3-phonon 6$^+$ state in our measurement, the value from Ref. [16] was adopted which, while in agreement with our value, is more precise (see Table I).

The γ-ray angular distributions performed at E_n=2.9 MeV were fitted with a Legendre polynomial expansion, allowing us to extract multipole-mixing ratios for the γ-ray transitions from the levels of interest. When two δ

values were possible, the one in better agreement with the tabulated values in Refs. [5,20] was chosen. In Table II the experimental values are compared with those from previous measurements [5,20]. Fig. 6 presents results of the angular distribution analysis for a few transitions of ^{110}Cd.
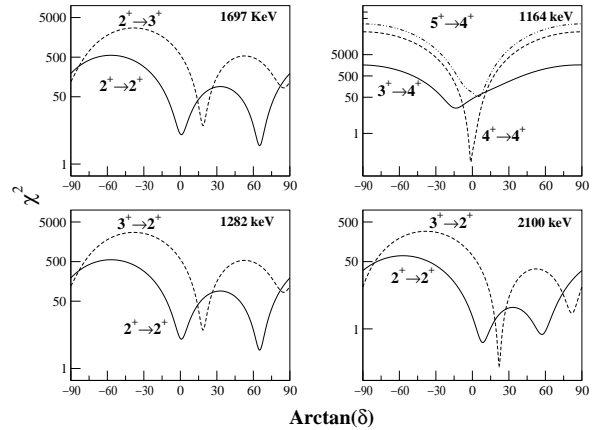
FIG. 6. Analysis of the angular distribution performed at 2.9 MeV of a few transitions in ^{110}Cd. Shown is the χ^2 calculated as a function of arctan(δ).

III. LEVEL SCHEME

In this section, we discuss levels which were expected to be observed but were not, those for which the decay is revised, and a new level. Transitions were placed on the basis of the excitation function thresholds and from γ-ray energy arguments. The experimental results are summarized in Table III. Some levels observed in transfer reactions have no known decay; from our data these levels cannot be confirmed and they must be regarded as doubtful. We placed 77 of the 128 γ rays assigned to ^{110}Cd in the measurement performed at E_n=3.4 MeV during the γ-ray excitation function. The energy calibrations of the spectra were performed using the well-known energies of the radioactive sources of ^{60}Co, ^{24}Na, and with 11 well-known γ rays in ^{110}Cd taken from Ref. [5].

1783.5-keV level: This level was known to decay by transitions of 1125.7 and 1783.6 keV. An additional 310-keV transition depopulating this level was observed by Meyer et al. [3] in their study of ^{110}Cd from β decay and by Araddad et al. [13] in their study of ^{110}Cd with the (n,n'γ) reaction. This γ ray was also observed in our study and, on the basis of its excitation function threshold, it was also placed as depopulating the 1783.6-keV level. In contrast to earlier work, its relative intensity was determined.

TABLE II. Comparison of measured multipole mixing ratios with previous work.

E_{level} [keV]	J_i^π	J_f^π	E_γ [keV]	$\delta_{(n,n'\gamma)}$	From Ref. [5]	From Ref. [20]
1783.5	$2_{1,intr}^+$	0^+	310.5	a)		
		2^+	1125.7	$0.13_{-0.02}^{+0.03}$, $1.69_{-0.11}^{+0.13}$		0.33(8)
		0^+	1783.6	E2		E2
2078.8	3_{oct}^-	2^+	603.1	0.04(2)	-0.14(22)	b)
		2^+	1421.1	$0.003_{-0.019}^{+0.028}$	0.01(8)	0.05(5)
2162.8	3_{3ph}^+	4^+	620.3	$-0.46_{-0.06}^{+0.07}$, $-1.61_{-0.19}^{+0.21}$		-0.70(4)
		2^+	687.0	$-1.66_{-0.06}^{+0.09}$	-1.26(41)	-1.76(6) or -1.48(15)
		2^+	1505.0	$-1.52_{-0.14}^{+0.11}$, $-0.39_{-0.05}^{+0.04}$	-1.48(23)	-1.21(4)
2220.1	4_{3ph}^+	4^+	677.6	-0.41(2)	-0.40(7)	-0.36(3)
		2^+	744.3	E2		-0(+16,-10)
		2^+	1562.3	E2	E2	-0.10(+2,-3)
2250.6	4_{intr}^+	2^+	467.1	E2	E2	(E2)
		4^+	708.1	$0.13_{-0.03}^{+0.04}$	-0.72(32)	-0.15(9)
		2^+	774.9	E2	E2	(E2)
		2^+	1592.8	E2	E2	(E2)
2287.4	$2_{2,intr}^+$	2^+	1629.7	$2.39_{-0.18}^{+0.13}$, -0.01(2)		0.06(3)
2355.7	2_{3ph}^+	0^+	624.5	E2		
		2^+	1697.9	-0.07(2), $2.86_{-0.22}^{+0.21}$		0.10(5) or 1.8(5)
2480.0	6_{3ph}^+	4^+	937.5	E2	E2	E2
2481.6	(2^+)	2^+	1823.8	$-0.91_{-0.12}^{+0.09}$, -2.88(56)		-0.70(10) or -5.2(20)
		3^-	402.8	E1		
2539.7	5_{oct}^-	3^-	460.8	(E2)	E2	(E2)
		4^+	997.2	E1	-0.030(46)	-0.025(+35,-75)
2561.3	4^+	4^+	1018.9	$-0.49_{-0.19}^{+0.16}$, $3.48_{-1.23}^{+2.25}$	-0.56(35)	b)
		2^+	1085.5	E2	E2	E2
		2^+	1903.5	E2		
2633.1	$(2^+, 3^+)$	2^+	1157.2	a)		
		2^+	1975.4	(E2)		
2705.6	4_{intr}^+	4^+	1163.1	E2	0.0(3)	

a) No reliable value was found.
b) Same value as in Ref. [5].

1809.5-keV level: This level was first observed by Sarantites et al. [23] who proposed $J^\pi = (1,2)^+$ based on ^{110m}In decay. From their study of the same decay, Bertschy et al. [12] noted this level as questionable. Such a low-spin state should be populated by the (n,n') reaction, but no evidence for its existence was observed in this study. We conclude that this earlier level placement is spurious.

2078.86 and 2078.88-keV levels: This doublet is well established. The main difficulty lies in separating the γ rays which decay from each of these states. We observe γ rays with energies of 295.6, 603.1 and 1421.1 keV. Taking into account the branching ratio given in Ref. [20], the measured intensities for these transitions agree with the proposed 0^+, 3^- doublet.

2332.0-keV level: This level was assigned by Blasi et al. [7] from $(\vec{d},t)$ reaction measurements as $J^\pi = 0^+$, while according to Ref. [20] it has $J^\pi = (0^+,1^+,2^+)$. The excitation function supports $J^\pi = (0^+,1^+)$ (see Fig. 2), and the angular distribution of the γ ray from this level is isotropic. Consequently, we assign this level as $J^\pi = 0^+$.

2355.7-keV level: The γ-ray excitation function measurement allowed us to improve our knowledge of the decay of this 3-phonon state (2_{3ph}^+) to the 2-phonon multiplet, because a transition of 624.5 keV from this state to the 0^+ state at 1731 keV is observed [17].

2477.5-keV level: This level was observed by Blasi et al. [7] and Bertschy et al. [12]. Based on its excitation function, the 2477.8-keV transition, which decays to the ground state, was also placed as in Ref. [12]. Moreover, the level decays by additional transitions of 1819.8 keV ($2477.5 \rightarrow 657.7(2_{1ph}^+)$) and 746.2 keV ($2477.5 \rightarrow 1731.3(0_{2ph}^+)$). From the E2 multipolarity of the latter transition, we assign this level as $J^\pi = 2^+$ in agreement with Ref. [7]. Bertschy et al. [12] observed a 1001-keV transition from this level, but this transition is placed in Ref. [20] as depopulating the 3078-keV level. The lower placement is supported by the γ-ray excitation function of this transition for which the observed threshold is about 2500 keV. Therefore, this transition was retained as depopulating the 2477-keV level.

2481.6-keV level: This level is known to be depopulated by a transition of 1823.9 keV to the 657.7-keV level

(2^+_{1ph}). From the excitation function data, a 402.8-keV transition is found which connects this level to the 2078.9-keV level (3^-_{oct}). This state was assigned by Araddad et al. [13] as $J^\pi = 3^-, 2^+$. As shown in Fig. 2, the excitation function favours a spin J=(2). Moreover, the multipolarities of the decaying transitions indicate positive parity. Consequently, we adopt the assignment $J^\pi = (2^+)$ for this level.

2633.1-keV level: A new transition of 1157.2 keV (2633.1 → 1475.8(2^+_{2ph})) from this level is observed. Araddad et al. [13] proposed $J^\pi = (3^+), 4^+$, Blasi et al.

[7] assigned $J^\pi = 2^+$, and Bertschy et al. [12] proposed $J^\pi = 2^+, (3^+)$. The excitation function of the 1975.4-keV transition, which was known to de-excite this level, supports a spin and parity of $J^\pi = (3^+)$. Combining all these data, we adopt $J^\pi = (2^+, 3^+)$

2649.5-keV level: The level energy has been improved from 2649.15(24) keV (from Ref. [20]) to 2649.54(11) keV. This state was assigned according to Ref. [20] as $J^\pi = (0^-, 1^-)$. Moreover, it decays only to 0^+ states and the excitation function favours a spin of J = 1. We adopt the spin and parity of $J^\pi = (1^-)$ for this level.

TABLE III. Observed transitions and levels (See text).

E_x [keV][a]	$J^\pi_{adopted}$	J^π_f	E_γ [keV]	δ	Mult.	B.R.[b]	$J^\pi_{prev.}$
0.0	0^+						0^+
657.765(9)	2^+	0^+	657.765(9)		E2	1.000	2^+
1473.053(30)	0^+	2^+	815.31(3)			1.000	0^+
1475.785(19)	2^+	2^+	818.03(4)	$1.49^{+0.28}_{-0.40}$	M1+E2	0.624(4)	2^+
		0^+	1475.75(4)		E2	0.376(4)	
1542.467(25)	4^+	2^+	884.68(4)		E2	1.000	4^+
1731.284(32)	0^+	2^+	255.55(5)			0.088(3)	0^+
		2^+	1073.62(7)			0.912(3)	
1783.529(32)	2^+	0^+	310.53(12)		E2	0.003(1)	2^+
		2^+	1125.71(2)	$0.13^{+0.03}_{-0.02}$	M1+E2	0.756(2)	
		0^+	1783.62(7)		E2	0.240(2)	
2078.853(30)	3^-	2^+	295.62(9)			0.032(6)	3^-
		2^+	603.10(4)		E1	0.127(3)	
		2^+	1421.08(4)		E1	0.841(3)	
2078.878(30)	0^+	2^+	295.62(9)			0.758(4)	0^+
		2^+	1421.08(4)			0.242(4)	
2162.798(26)	3^+	4^+	620.33(4)	$-0.46^{+0.07}_{-0.06}$	M1+E2	0.165(5)	3^+
		2^+	687.02(4)	$-1.66^{+0.09}_{-0.08}$	M1+E2	0.247(7)	
		2^+	1505.03(4)	$-1.52^{+0.11}_{-0.14}$	M1+E2	0.587(9)	
2220.083(31)	4^+	4^+	677.62(4)	-0.41(2)	M1+E2	0.638(8)	4^+
		2^+	744.29(4)		E2	0.281(7)	
		2^+	1562.33(8)		E2	0.081(3)	
2250.564(35)	4^+	2^+	467.08(6)		E2	0.081(4)	4^+
		4^+	708.10(4)	$0.13^{+0.04}_{-0.03}$	M1+E2	0.817(6)	
		2^+	774.88(20)		E2	0.033(4)	
		2^+	1592.79(10)		E2	0.069(4)	
2287.425(61)	2^+	2^+	1629.66(55)	-0.01(2)		1.000	2^+
2332.045(71)	0^+	2^+	1674.28(7)			1.000	$(0^+, 1^+, 2^+)$
2355.717(57)	2^+	0^+	624.47(9)		E2	0.030(2)	2^+
		2^+	1697.93(7)	-0.07(2)	M1+E2	0.970(2)	
2433.206(33)	3^+	2^+	957.41(4)			0.641(7)	3^+
		2^+	1775.48(5)			0.359(7)	
2477.544(98)	2^+	0^+	746.19(17)		E2	0.164(7)	$1^+, 2^+$
		2^+	1001.65(17)		(E2)	0.394(6)	
		2^+	1819.82(24)			0.080(4)	
		0^+	2477.81(22)		E2	0.360(7)	
2480.019(74)	6^+	4^+	937.55(7)		E2	1.000	6^+
2481.644(121)	(2^+)	3^-	402.84(17)		E1	0.119(12)	$3^-, 2^{+c)}$
		2^+	1823.83(17)	$-0.91^{+0.09}_{-0.12}$	M1+E2	0.881(12)	
2539.690(47)	5^-	3^-	460.83(17)		(E2)	0.030(4)	5^-
		4^+	997.22(4)		E1	0.970(4)	

TABLE III. Observed transitions and levels (See text) [cont].

E_x [keV][a]	$J^\pi_{adopted}$	J^π_f	E_γ [keV]	δ	Mult.	B.R.[b]	$J^\pi_{prev.}$
2561.278(39)	4^+	4^+	1018.86(8)	$-0.49^{+0.16}_{-0.19}$	M1+E2	0.136(6)	4^+
		2^+	1085.49(5)		E2	0.683(8)	
		2^+	1903.48(7)		E2	0.182(7)	
2633.070(121)	$(2^+,3^+)$	2^+	1157.24(17)			0.030(4)	$2^{+d)},(3^+),4^{+c)}$
		2^+	1975.35(17)		(E2)	0.970(4)	
2649.537(108)	(1^-)	0^+	1176.60(8)			0.094(4)	$(0^-,1^-)$
		0^+	2649.39(9)			0.906(4)	
2659.955(60)	5^-	4^+	409.51(14)			0.078(10)	5^-
		4^+	1117.46(6)			0.922(10)	
2661.988(74)	0^+	2^+	1186.13(5)			0.535(7)	0^+
		2^+	2004.33(6)			0.465(7)	
2705.589(65)	4^+	4^+	1163.12(6)		E2	1.000	$4^{(-)}$
2707.443(51)	4^+	3^+	544.67(6)		(M1+E2)	0.307(9)	(4^+)
		4^+	1164.94(7)		DP	0.693(9)	
2758.173(71)	$(2^+,3^+)$	2^+	1282.28(7)			0.725(6)	$(1^+,2^+,3^+)$
		2^+	2100.57(9)			0.275(6)	
2787.375(71)	(2^+)	2^+	2129.61(7)		M1+E2	1.000	$1^+,2^+$
2793.400(56)	(4^+)	4^+	573.23(9)			0.311(15)	(4^+)
		3^+	630.59(9)			0.336(17)	
		4^+	1251.02(9)			0.353(19)	
2842.688(64)	5^-	5^-	182.83(60)[e]				(5^-)
		3^+	409.51(14)			0.081(27)	
		4^+	1300.21(7)		(E1)	0.922(27)	
2868.998(43)	(2^+)	2^+	1085.49(5)		E2	0.354(5)	$1^+,2^+$
		2^+	2211.27(7)			0.646(5)	
2917.590(61)	$2^+,3^-$	4^+	356.40(10)			0.120(14)	$2^+,3^-$
		2^+	1441.85(12)			0.480(33)	
		2^+	2259.73(9)			0.400(26)	
2926.723(79)	5^+	3^+	763.95(9)			0.576(26)	5^+
		4^+	1384.19(14)			0.424(26)	
2975.164(90)	2^+	2^+	2317.40(9)			1.000	2^+
2984.501(94)	5^-	3^-	905.71(7)			0.445(21)	5^-
		4^+	1441.85(12)			0.555(21)	
2993.615(171)	(0^+) [f]	2^+	1517.83(17)			1.000	$0^+,3^+,4^{+d)}$
2994.089(84)	$(3^+,4^+)$[f]	4^+	1451.62(8)			1.000	$0^+,3^+,4^{+d)}$
3042.841(83)	(2^+)	2^+	1566.92(10)			0.158(8)	
		2^+	2385.22(11)			0.352(10)	
		0^+	3042.98(28)			0.491(10)	

[a] Energy calculated using a least-square procedure involving all transitions placed in the present level scheme.

[b] From this experiment.

[c] From Ref. [13].

[d] From Ref. [7].

[e] This transition was not observed in our experiments due to the attenuation of low-energy γ rays in the sample. We have accepted the value given in Ref. [5].

[f] See discussion in the text.

2707.4-keV level: This level was assigned by Kern et al. [5] in their study of the ^{108}Pd$(\alpha,2n)^{110}$Cd reaction and Blasi et al. [7] as $J^\pi = 4^+$, but this assignment is listed as uncertain in Ref. [20]. The excitation function data also support a spin of 4 for this level. As shown in Fig. 6, the angular distribution analysis of the 1164-keV transition favours also a spin of 4. Therefore, we confirm $J^\pi = 4^+$ for this level.

2758.2-keV level: This level is assigned in Ref. [20] as $J^\pi = 1^+,2^+,3^+$. Araddad et al. [13] observed a spin and parity of $J^\pi = 3^+$ and Blasi et al. [7] assigned this level as $J^\pi = 1^+,2^+$. As one can see in Fig. 6, the angular distribution of the 1282-keV transition seems to favour $J^\pi = 2^+$ while the 2100-keV transition favors $J^\pi = 3^+$. The multipole mixing ratios of the transitions support positive parity, so we adopt for this level the assignment

of $J^\pi = (2^+, 3^+)$.

2787.3-keV level: This level was assigned by Bertschy et al. [12] and Blasi et al. [7] as $J^\pi = 1^+, 2^+$. The excitation function favours $J^\pi = (2^+)$ for this level.

2842.7-keV level: This level was known to decay by transitions of 182.8, 409.5 and 1300.2 keV. The spin and parity were proposed to be $J^\pi = 5^-$ by Kern et al. [5], but it is listed as uncertain in Ref. [20]. From the excitation function data and the multipole character of the 1300-keV transition, we also assign this level as $J^\pi = 5^-$.

2869.0-keV level: The spin of this level was assigned by Bertschy et al. [12] and Blasi et al. [7] as $J^\pi = 2^+$, and according to Ref. [20] it has $J^\pi = 1^+, 2^+$. From the excitation function data, this level seems to have a spin and parity of $J^\pi = (2^+)$, which is the value we adopt.

2984.5-keV level: This level was observed by Kern et al. [5] to decay by only a 1441.8-keV transition. A new transition of 905.7 keV ($2984.5 \rightarrow 2078.8(3^-_{oct})$) has been placed. This γ ray was also observed by Kern et al. [5], but was not placed in the level scheme. From the excitation function data, the spin and parity of $J^\pi = 5^-$, assigned by Kern et al. [5] are supported.

2994-keV doublet: Blasi et al. [7] observed an unresolved doublet at this energy. New transitions of 1451.6 and 1517.8 keV from the decay of these levels have been added. As the 1451.6-keV transition decays to the state at 1542 keV with $J^\pi = 4^+$, we can support the $J^\pi = (3^+, 4^+)$ assignment proposed by Blasi et al. [7]. The corresponding excitation energy would be 2994.0 keV. The second transition has an energy of 1517.8 keV.

This γ ray is placed as a transition depopulating the second member of the doublet at an excitation energy of 2993.4 keV. According to Ref. [7], the second level has $J^\pi = (0^+)$.

3042.8-keV level: This new level decays by transitions of 1566.9, 2385.2 and 3043.0 keV, but no multipolarities could be extracted for these transitions from the present data. The γ-ray excitation functions of the lines seem to indicate a spin and parity of $J^\pi = (2^+)$, which is in agreement with the decay pattern of this new level.

IV. COMPARISON WITH THEORY

We limit ourselves here to the states below 2.55 MeV. This limitation is due to uncertain spin assignments of higher-lying states and the clear non-collective decay of other states, e.g., the 2561-keV state.

A. Positive-parity states

In Table IV, the experimental B(E2) values for transitions depopulating the states of interest are compared with theoretical predictions. Only states for which the spin-parity assignments have been unambiguously determined are given. In Ref. [17], several theoretical predictions available in the literature were compared with our data for the decay of the 3-phonon states.

TABLE IV. Comparison of experimental and theoretical B(E2) values for states in ^{110}Cd.

Transition	E_γ [keV]	Exp.[W.u.]	Theory [W.u.] U(5)-O(6)		IBM-2 [28]
			Lehmann et al. [25]	This work	
$2^+_{1,intr} \rightarrow 0^+_{intr}$ [a]	310.5	23^{+27}_{-18}	15	52	44
$2^+_{1,intr} \rightarrow 2^+_{1ph}$ [a]	1125.7	$0.16^{+0.12}_{-0.09}$	0.23	0.23	0.005
$2^+_{1,intr} \rightarrow 0^+_{1ph}$ [a]	1783.5	0.30(10)	0.08	0.06	0.34
$3^+_{3ph} \rightarrow 4^+_{2ph}$	620.3	7^{+6}_{-4}	16	17	15
$3^+_{3ph} \rightarrow 2^+_{2ph}$	687.0	25^{+13}_{-11}	39	43	43
$3^+_{3ph} \rightarrow 2^+_{1ph}$	1505.0	$1.1^{+0.6}_{-0.5}$	0.002	0.002	0.4
$4^+_{3ph} \rightarrow 4^+_{2ph}$	677.6	17^{+8}_{-6}	26	29	23
$4^+_{3ph} \rightarrow 2^+_{2ph}$	744.3	33(11)	29	32	32
$4^+_{3ph} \rightarrow 2^+_{1ph}$	1562.3	0.23(8)	0.002	0.002	0.100
$4^+_{intr} \rightarrow 2^+_{intr.}$	467.1	109^{+62}_{-53}	27	113	124
$4^+_{intr} \rightarrow 4^+_{2ph}$	708.1	2^{+4}_{-1}	2	2	1
$4^+_{intr} \rightarrow 2^+_{2ph}$	774.9	3^{+3}_{-1}	0.30	0.30	0.02
$4^+_{intr} \rightarrow 2^+_{1ph}$	1592.8	$0.20^{+0.27}_{-0.10}$	0.0003	0.05	0.22
$2^+_{2,intr} \rightarrow 2^+_{1ph}$ [b]	1629.7	< 0.004	0.62	0.06	0.005
$2^+_{3ph} \rightarrow 0^+_{2ph}$	624.5	16(5)	18	26	19
$2^+_{3ph} \rightarrow 2^+_{1ph}$	1697.9	$0.02^{+0.02}_{-0.01}$	0.02	0.02	0.08
$6^+_{3ph} \rightarrow 4^+_{2ph}$	937.5	62^{+18}_{-17}	56	61	59
$5^-_{oct} \rightarrow 3^-_{oct}$	460.8	48^{+27}_{-22}	32	32	–

[a] First 2^+ intruder state at $E_x = 1783.5$ MeV
[b] Second 2^+ intruder state at $E_x = 2287.5$ MeV

The influence of two-particle, four-hole intruder configurations, which leads to a second collective structure, is studied in the present work. In order to take account of the shape coexistence [24] in ^{110}Cd, which manifests itself at an energy near 1.5 MeV [5], models incorporating this feature are considered. The U(5)-O(6) model of Lehmann and Jolie [25] describes the normal states interacting with the intruder states by mixing the U(5) dynamic symmetry for the normal states and the O(6) limit for the intruder states. This model is very simple and has a reduced set of parameters.

Before comparing the U(5)-O(6) model and the experimental data, one should consider two facts. In Ref. [25], few absolute transition rates involving intruder states were used in the fit, and these involved analytic expressions between states that were assumed to interact only via two-level mixing. In order to include all mixings, numerical calculations with the code OCTUPOLE [26] were performed. Using the parameters of the U(5)-O(6) model given in Ref. [25], the numerical results given in Table IV (fourth column) are obtained.

In order to improve this model, we consider the electric quadrupole transition operator given by

$$T^{(E2)} = e_2[\delta_{N,N'}T_{U5} + \delta_{N+2,N'}\epsilon_{rel}T_{O6}], \qquad (2)$$

with the operators

$$T_{U5} = e_2([s^\dagger \tilde{d} + d^\dagger s]_\mu^{(2)} + \chi[d^\dagger \tilde{d}]_\mu^{(2)}), \qquad (3)$$

and

$$T_{O6} = e_2([s^\dagger \tilde{d} + d^\dagger s]_\mu^{(2)}), \qquad (4)$$

In Eq. 2, e_2 is the effective charge and N' is the number of bosons. Each operator is applied to the respective states in each configuration. The parameter ϵ_{rel} weights the O(6) operator relative to the U(5) transition operator. In Ref. [25], e_2=0.11[eb], χ=-2.7 and $\epsilon_{rel} = 0.48$ were obtained. In order to remove the discrepancy in the description of the transition probabilities between the intruder states, in particular for the $4_{intr}^+ \rightarrow 2_{1,intr}^+$ transition, the calculation was improved by changing the ϵ_{rel} parameter from 0.48 to 1.0 in Eq. 2. As can be observed in the fifth column of Table IV, this parameter value yields better agreement with the experimental results. This value for ϵ_{rel} is also more in line with the results obtained for the other Cd isotopes [25].

A more sophisticated calculation can be performed using the IBM-2 approach. In this model, neutron and proton bosons are considered. This distinction allows one to discern the effects due to the proton 2p-4h configurations in more detail. Notably, it predicts the energy of these states on a semi-microscopic basis (see Ref. [27]), but at the cost of a greatly increased parameter set. Using this IBM-2 approach, calculations were performed by M. Délèze et al. [28] for ^{110,112,114}Cd nearly a decade ago. These calculations were extensively tested for ^{112}Cd in

Ref. [29,30] and proved to be reliable. They are compared to our data in the last column of Table IV. Once more, excellent agreement is obtained. If we examine the fourth and fifth columns of Table IV, we see that changing the ϵ_{rel} from 0.48 to 1.00 in the U(5)-O(6) model yields results that are very close to the IBM-2 results. This can be illustrated by the presence of coherent mixing of intruder and three-phonon states as described in [31]. If all transitions decaying from the 3_{3ph}^+, 4_{3ph}^+ and 6_{3ph}^+ states to the 2^+ and 4^+ two-phonon states are summed for each state, the common O(5) symmetry imposes equal mixing amplitudes for these two and three-phonon states and hence the same sum for each state. This is not the case for the 2_{3ph}^+ state which has another O(5) quantum number. Inspection of Table IV shows that indeed the summed decay probabilities are nearly equal in the U(5)-O(6) model. In Table V these values are compared to those in the IBM-2 and the experimental sums. One notices that the IBM-2 values are very close to each other. Unfortunately, the experimental sums still have errors that are too large to permit a definite experimental confirmation about the observation of this coherent mixing.

For both models, the experimental and theoretical level energies are in good agreement, as is illustrated in Fig. 7, in which level energies and B(E2) values calculated using the U(5)-O(6) model are compared with the experimental results. More details concerning the description of the models and the Hamiltonians can be found in Ref. [32].

Table VI shows a comparison between the experimental and theoretical B(M1) values for the transitions of Table IV with mixed multipole character. They are compared to the theoretical IBM-2 values from Ref. [28]. Note that all M1 transitions are strictly forbidden in the U(5)-O(6) model. We remark as for the B(E2) values that there is good agreement between theory and experiment and that all observed transition probabilities are quite small. One can also now clearly exclude the mixed symmetry character of the third experimental 2^+ state which in the original calculation of Ref. [28] was associated with the theoretical lowest mixed-symmetry state. Note that at that time there was an additional experimental 2^+ state at 1809.5 keV, which was shown not to exist by Bertschy et al. [12]. Although the presence in the theory of a low-lying mixed-symmetry state does not strongly affect the other states, one notices its presence in the overpredicted B(M1;$2_{intr}^+ \rightarrow 2_{1ph}^+$) value.

TABLE V. The sum of $B(E2; J_{3ph}^+ \rightarrow J_{2ph}^+)$ for the three-phonon states which mix coherently in the U(5)-O(6) model, is compared to the IBM-2 and experimental sums.

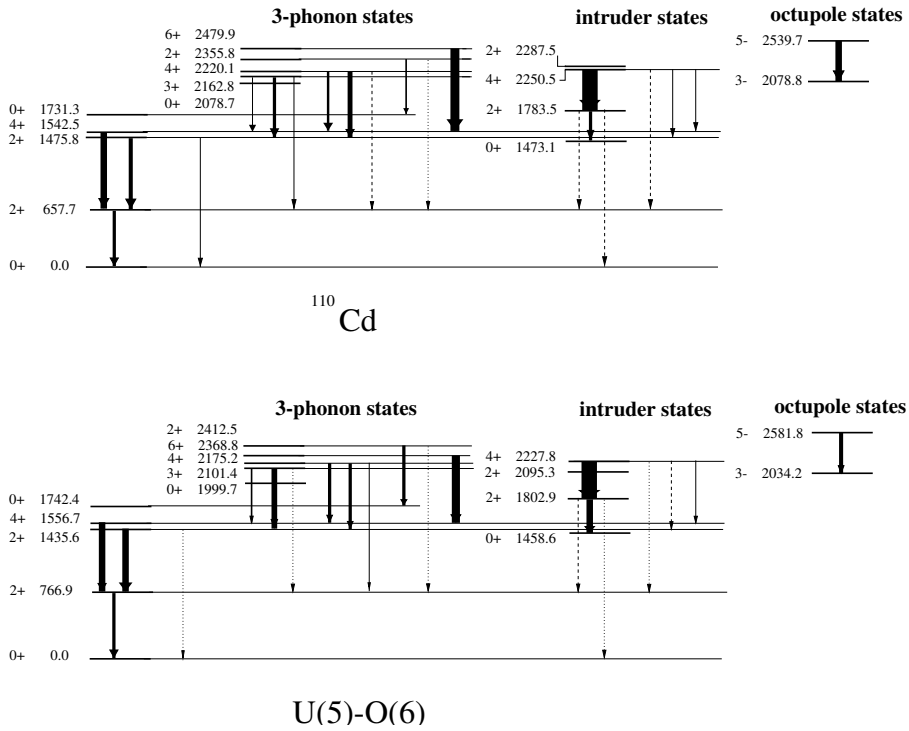| J^π	U(5)-O(6)	IBM-2	EXP
3_{3ph}^+	61	58	32(14)
4_{3ph}^+	61	55	50(14)
6_{3ph}^+	61	59	62(18)

FIG. 7. Comparison between the experimental and theoretical level energies and B(E2) values for the U(5)-O(6) model (see text). The widths of the arrows correspond to the magnitude of the experimental and theoretical B(E2) values.

In this context it is worth noting that the predicted $B(M1;2^+_{ms} \to 2^+_{1ph})$ value equals 0.38 μ^2_n, which is clearly not observed for any 2^+ state, including the state at 2.355 MeV proposed as a possible candidate in Ref. [12]. This absence of a mixed-symmetry state, combined with the relatively small B(M1) values observed in ^{112}Cd [33] casts some doubt on the existence of a low-lying mixed-symmetry state in ^{112}Cd. While the magnetic dipole decay of the 3^+ and 2^+ states are well described in the model, strong underprediction of the decay of the two 4^+ states is observed. A possible explanation could be that these states are partially mixed with a two quasi-particle state, although the good agreement of their electric quadrupole decay with experiment seems to contradict this.

TABLE VI. Comparison of experimental and theoretical B(M1) values for states in ^{110}Cd.

Transition	E_γ [keV]	$B(M1)_{Exp.}[\mu^2_n]$	Theory $[\mu^2_n]$
$2^+_{1,intr} \to 2^+_{1ph}$	1125.7	0.026(8)	0.007
$3^+_{3ph} \to 4^+_{2ph}$	620.3	0.027(11)	0.021
$3^+_{3ph} \to 2^+_{2ph}$	687.0	0.010(4)	0.018
$3^+_{3ph} \to 2^+_{1ph}$	1505.0	0.002(1)	0.001
$4^+_{3ph} \to 4^+_{2ph}$	677.6	0.103(32)	0.003
$4^+_{intr} \to 4^+_{2ph}$	708.1	0.148^{+73}_{-68}	0.001
$2^+_{2,intr} \to 2^+_{1ph}$	1629.7	0.031(6)	0.007
$2^+_{3ph} \to 2^+_{1ph}$	1697.9	0.022(5)	0.021

B. Negative parity states

The OCTUPOLE code also describes the negative-parity states based on the octupole vibration, using the *spdf* IBM-1 hamiltonian, described in detail in [34]. Adopting the parameters describing the negative-parity states obtained in [28] for ^{112}Cd excellent results are obtained. The theoretical octupole vibration is calculated at 2034 keV and the 5^- member of the quadrupole-octupole coupled (QOC) states at 2581 keV. Besides the good agreement in excitation energy, the theory also nicely reproduces the observed collective quadrupole transition between these states (see Table IV), confirming the QOC character of the 5^- state at 2539.7 keV.

TABLE VII. Comparison of experimental and theoretical B(E1) values for states in ^{110}Cd.

Transition	E_γ [keV]	$B(E1)_{Exp.}$ [mW.u.]	spdf-IBM-1 [mW.u.]
$3^-_{oct} \to 2^+_{1ph}$	1421.1	0.2(1)	0.4
$3^-_{oct} \to 2^+_{2ph}$	603.1	0.4(1)	0.03
$3^-_{oct} \to 2^+_{1,intr}$	295.6	0.8^{+4}_{-3}	0.0002
$5^-_{oct} \to 4^+_{2ph}$	997.2	2.6(2)	0.7

Table VII compares the experimental B(E1) values with the ones obtained with the *spdf* IBM-1 calculation using the transition operator described in [34]. In general the theoretical values are within the order of magnitude of the experimental values, except for the decay of the octupole state to the $2^+_{1,intr}$ which is greatly underestimated. While the low transition probability is easily understood from the theoretical point of view, the large experimental value seems to confirm the insensitivity of B(E1) transitions to the nature of states in this mass region, as discussed by Garrett et al. [35].

V. CONCLUSION

The primary goal of this work was to examine the character of the states in ^{110}Cd in the region up to 3 MeV. Toward this end, the (n,n'γ) reaction has been used to perform a set of measurements consisting of γ-ray excitation functions and angular distributions. The former allowed us to add 10 new transitions and one new level to the level scheme of ^{110}Cd. The latter permitted the extraction of lifetimes of 16 excited states, of which 12 were previously unknown, and the determination of the multipole-mixing ratios. At the same time, we were able to determine the B(E2,$2^+_{1,intr} \to 0^+_{intr}$) value. Unfortunately, the lifetime of the 0^+_{intr} state at 1473.1 keV was too long to be determined by this method. As expected, the transition $4^+_{intr} \to 2^+_{1,intr}$ is very collective. As discussed in Ref. [17], we see that the 3-phonon states have transitions to the 2-phonon states which are clearly collective.

Our data also permitted us to identify the 5^- member of the quadrupole-octupole coupled state via the collective electric quadrupole transition to the octupole state and to exclude the presence of a low-lying mixed symmetry state.

To study the intruder states, the data were compared to calculations using IBM-2 with configuration mixing and the U(5)-O(6) model. Both models yield good agreement with the experimental results with a slight preference for IBM-2. However, in view of the very reduced set of parameters and the use of dynamical symmetries in the U(5)-O(6) model, ^{110}Cd should be considered as an excellent example of a nucleus described by this model. Therefore, this nucleus is not only a good vibrational nucleus but it also illustrates clearly the coexistence of two dynamical symmetries in a single nucleus and the influence of the common O(5) subgroup [31] needed to explain the $2^+_{3ph} \to 0^+_{2ph}$ decay [17]. This conclusion is not only of importance in the context of the U(5)-O(6) model [25], but more generally for particle-hole symmetries as discussed in Ref. [36–39].

[1] G. Scharff-Goldhaber and J. Weneser, Phys. Rev. **98**, 212 (1955).
[2] A. Arima and F. Iachello, Ann. of Phys. **99**, 253 (1976).
[3] R.A. Meyer and L. Peker, Z. Phys. **A283**, 379 (1977).
[4] K. Heyde, P. Van Isaker, M. Waroquier and G. Wenes, Phys. Ref. **C25**, 3160 (1982).
[5] J. Kern, A. Bruder, S. Drissi, V.A. Ionescu, and D. Kusnezov, Nucl. Phys. **A512**, 1 (1990).
[6] B.L. Cohen, R. Patell, A. Prakash, and E.J. Schneid, Phys. Rev. **135**, B383 (1964).
[7] N. Blasi, S. Micheletti, M. Pignanelli, R. De Leo, R. Hertenberger, M. Bisemberger, D. Hofer, H. Kader, P. Schiemenz, and G. Graw, Nucl. Phys. **A536**, 1 (1992).
[8] M. Pignanelli, N. Blasi, S. Micheletti, R. De Leo, M.A. Hofstee, J.M. Schippers, S.Y. van der Werf, and M.N. Harakeh, Nucl. Phys. **A519**, 567, (1990).
[9] J. Kumpulainen, R. Julin, J. Kantele, A. Passoja, W.H. Trzaska, E. Verho, J. Väärämäki, C. Cutoiu, and M. Ivascu, Phys.Rev. **C45**, 640 (1992).
[10] Y. Kawase, K. Okano, S. Uehara, and T. Hayashi, Nucl. Phys. **A193**, 204 (1972).
[11] L.L. Kiang, P.K. Teng, G.C. Kiang, W.S. Chang, and P.J. Tu , J. Phys. Soc. Jpn. **62**, 888 (1993).
[12] M. Bertschy, S. Drissi, P.E. Garrett, J. Jolie, J. Kern, S.J. Mannanal, J.P. Vorlet, N. Warr, and J. Suhonen, Phys. Rev. **C51**, 103 (1995);**C52**, 1148 (1995).
[13] S.Yu. Araddad, A.M. Demidov, M.M. Dyufani, S.M. Zlitni, V.A. Kurkin, I.V. Mikhailov, D.M. Rateb, and S.M. Sergiwa, Yad. Fiz. **52**, 3 (1990); Sov. J. Nucl. Phys. **52**, 1 (1990).
[14] A.M. Demidov, S.M. Zlitni, V.A. Kurkin, J.M. Rateb, S.M. Sergiva, and A.M. Shermit, Bull. Rus. Acad. Sci. Phys. **56**, 8 (1992).
[15] M. Piiparinen *et al.*, Nucl. Phys. **A565**, 671 (1993).
[16] Yu. N. Lobach, A.D. Efimov, and A.A. Pasternak, Eur. Phys. J. **A6**, 131 (1999).
[17] F. Corminboeuf, T.B. Brown, L. Genilloud, C.D. Hannant, J. Jolie, J. Kern, N. Warr, and S.W. Yates, Phys. Rev. Lett. **84**, 4060 (2000).
[18] P.E. Garrett, N. Warr, and S.W. Yates, J. Res. Natl. Inst. Stand. Technol. **105**, 141 (2000).
[19] E. Sheldon and V.C. Rogers, Comput. Phys. Commun. **6**, 99 (1973).
[20] D. De Frenne, Nucl. Data Sheets **67**, 809 (1992).
[21] K.B. Winterbon, Nucl. Phys. **A246**, 293 (1975).
[22] T. Belgya, G. Molnár, and S.W. Yates, Nucl. Phys **A607**, 43 (1996).
[23] D.G. Sarantites, N.R. Johnson, and H.W. Boyd, Nucl. Phys. **A138**, 115 (1969).
[24] J.L. Wood, K. Heyde, W. Nazarewiecz, M. Huyse, and P. Van Duppen, Phys. Rep. **215** 101, (1992), and references therein.
[25] H. Lehmann and J. Jolie, Nucl. Phys. **A588**, 623 (1995).
[26] D. Kusnezov, the computer code OCTUPOLE (1987), unpublished.

[27] K. Heyde, J. Jolie, J. Moreau, J. Ryckebusch, M. Waroquier, P. Van Duppen, M. Huyse, and J.L. Wood, Nucl. Phys. **A466**, 189 (1987).

[28] M. Délèze, S. Drissi, J. Kern, P.A. Tercier, J.P. Vorlet, J. Rikovska, T. Otsuka, S. Judge, and A. Williams, Nucl. Phys. **A551**, 269 (1993).

[29] H. Lehmann, P.E. Garrett, J. Jolie, C.A. McGrath, Minfang Yeh, and S.W. Yates, Phys. Lett. **B387**, 259 (1996).

[30] S. Drissi *et al.*, Nucl. Phys. **A614**, 137 (1997).

[31] J. Jolie and H. Lehmann, Phys. Lett. **B342**, 1 (1995).

[32] N. Warr, S. Drissi, P.E. Garrett, J. Jolie, J. Kern, H. Lehmann, S.J. Mannanal, and J.-P. Vorlet, Nucl. Phys. **A636**, 379 (1998).

[33] P.E. Garrett, H. Lehmann, C.A. McGrath, Minfang Yeh, and S.W. Yates, Phys. Rev. **C54**, 2259 (1996).

[34] H. Lehmann et al., Phys. Rev. **C60**, 024308 (1999).

[35] P.E. Garrett, H. Lehmann, J. Jolie, C.A. McGrath, Minfang Yeh, and S.W. Yates, Phys. Rev. **C59**, 2455 (1999).

[36] C. De Coster, K. Heyde, B. Decroix, P. Van Isaker, J. Jolie, H. Lehmann, and J.L. Wood, Nucl. Phys. **A600**, 251 (1996).

[37] H. Lehmann, J. Jolie, C. De Coster, B. Decroix, K. Heyde, and J.L. Wood, Nucl. Phys. **A621**, 767 (1997).

[38] C. De Coster, B. Decroix, K. Heyde, J.L. Wood, J. Jolie, and H. Lehmann, Nucl. Phys. **A621**, 802 (1997).

[39] C. De Coster, B. Decroix, K. Heyde, J. Jolie, H. Lehmann, and J.L. Wood, Nucl. Phys. **A651**, 31 (1999).

Study of ^{114}Te by the ^{112}Sn(α,2nγ) reaction. *

F. Corminboeuf [a], L. Genilloud [a], S. Drissi [a], J. Jolie [a,b],
J. Kern [a], H. Lehmann [a], N. Warr [a,b,c].

[a]*Institut de Physique, Université de Fribourg, CH-1700 Fribourg, Switzerland*

[b]*Institut für Kernphysik, Universität zu Köln, Zülpicher Strasse 77, D-50937 Köln, Germany*

[c]*University of Kentucky, Lexington, KY 40506-0055, USA*

Abstract

The ^{114}Te nuclear levels were populated using in-beam γ-ray spectroscopy. On the basis of the $\gamma\gamma$-coincidences, a level scheme was constructed with over 50 levels and it was possible to place 74 transitions. The level scheme was extended by 16 new levels. Excitation-function and angular-distribution measurements yielded spin assignments for a large number of the levels. The experimental results were compared to the U(5) dynamical symmetry calculation of the Interacting Boson Model, the broken pair model and the Quasiparticle Phonon Nuclear Model. This comparison allows us to show that ^{114}Te mimics a good U(5) nucleus.

PACS: 21.10.Re,21.60.Fw,23.20.Lv,27.60.+j

Key words: NUCLEAR REACTION: ^{112}Sn(α,2n), $E = 24.0, 28.0, 37.0, 43.0$ MeV; Measured E_γ, $I_\gamma(\theta)$, $\gamma\gamma$-coin. ^{114}Te deduced levels, J, π; enriched targets; Compton-suppressed Ge detectors.

1 Introduction

During the last few years the nucleus ^{110}Cd has been intensively studied. This nucleus exhibits a shape coexistence structure due to 4h-2p excitations across the Z=50 shell, which can be described as the so-called intruder states [1]. In the context of the concept of particle-hole invariance formulated in terms of intruder spin [2,3], ^{114}Te can be expected to show an excitation pattern similar

* Work supported by the Swiss National Science Foundation

to that of ^{110}Cd, but based on 2p excitations instead of 2h ones, and may thus also exhibit a level structure characteristic of the U(5) dynamical symmetry.

As mentioned in Ref. [4] there are four criteria to test whether a nucleus is vibrational or not. They are: a ratio $R_{4/2}$ equal to 2, a nearly degenerate two-phonon triplet, the levels energies follow the analytical expression for the U(5) limit of the IBM, electric quadrupole transitions between states differing by more than one phonon are strongly hindered. Despite the $R_{4/2}$ ratio of 2.09, Ref. [4] did not consider ^{114}Te as a good vibrational nucleus due to the lack of experimental data [5]. According to the present work it seems that this nucleus mimics the U(5) dynamical symmetry not only because the ratio $R_{4/2}$ is near to the harmonic value of 2 but also because it fullfills three out of the four criteria. Nevertheless the lst criterion, the absolute transition rates, is badly violated.

Unlike ^{110}Cd, ^{114}Te has not been extensively studied. Only a few experimental works exist. ^{114}Te was previously studied only by few reactions and, notably at low spin, knowledge on the structure of ^{114}Te was lacking. The results are compiled in Ref. [6]. We can mention the works of Lonnroth et al. [7] in their study of the ^{114}Sn(^{3}He,nγ)^{114}Te reaction, Zimmermann [8] in his study from ^{114}I β decay, Moon et al. [9] using the ^{89}Y(^{28}Si,p2n) and ^{89}Y(^{29}Si,p3n) reactions and Janzen [10] in his study of the ^{94}Mo(^{23}Na,p2nγ)^{114}Te reaction.

With the aim of elucidating the structure of ^{114}Te and to test the validity of the intruder-spin invariance, a set of in-beam measurements was performed using α particles accelerated with the Philips variable energy cyclotron at the Paul Scherrer Institute, Switzerland.

The experiments will be described in Section 2. The analysis and the resulting level scheme are presented in Section 3, including a discussion of the individual levels when there are differences with the tabulated ones [6]. The last section presents the comparison of our results with theoretical calculations in the framework of the Interacting Boson Model [11] (IBM), Broken-Pair Model [12] and Quasiparticle-phonon Model (QPNM) [13].

2   In-beam study using the ^{112}Sn(α,2n) reaction

The in-beam experiments consisted of the measurement of γ-ray excitation functions, γ-ray angular distributions and $\gamma\gamma$-coincidences. The excited nucleus ^{114}Te was produced by bombarding a 10 mg/cm^2 metallic target enriched in ^{112}Sn (98% isotopically enriched), with a beam of α particles from the Philips variable energy cyclotron at the Paul Scherrer Institute (PSI), Switzerland.
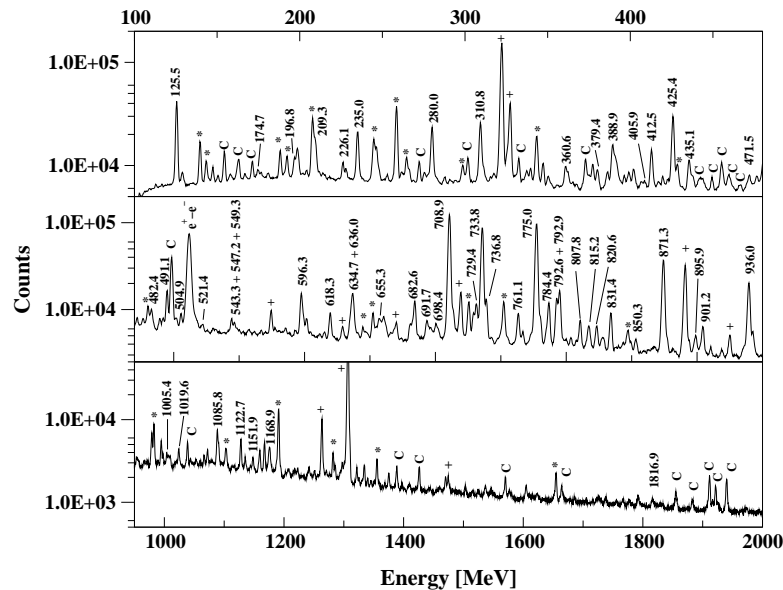
Fig. 1. Singles γ-ray spectrum acquired during the excitation-function measurement bombarding a ^{112}Sn target at an α-beam energy of 37 MeV. The prominent peaks from ^{114}Te are labelled by their energies. The peaks marked with * are γ lines belonging to ^{114}Sb, the ones with $^+$ to ^{114}Sn, and the ones belonging to other nuclei are marked with C.

2.1 Excitation functions

The excitation-function measurement was performed at beam energies of 24.6, 28.7, 36.7 and 42.7 MeV using a Compton-supression spectrometer [14] placed at 55° with respect to the beam-line direction. The central detector consisted of a 114 cm^3 intrinsic Ge detector with a FWHM resolution of 1.2 keV at 122 keV and 2.3 keV at 1.4 MeV. Relative efficiency was determined by the use of radioactive sources of ^{60}Co and ^{152}Eu placed at the target position. In order to provide accurate energy and intensity calibration of the γ rays, a spectrum was acquired using both the ^{152}Eu source and the in-beam reaction simultaneously. The γ-ray yields were normalized to an intensity of 1000 for the 708.9-keV transition at each bombarding energy.

The beam energy corresponding to the largest cross section for the $(\alpha,2n)$ reaction was found to be approximately 37 MeV. This energy was used for the γ-ray angular distribution and $\gamma\gamma$-coincidences measurements. A γ-ray spectrum acquired at an energy of 37 MeV is shown in Fig. 1

Table 1
Transitions properties belonging to ^{114}Te determined by our data.

E_γ [keV][a]	Ang. distr. coef				Observed multip. and mixing ratios			Assignments	Comments
	A_0 (I_γ)	A_2/A_0	A_4/A_0	Slope[b]	Previous work[c]	δ[d]	This work	$E_i - E_f$	
125.522(19)	94.7(20)			3.7(1)	(M1)			3279.3-3153.8	
174.676(40)	3.9(2)	0.632(60)	0.233(77)	15.4(3)		-1.25(16)	M1+E2	5434.6-5259.9	
196.777(23)	9.1(4)	-0.222(22)	0.037(31)	6.7(4)	M1,E2		M1+E2	3920.3-3723.5	
201.642(94)	1.1(2)			4.7(12)				3716.0-3514.3	
209.266(45)	15.4(13)	0.350(31)		5.1(6)		-0.010(9)	E1	3723.5-3514.3	
226.12(50)	8.7(2)	-0.619(25)	0.101(34)	12.6(5)		-0.20(2)	M1+E2	5259.9-5034.0	
234.992(16)	7.1(28)	0.133(13)		4.9(2)		0.22(1)	M1+E2	3514.3-3279.3	
279.993(15)	4.3(6)	0.050(17)		-3.4(11)		-0.15(2)	M1+E2	4834.7-4554.7	
310.776(62)	8.6(7)							1794.7-1483.9	
360.568(35)	14.3(6)	0.222(15)	-0.045(21)	4.6(5)			(E2)	3514.3-3153.8	
379.405(94)	6.5(11)							3658.6-3279.3	
388.891(24)	38.5(9)	0.305(16)	-0.030(22)	4.3(39)	M1+E2	-0.15(4)	M1+E2	2606.6-2217.7	
402.73(50)	4.8(11)	0.084(14)					M1+E2	1794.7-1391.5	
405.920(72)	7(6)	-0.689(46)	-0.089(15)	8.1(10)		-0.021(2)	E1	3920.3-3514.3	
412.474(23)	36.8(7)	0.264(10)		6.1(3)			E2	3920.3-3507.8	
425.413(16)	110.1(20)	-0.278(11)	-0.079(18)	10.6(3)	E1+M2	-0.009(1)	E1	3514.3-3088.9	
435.096(28)	27.9(7)	0.094(12)		7.1(6)			E2	5259.9-4824.8	
471.504(43)	9.3(4)							5781.7-5310.0	
482.388(40)	20.8(7)	0.471(30)	0.094(39)	6.7(5)		0.21(10)	M1+E2	3088.9-2606.6	

Table 1
Transitions properties belonging to ^{114}Te determined by our data [cont].

E_γ [keV][a]	Ang. distr. coef.			Slope[b]	Observed multip. and mixing ratios			Assignments	Comments
	A_0 (I_γ)	A_2/A_0	A_4/A_0		Previous work[c]	δ[d]	This work	$E_i - E_f$	
491.061(32)								4554.7-4063.7	e)
491.061(32)								2518.5-2027.4	e)
504.894(134)	13.8(11)	-0.578(50)	0.142(84)			0.39(3)	M1+E2	3658.6-3153.8	
517.392(98)	8.0(9)	0.089(49)		9.0(9)			(E1)	5034.0-4516.6	
521.43(50)	6.5(7)	-0.753(65)	0.17(12)	13.6(10)		2.84(51)	M1+E2	5781.7-5259.9	
543.28(50)	15.6(4)	0.119(16)	-0.063(24)	-2.4(6)	M1+E2	0.25(3)	M1+E2	2027.4-1483.9	
547.220(76)	3.3(9)	-0.488(50)		0.3(16)			(E1)	3153.8-2606.6	
549.271(70)	3.3(4)			9.7(12)				4063.7-3514.3	
579.217(23)	3.5(6)	0.555(64)	-0.08(12)				(M1+)E2	2606.6-2027.5	
596.296(19)	68.8(7)	0.445(15)	-0.038(21)	10.6(4)	E2		(E2)	4516.6-3920.3	
618.323(25)	33.9(15)	0.348(24)	-0.110(32)	-1.8(6)	(M1)	$0.026^{+0.014}_{-0.028}$	M1	2645.8-2027.4	
634.657(89)	36.8(33)			6.6(13)				3723.5-3088.9	
635.990(59)	53.4(56)			-5.2(22)				2027.4-1391.5	
639.162(135)	4.3(7)			6.1(42)				1348.0- 708.9	
655.336(53)	22.1(9)	0.103(61)		-4.1(7)			M1+E2	2450.0-1794.7	e)
655.93(50)	18.2(11)	0.036(14)	-0.033(20)	2.9(11)			M1+E2	3301.1-2645.8	e)
682.595(26)	68.4(9)	-0.019(10)		-7.3(20)				1391.5- 708.9	
691.682(56)	20.1(7)			13.7(7)	E2			5945.0-5253.4	
698.419(72)	12.8(7)	0.154(55)		1.5(38)			(E2)	4357.0-3658.6	
708.883(16)	1000(8)	0.278(19)	-0.047(37)	0.0	E2		E2	708.9- 0.0	

Table 1
Transitions properties belonging to ^{114}Te determined by our data [cont].

E_γ [keV] [a]	Ang. distr. coef.			Slope [b]	Observed multip. and mixing ratios			Assignments	Comments
	A_0 (I_γ)	A_2/A_0	A_4/A_0		Previous work [c]	δ [d]	This work	$E_i - E_f$	
729.395(35)	54.9(15)				E2			5034.0-4304.6	
733.818(17)	736.4(45)	0.327(21)	-0.077(41)		E2		E2	2217.7-1483.9	
736.823(28)	29.9(58)	0.421(14)	-0.110(23)		E2		E2	5253.4-4516.6	
747.677(89)	11.7(9)	0.175(34)	0.045(46)	7.1(8)		0.24(2)	M1+E2	5781.7-5034.0	
761.148(27)	47.2(11)	0.345(19)	-0.116(35)		E2		E2	4824.8-4063.7	
775.004(16)	866.8(67)	0.318(27)	-0.065(44)	1.2(1)	E2		E2	1483.9- 708.9	
784.352(24)	73.8(13)	0.325(16)	-0.131(24)	5.7(2)	E2		E2	4063.7-3279.3	
790.288(23)	83.9(11)	0.330(13)	-0.088(21)		E2		E2	4304.6-3514.3	
792.559(20)	116.4(13)	0.318(17)	-0.111(26)	5.3(1)	E2		E2	3881.5-3088.9	
792.870(151)								4516.6-3723.5	f)
797.478(109)	6.7(6)	0.288(26)	-0.181(40)			E2		6307.9-5510.0	
807.801(56)	38.5(6)	0.302(20)	-0.128(30)	8.4(3)			E2	4689.4-3881.5	
815.241(54)	13(3)	-0.479(29)	-0.121(43)	4.5(15)		-0.15(3)	M1+E2	3461.0-2645.8	
820.560(13)	24.6(47)	-0.216(13)		7.0(5)	E2		M1	5510.0-4689.4	
825.845(146)	11.3(7)	0.308(50)	-0.101(68)	0.2(17)			E2	2853.3-2027.4	
831.392(25)	58.2(7)	0.355(11)	-0.109(16)	8.8(2)			E2	3920.3-3088.9	
842.717(91)	7.8(7)	0.173(75)	0.17(11)			-0.24(3)	M1+E2	4357.0-3514.3	
850.338(69)	14.1(7)	0.088(12)	-0.103(16)	4.4(6)			(E2)	2241.8-1391.5	
859.927(155)	1.9(7)	0.82(27)				1.25(59)	M1+E2	4320.8-3461.0	
871.255(16)	362.7(37)	-0.172(27)	0.105(41)	5.4(12)	E2		E2	3088.9-2217.7	

Table 1
Transitions properties belonging to ^{114}Te determined by our data [cont].

E_γ [keV][a]	Ang. distr. coef.				Observed multip. and mixing ratios			Assignments	Comments
	A_0 (I_γ)	A_2/A_0	A_4/A_0	Slope[b]	Previous work[c]	δ[d]	This work	$E_i - E_f$	
895.885(99)	22.7(11)	-0.113(90)		6.9(8)			M1+E2	5929.9-5034.0	
901.177(24)	40.0(7)	0.324(25)	-0.159(37)	4.4(6)	E2		E2	3507.8-2606.6	
936.034(17)	204.8(19)	-0.258(13)		4.2(1)	(E1+M2)		E1	3153.8-2217.7	
1005.424(74)	11.0(7)	-0.625(25)					M1	5310.0-4304.6	
1019.645(64)	19.7(7)	0.172(41)	-0.118(57)	2.2(8)			(E2)	4320.8-3301.3	
1034.395(29)	34.8(9)	-0.248(22)		-2.2(7)	M1		M1	3252.1-2217.7	
1054.600(36)	3.9(7)			4.3(20)				6307.9-5253.4	
1085.820(45)	29.4(7)	-0.239(15)	0.070(22)	-5.3(7)		-2.22(30),-0.18(3)	M1+E2	1794.7- 708.9	
1091.086(312)	1.5(6)							1800.0- 708.9	
1122.656(28)	50.2(9)	0.264(33)	-0.049(45)		E2		E2	2606.6-1483.9	
1151.939(169)	6.5(9)	0.452(88)	0.10(13)	-7.3(18)		$1.28^{+0.91}_{-0.46}$	M1+E2	1860.8- 708.9	
1168.914(70)	19.9(11)			4.7(7)				6603.5-5434.6	
1290.310(236)	16.2(11)			2.3(8)				3507.8-2217.7	
1367.421(45)	13.8(7)	0.199(41)	-0.148(56)				(E2)	2851.3-1483.9	
1816.924(364)	2.2(4)							3301.1-1483.9	

[a] Energy taken from the excitation measurement performed at E_α=37 MeV.
[b] Excitation-function slope computed using Equ. 2.
[c] Data taken from Ref. [6].
[d] Multipole-mixing ratio obtained from this analysis of the angular distribution.
[e] Double assignment supported by coincidences data.
[f] Energy determined from coincidence data.

2.2   Angular distributions

The same Compton-supression spectrometer setup was used to record singles spectra at nine angles in the range of 25° to 90 ° with respect to the beam direction at a distance of about 80 cm from the target. Normalization of the angular distribution was performed using a strong and isotropic γ-ray of 1299.9 keV emitted after the β decay of ^{114}Sb. The experimental angular distributions were fitted with a Legendre polynomial expansion:

$$W(\theta) = A_0 + A_2 P_2(cos\theta) + A_4 P_4(cos\theta) \tag{1}$$

where W(θ) is the normalized peak area and P_k are Legendre polynomials. The coefficients $A_0(=I_\gamma)$,A_2/A_0 and A_4/A_0 determined for the γ rays of ^{114}Te are reported in Table 1.

2.3   The $\gamma\gamma$ – coincidence experiment

A system of five HPGe detectors with BGO-NaI(Tl) anti-Compton shields, with volumes ranging from 83 to 160 cm^3 was used for the coincidence experiments. They were placed at a distance of 15 cm from the target. The experimental arrangement and more details concerning the features of the system can be found in Ref. [17]. For coincidence events, the energies E_i and times (T$_{i-RF}$) relative to the cyclotron radio frequency were recorded for each detector in list-mode on streamer tapes. The coincidence matrix was constructed off-line with narrower gates on the times T$_{i-RF}$ and T$_{ij}$= T$_{i-RF}$- T$_{j-RF}$.

The coincidence rate was about 300 Hz for a beam current of 1.5 nA. In total approximately 5x10^7 events satisfying the off-line time conditions were stored in the $\gamma\gamma$-coincidences matrix. Table 2 presents selected coincidences gates, and Fig. 2 presents a few selected coincidence spectra.

2.4   Identification of the lines attributed to ^{114}Te

As shown in Fig. 1, the observed spectra are complex due to the high level density of excited states populated by the (α,2nγ) reaction, and due to the presence of γ rays produced by several competing reactions and the subsequent β-decays.

The latter are important because ^{114}Te is situated at the proton rich side of the line of stability. Fig. 3 illustrates the different competing reactions.

Table 2
Qualitative results of selected coincidence gates

Gate [keV]	Display [keV] [a]
174	**125***, 139^C, **226***, 234*, 321^C, 425*, 435*, 708*, 729*, 734*, (751), 761*, 775*, 784*, 790*, 871*, **935***, **1168***
311	**(125)**, 208^C, 341^C, 494^C, 573^C, (635), **655***, 709*, 734*, **775***, 1272^C
504	**698***, 709*, 734*, 775*, 935*
618	**543***, **635***, **655***, **682***, 709*,(734)*, 775*, **815***, **1019** *
655	309*, 618*, 635*, 682*, **709***, 763^C, 775*, 935*, **1019***, **1085***
698	**125***, **209***, 258^C, 379*, **425***, **504***, (596)*,(635)*,708*, 729*, 734*, 775*, (790)*, 871*, **935***
825	(125)*, (235)∗, 543*, **635***, **682***, **708***, (734)*, (775)*, **935***
842	**234***, **425***, **471***, 511^C, 708*, 734*, 775*, 871*, 935*
1168	125*, **174***, **226***, 234, 342^C, 414, 435*, (596)*,(658), 708*, 733*,775*, 784*, 935*
1367	(655)*, **708** *, **774** *, (1085)*

[a] Bold types indicates that this line appears clearly in the coincidence gate, parentheses indicate questionable presence, a C denotes a line from a contaminant nucleus, and an asterisk means that this line has been placed in the level scheme.

Concerning the β decay channels, two methods were used to identify the γ rays belonging to the different nuclei. The first one was to build a $\gamma\gamma$-coincidence matrix with time conditions out of burst so that only the delayed γ rays were sorted. This method allowed the identification of the most intense γ rays produced by the β disintegration. Fig. 4 shows singles spectra and some selected coincidence gates from this matrix. Because of the relative long lifetimes of the β decays, all the γ rays observed in the angular distribution were isotropic. This second criterion and the coincidence relations were used to identify unambiguously the transitions not belonging to Te isotopes.

Further competing channels are the different (α,xn) reactions. The γ rays belonging to these reactions were identified using the shape of the excitation function and the coincidence relations. However, as the threshold of the (α,n) channel is about 24 MeV and that of the $(\alpha,3n)$ channel is about 49 MeV, the production of ^{113}Te and ^{115}Te was not significant and only the strongest γ rays belonging to these nuclei are observed. Moreover, the (α, np) channel also has its maximum cross-section at the same energy as the $(\alpha, 2n)$ reaction.
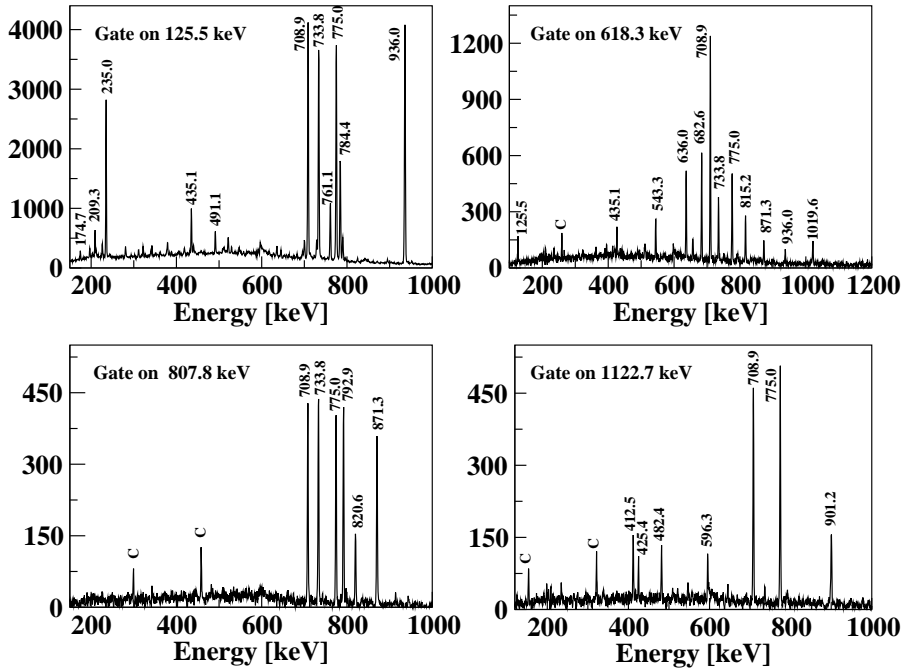
Fig. 2. Selected $\gamma\gamma$-coincidence spectra from the (α,2nγ) reaction supporting parts of the proposed level scheme

Consequently some transitions of ^{114}Sb not observed after β decay appear in the spectra. These transitions have been identified using the coincidence matrix.

3 Data analysis and results

3.1 Analysis of the angular distributions

The spin and parity of the observed levels were first obtained from the γ-ray angular distributions. The analysis of the angular distribution data is based on the suggestion of Taras and Haas [18] and Ionescu et al. [19] that the magnetic-substate population after a light ion induced reaction is not purely Gaussian. This hypothesis is based on the fact that a state is populated by two mechanisms (i) discrete population from parent levels and (ii) the side-feeding. The contribution of the first one is taken explicitly into account using de-orientation coefficients. Due to the huge number of feeding paths from the entry states, the side-feeding contribution is considered to be Gaussian, the variance parameter being σ. This σ-value was determined by considering only the pure E2 transitions. For ^{114}Te it was found to be 1.9(3). This value was
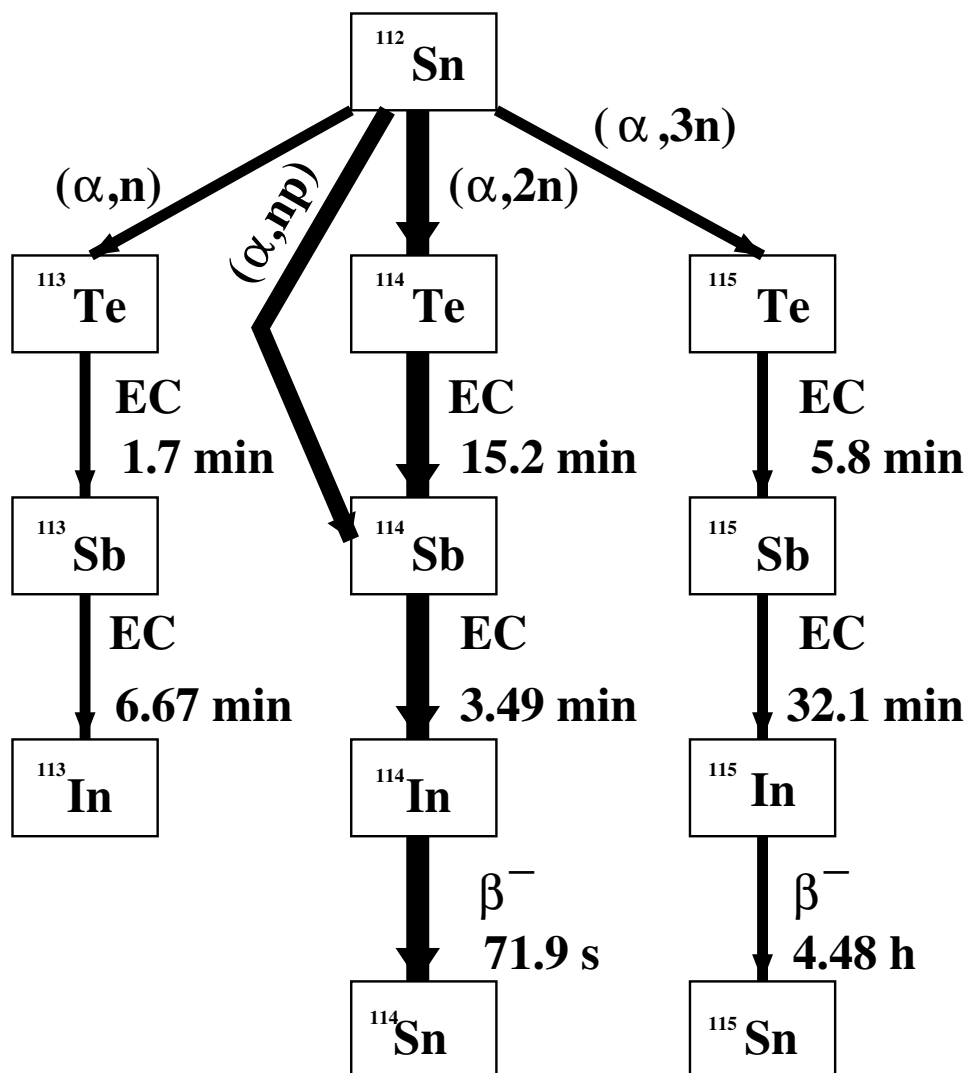
Fig. 3. The different competing channels and nuclei produced during our experiments.

then used in the χ^2 analysis of dipole and mixed transitions as a function of the multipole-mixing ratio δ. Some examples of the analysis of the angular distribution are shown for a few transitions in Fig. 5. When the χ^2 analysis gives more than one acceptable value for δ, both are listed in Table 1.
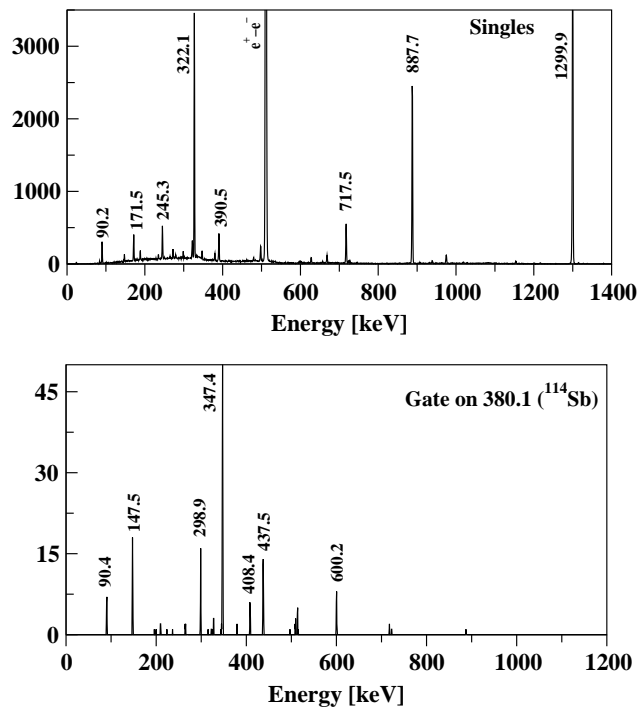
Fig. 4. Matrix projection and selected coincidence gate from the $\gamma\gamma$-coincidence matrix build out of burst.
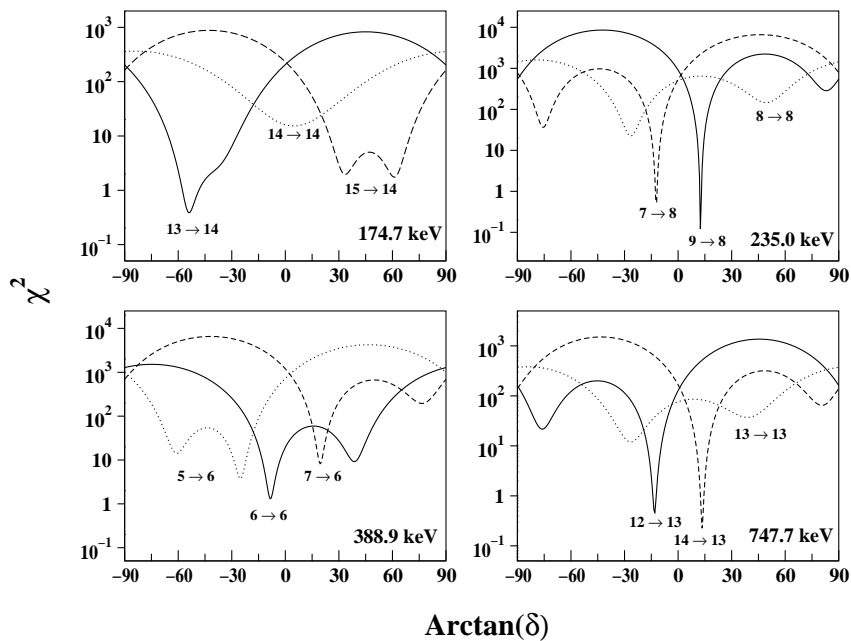

Fig. 5. Analysis of the angular distribution of a few transitions in ^{114}Te. The value of χ^2 is reported as a function of arctan δ for the three possible spin sequences.
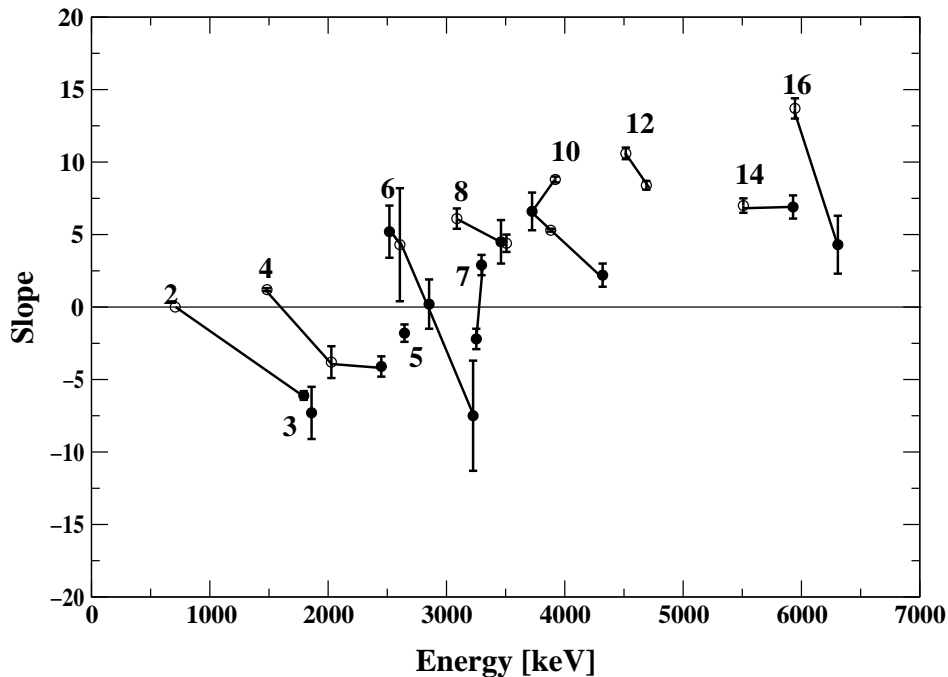
53

Fig. 6. Slopes of the excitation function for the positive-parity states. The lines connect points of levels with the same spins. Open circles denotes levels with previously known spins.

3.2 Excitation-function slopes

The excitation-function slope SL is defined as in Ref. [20] :

$$SL = \frac{200}{E_2 - E_1}\left(\frac{I_2 - I_1}{I_1 + I_2}\right) \qquad (2)$$

where I_1 and I_2 are the γ-ray intensities at the α-particle energies E_1=32.4 MeV and E_2=42.7 MeV, respectively. It has been shown in Ref. [20] that the excitation-function slopes of the depopulating transitions depend on the spin of the levels. So it is possible to determine the spin of levels by comparing the slopes with those of levels with known spins (see Fig. 6). The measured excitation-function slopes are reported in Table 1.

3.3 Discussion of individual levels

In this section, we discuss levels which were expected to be observed but were not, those for which the decay is revised, and new levels. The experimental results are summarized in Table 3.

Table 3
Levels of ^{114}Te. Only the levels observed in our experiments are listed.

E_{exc}		Observed in experiment[c]	I^{π} [b]	Slope	$I^{\pi}_{a.d.}$ [d]	I^{π} [e]	Comments
This work[a]	Previous[b]		previous			adopted	
0.0	0.0	ABCD	0^+				
708.883(16)	708.9(2)	ABCD	2^+	0.0	2^+	2^+	E2 to 0^+
	1342.6(3)	B	$(1,2)^+$				f),g)
1348.045(136)	1348.1(3)	A		6.1(42)	$(0)^+$	(0^+)	f)
1391.477(31)	1391.2(3)	A	2^+	-7.3(20)	$(2,3^+)$	2^+	
1483.889(22)	1484.2(3)	ABCD	4^+	1.2(1)	4^+	4^+	E2 to 2^+
1794.690(40)	1794.4(3)	A	(2^+)	-6.1(3)	(3^+)	(3^+)	
1799.969(312)					(0^+)	(0^+)	f)
1860.822(170)	1860.0(3)	A	(0^+)	-7.3(18)	(3^+)	(3^+)	f)
	1949.6(4)	A	$(2,3)^+$				f),g)
	1960.4(4)	A	(3^+)				f),g)
2027.463(66)	2026.8(5)	AB	4^+	-3.8(11)	(4^+)	4^+	E2 to 4^+
2217.696(27)	2217.8(5)	ABCD	6^+		6^+	6^+	E2 to 4^+
2241.815(75)	2241.3(5)	A			(4^+)	(4^+)	f)
	2275.7(5)	A					g)
	2296.1(5)	A					g)
2450.026(67)				-4.1(7)	(4^+)	(4^+)	f)
	2482.3(4)	A					f),g)
2518.524(73)							f)
2606.576(29)	2606.9(8)	BC	6^+	4.3(39)	6^+	6^+	

Table 3
Levels of ^{114}Te [cont].

$E_{exc}^{a)}$		Observed in experiment$^{c)}$	$I^{\pi b)}$	Slope	$I^{\pi}_{a.d.}$ $^{d)}$	$I^{\pi e)}$	Comments
This work$^{a)}$	Previous$^{b)}$		previous		adopted	adopted	
2645.786(71)				-1.8(6)	5$^+$	5$^+$	$f)$
	2695.0(3)	A					$f),g)$
2851.310(50)					(6$^+$)	6$^+$	$f)$
2853.308(160)				0.2(17)	6$^+$	6$^+$	(E2 to 4$^+$),$f)$
	3008.2(5)	A					$f),g)$
3088.926(30)	3089.1(6)	ABCD	8$^+$	6.1(7)	8$^+$	8$^+$	E2 to 6$^+$
	3121.4(6)	B					$f),g)$
	3143.9(4)	A					$f),g)$
3153.753(30)	3154.3(6)	BC	(7$^-$)	4.4(6)	7$^-$	7$^-$	
3252.091(40)	3253.4(6)	B	(7$^+$)	-2.2(7)	7$^+$	7$^+$	
3279.303(32)	3279.7(8)	BC	(8$^-$)	3.7(1)	8$^-$	8$^-$	
3301.138(87)	3301.6(5)	A		-4.1(7)		(7$^\pm$)	$f)$
	3346.0(4)	A					$g)$
3461.011(87)				4.5(15)	(7$^+$)	(7$^+$)	$f)$
3507.783(34)	3508.1(9)	C	8$^+$	4.4(6)	8$^+$	8$^+$	E2 to 6$^+$
3514.315(31)	3514.1(8)	BC	(9$^-$)	4.8(3)	9$^-$	9$^-$	(E2 to 7$^-$)
	3550.3(5)	A					$g)$
3658.627(93)					(6$^-$)	(6$^-$)	$f)$

Table 3
Levels of ^{114}Te [cont].

E_{exc}		Observed in experiment[c]	I^{π}[b]	Slope	$I^{\pi}_{a.d.}$[d]	$I^{\pi e}$	Comments
This work[a]	Previous[b]		previous			adopted	
3715.957(99)				4.7(12)		$8^+,(9^+)$	
3723.524(37)	3723.5(8)	C	9^+	6.6(13)	(10^+)	10^+	f)
3881.499(48)	3880.6(6)	BCD	10^+	5.3(1)	10^+	10^+	E2 to 8^+
3920.282(33)	3920.1(7)	C	10^+	8.8(2)	10^+	10^+	
4063.658(39)	4063.7(9)	BC	(10^-)	5.7(2)	10^-	10^-	E2 to 8^-
4304.600(38)	4304.0(4)	C	(11^-)	8.5(4)	11^-	11^-	E2 to 9^-
4320.805(102)				2.2(8)	$(8,9)^+$	$(9)^+$	f)
4357.041(84)				1.5(38)	8^-	8^-	f)
4516.566(38)	4516.1(8)	C	12^+	10.6(4)	12^+	12^+	(E2 to 10^+)
4554.719(51)							f)
4689.419(80)	4688.6(7)	C	12^+	8.4(3)	12^+	12^+	E2 to 10^+
4824.807(48)	4824.7(9)	C	(12^-)		12^-	12^-	E2 to 10^-
4834.712(53)				-3.4(11)			h)
5033.981(48)	5033.4(9)	C	(13^-)	9.0(9)		(13^-)	f)
5253.359(46)	5253.2(9)	C	14^+		14^+	14^+	E2 to 12^+
5259.905(55)	5259.3(3)	C	(14^-)		(14^-)	14^-	E2 to 12^-

Table 3
Levels of ^{114}Te [cont].

E_{exc}		Observed in experiment[c]	I^{π}[b]	Slope	$I^{\pi}_{a.d.}$[d]	I^{π}[e]	Comments
This work[a]	Previous[b]		previous			adopted	
5310.068(71)	5308.9(10)	C	(13^-)		13^-	13^-	
5434.581(68)				15.4(3)	(13^-)	$(13,15^-)$	
5509.985(201)	5509.3(9)	C	14^+	7.0(5)	$(11,13)^+$	13^+	f)
	5636.0(12)	C	(14^-)				g)
5781.587(73)	5779.9(10)	C	15^-	7.1(8)	13,14,15	(15^-)	
5929.866(110)				6.9(8)		$(14,15)^+$	
5945.041(72)	5944.9(9)	C	16^+	13.7(7)		(16^+)	
6307.910(185)	6306.3(9)	C	16^+	4.3(20)	$13^+,15^+$	15^+	
	6425.8(12)	C	(15^-)				
	6472.0(16)	C	(16^-)				
	6599.9(13)	C	(16^-)				
6603.495(98)				4.7(7)		(16^-)	

a) Excitation energies are calulculated by a least-squares procedures involving all transitions observed in the present work.
b) According to Ref. [6].
c) Levels have been observed previously in A: ^{114}I decay from Ref. [8], B: ^{114}Sn(^{3}He,3nγ) reaction from Ref. [7], C: (HI,xnγ) from Ref. [10,15], D: (α,2n) reaction from Ref. [16].
d) Spins and parities according to angular-distribution analysis.
e) Adopted spins and parities using all available experimental informations.
f) See discussion in Sect. 3.3.
g) Level not observed in the present data. Existence is uncertain.
h) Based on the multipole character of the decay, this level seems to be a negative-parity state.
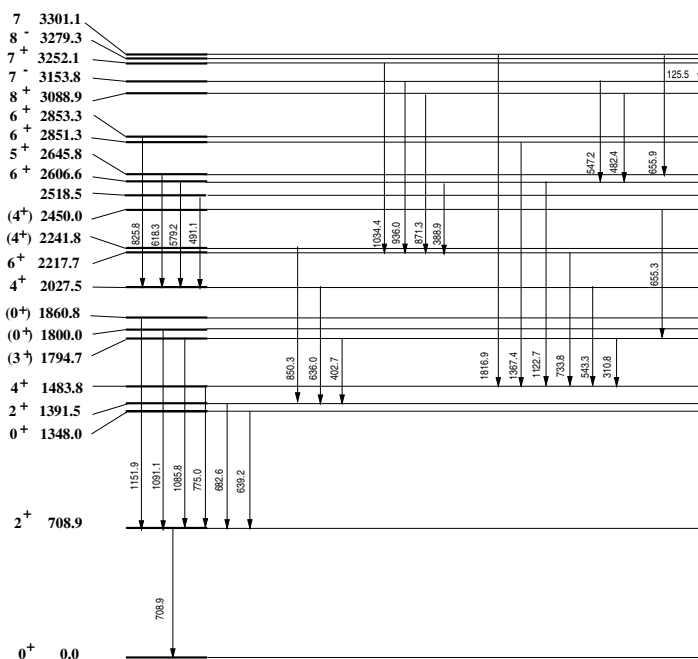
Fig. 7. First part of the proposed level scheme of ^{114}Te based on the present experiments.

Moreover, Figs. 7 and 8 present the level scheme based on the analysis of the present work.

1342.6-keV level: This level was only observed by Lonnroth et al. [7]. They observed 1342- and 633-keV γ rays, but our coincidence experiment does not support these placements. The coincidence relation for the 1342-keV transition shows that it belongs to ^{114}Sb. Moreover, the coincidence relation does not support their placement of the 633-keV transition because they show that it belongs to ^{114}Sb. Note that the statistical population of states by the (α, 2n) reaction should show a similar population for this state as for the 0^+ at 1348 kev which is observed in the work. So the existence of this level is doubtful.

1348.0-keV level: This level was previously observed by Zimmerman [8]. He assigned this level as (0^+). From our $\gamma - \gamma$ coincidence, we only observed one γ ray of 639.2 keV depopulating this level. From the γ-ray angular distribution experiment, this γ ray is isotropic. So we confirm the assignment of this level as $I^\pi = 0^+$.

1800.0-keV level: This level is observed for the first time. From our $\gamma\gamma$-coincidences experiment only a 1091.1-keV transition was found to depopulate this new level. This transition was placed by Zimmerman [8] as decaying from a 2482-keV level. According to the present experiments, this placement does not match because we observe only the 708 keV γ-ray in the $\gamma\gamma$-coincidence
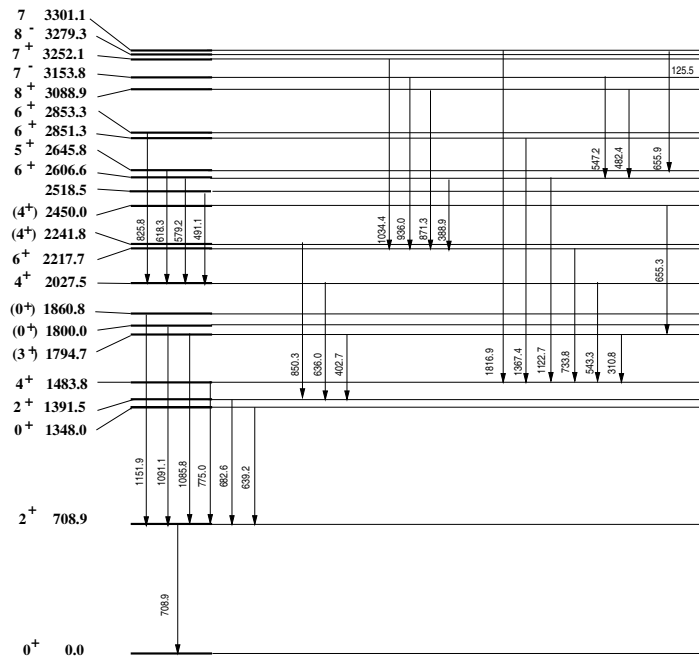
Fig. 8. Second part of the proposed level scheme of ^{114}Te based on the present experiments.

relation of the 1091-keV transition and not the 682-keV one. We assign to this level the spin and parity of $I^\pi=(0^+)$ because the angular distribution of the 1091-keV transition is isotropic.

1860.8-keV level: This level was first observed by Zimmermann [8] and has been assigned as $J^\pi=(0^+)$. It was known to decay by one 1151-keV transition. According to our angular distribution data, this transition shows a M1+E2 character. According to our analysis this state can be assigned as $J^\pi=(3^+)$. This assignment is also supported by the excitation-function slope (see Fig. 6).

1949.6-keV level: This level was only observed by Zimmerman [8] and was known to decay only by one 558-keV transition. Because the 558-keV transition was not observed in any of our experiments, it is assumed that the existence of this level is uncertain.

1960.4-keV level: This level was proposed by Lonnroth et al. [7] and decays by only one 617-keV transition. According to our $\gamma\gamma$-coincidences data (see Fig. 2), this γ ray has been placed as depopulating the 2645-keV level in accordance with C.B Moon et al. [9]. Moreover, the existence of the final level connected by the 617-keV γ ray is also doubtful (see discussion of 1342-keV level). Consequently, we conclude that the 1960-keV level does not exist.

2241.8-keV level: This level was previously observed by Zimmerman [8] and was known to decay by transitions of 850.3 and 758.2 keV. Based on the intensity of the 850.3-keV transition and the branching ratio in Ref. [8], the intensity of the 758.2-keV transition is below our detection threshold. The 850-keV transition seems to have an E2 multipole character suggesting a spin and parity $I^\pi=(4^+)$.

2450.0-keV level: This new level decays by one transition of 655.3 keV. It gives a clear coincidence signal (see Table 2, 655-keV gate). The complexity of the signal supports a second placement of a resolved doublet with an energy of 655.9 keV. The γ-ray angular distribution analysis of the 655.3-keV γ ray leads to a spin and parity of $I^\pi=(3,4)^+$. The excitation-function slope supports a spin and parity of $I^\pi=4^+,5^+$. Consequently we adopt the assignment $I^\pi=(4^+)$.

2482.3-keV level: This level was first observed by Zimmerman [8] and was known to decay by only one transition of 1091.1 keV. According to the coincidence signal of the 1091-keV transition, only the 708-keV γ ray ($2^+ \rightarrow 0^+$) was observed, and this is why the 1091-keV transition has been placed as depopulating the 1800-keV level. For this reason the existence of this level is highly doubtful.

2518.5-keV level: This new level decays by one transition of 491.1 keV. The coincidence signal is very complicated and supports a second placement of this line (see discussion of level 4554.7 keV). But the doublet structure of this γ ray cannot be resolved. Consequently, we cannot give an assignment to this level.

2645.8-keV level: This level was observed for the first time by Moon et al. [9] and was known to decay by one 618-keV transition. Our coincidence data confirm this placement(see Table 2, 618-keV gate, and Fig. 2). The γ-ray angular distribution leads to a M1 multipole character and favours a spin and parity $I^\pi = 5^+$. The excitation-function slope also supports this assignment.

2695.0- and 3008.2-keV levels: These levels were only observed by Zimmerman [8]. The four transitions proposed to depopulate these levels are too weak to be observed in this work.

2851.3-keV level: This new level decays by one transition of 1367.4 keV. This placement is confirmed by the coincidence data (see Table 2, 1367-keV gate). According to the γ-ray angular distribution this transition seems to have an E2 multipole character which implies a spin and parity $I^\pi = 6^+$. This assignment is also supported by the excitation-function slope analysis.

2853.3-keV level: This new level is depopulated by one transition of 825.8 keV. This placement is confirmed by the coincidence data (see Table 2, 825-keV gate). The analysis of the γ-ray angular distribution of the 825-keV transition

favours a spin value of $I^\pi = 6^+$. The positive parity is confirmed by the experimental mixing-ratio $\delta=0.84^{+0.16}_{-0.20}$. Moreover, the excitation-function slope also support the proposed assignment.

3301.2-keV level: This level was known to decay by one transition of 1816.9 keV. This placement seems correct but not certain due to the weakness of the coincidence signal. A new transition of 655.9 keV has been added to the decay. This line is a doublet, but this placement is supported by the coincidence gate (see Table 2, gate 655 keV). The analysis of the excitation-function slope seems to support the assignment of $I^\pi = (7^+)$.

3461.0-keV level: This new level is depopulated by one transition of 815.2 keV which is clearly observed in the 618-keV gate (see Table 2, gate 618 keV and Fig. 2). According to the angular distribution, it has a M1+E2 multipole character and the analysis gives a mixing ratio value of $\delta=-0.15(3)$. The analysis of the angular distribution favours a spin and parity $I^\pi = 7^+$. The excitation-function slope data are less clear and give a spin and parity $I^\pi = 7^+, (8^+)$. According to the present data, we adopted the spin and parity $I^\pi = 7^+$.

3658.6-keV level: This new level is depopulated by two transitions of 504.9 and 379.4 keV. The 505-keV transition gives a clear coincidence signal (see Table 2, gate 504). The second one also gives a coincidence signal but it is not so clear due to the presence of a contaminant γ-ray line. The angular distribution of the 505-keV transition gives a clear M1+E2 multipole character with a mixing ratio value $\delta=0.39(3)$ confirming the negative parity of this state. The determination of the spin is not so clear and the analysis of the γ-ray angular distribution favours a spin $I_i = 6$. We adopt the spin and parity of $I^\pi=(6^-)$.

3723.5-keV level: This level was observed by Janzen [10] and by C.B. Moon et al. [9]. Janzen assigned this level as $I^\pi = 9^+$ while Moon et al. assigned it as $I^\pi = 10^+$. According to the angular distribution of the 209-keV transition, which has a clear E1 multipole character, and the feeding of the level from the 12^+ state at 4516 keV, we adopt a spin and parity of $I^\pi = 10^+$. This assignment is also supported by the excitation-function slope.

4320.8-keV level: We found two transitions of 859.9 and 1019.6 keV decaying from this new level. The angular distribution of the first transition give a M1+E2 multipole character with a mixing ratio value $\delta=1.25(59)$. The analysis of the angular distribution favoured two possible spins which could be $I^\pi = (8,9)^+$ depending on the final spin. The second one seem to have an E2 multipole character giving a spin and parity $I^\pi = (9^+)$. The excitation-function slope gives two possible spins $I_i = 9, 10$. But the spin $I_i = 10$ is incompatible with the decay to the 7^+ level. So we adopt the assignment $I^\pi = (9^+)$.

4357.0-keV level: This level is observed for the first time. Two transitions of

698.4 and 842.7 keV were placed. The two transitions give clear coincidence signals (see Table 2, gate 698 and 842). The angular distribution of the 843-keV transition shows a M1+E2 multipole character with a mixing ratio δ=-0.24(3) confirming a negative parity. The second one seems to give a E2 multipole character. Consequently we assign $I^\pi = 8^-$ to this level. This spin is also favoured by the angular distribution analysis of the 843-keV transition.

4554.7-keV level: This new level has one transition of 491.1 keV. The complex coincidence spectra justify this second placement of this transition. As for the 2519-keV level, no spin assignment is possible.

5034.0-keV level: This level was previously observed by Moon et al. [9] and was known to decay only by a 729.0-keV transition. A new decay of 517.4 keV has been added. The angular distribution of the latter gives a dipole character implying a spin and parity $I^\pi = 13^-$ in agreement with that proposed by Moon [9].

5510.0-keV level: This level was previously observed by Moon et al. [9] and Janzen [10]. The latter assigned this level as $I^\pi = 14^+$. But according to our data the transition of 820.6 keV decaying from this level has a M1 multipole character implying a spin and parity $I^\pi = 13^+$. This assignment is also confirmed by the excitation-function slope.

4   Interpretation of the results.

In this section, we will compare our results to the IBM, which describes the valence nucleon pairs by s and d bosons; the one-broken-pair model, which allows one of the nucleon pairs to be broken and the QPNM which explicitly constructs the phonon from two-quasiparticles components. The comparison will be restricted to the vibrational structures, since no clear candidate for the band head of the intruder band was identified.

4.1   Band structure

Figs. 9 and 10 present the level scheme of the proposed band structure for ^{114}Te.

Ground-state band: as in other even Tellurium isotopes, the ground-state band in ^{114}Te is vibrational with the ratio $E(4^+)/E(2^+)$ equal to 2.09, a value close to the pure vibrational limit. The ground-state band is clearly identified up to spin I=8. The band was tentatively extended up to spin I=12. In Ref. [6], the 10^+ level belonging to this band is the 3880-keV level. Using the formula
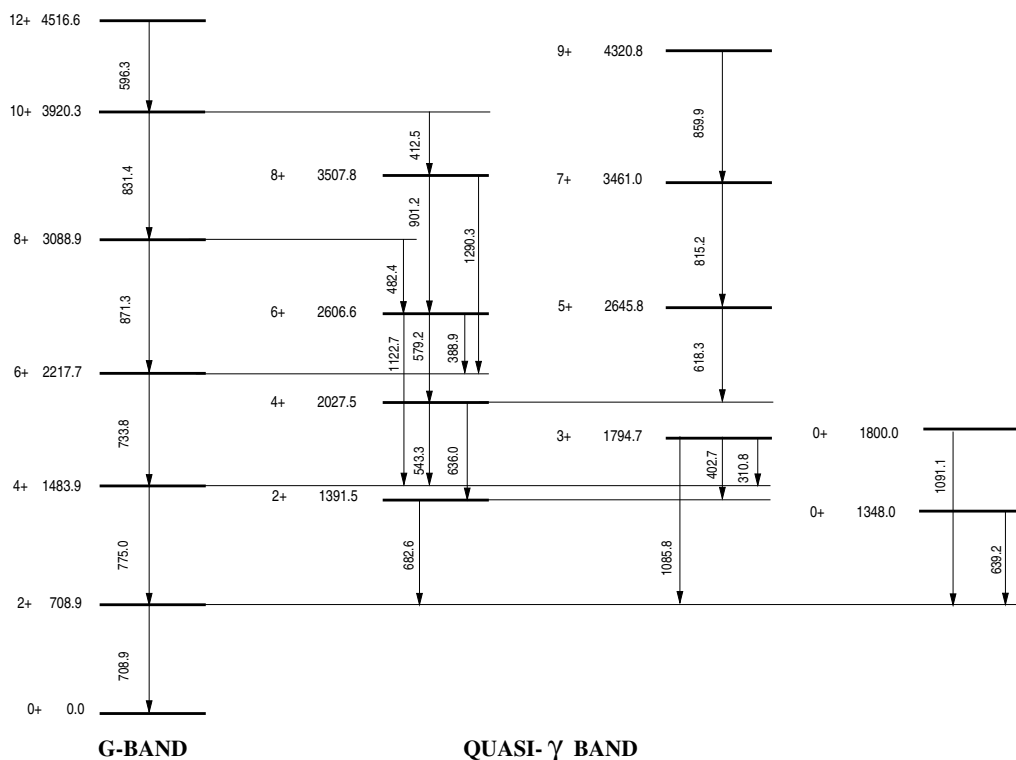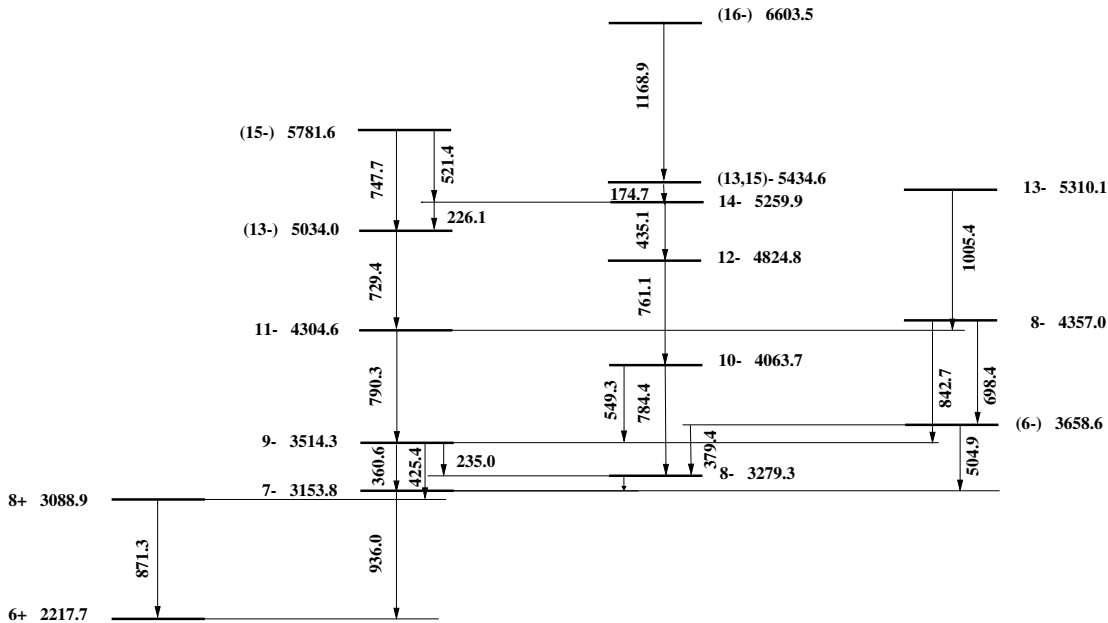
Fig. 9. Partial level scheme of ^{114}Te based on the present experiments showing states of positive-parity bands. Spin and parity are indicated for each level.

4 given below for the U(5) excitation energy, a 3920-keV excitation energy is obtained, which is in better agreement with the proposed band structure of this work. The relative excitation functions concerning this band structure are given in Fig. 11.

Quasi-γ band: for the first time, 8 levels belonging to what appears to be a quasi-γ band were identified up to a spin $J^\pi = 9^+$. While the high-spin states of these band show stretched E2 in-band transitions and transitions toward the yrast band, the odd low-spin members deviate strongly because no decay between the 5^+ and 3^+ is found. Another possible candidate exists for the 3^+ state but it also has no known γ ray connecting this level with the 5^+ level and its spin assignment is not certain. Note that both states decay only to the 2^+ level of the ground-state band.

Band A: this negative-parity band was previously observed up to a spin I=13 [9]. According to the present work, it was extended up to a spin I=(16). It decays principally by intraband transitions.

(16-) 6603.5

1168.9

(15-) 5781.6

747.7   521.4

(13,15)- 5434.6

174.7

14- 5259.9

13- 5310.1

226.1

435.1

1005.4

(13-) 5034.0

729.4

12- 4824.8

761.1

11- 4304.6

8- 4357.0

790.3

10- 4063.7

842.7   698.4

549.3   784.4

(6-) 3658.6

9- 3514.3

379.4

360.6   425.4   235.0

8- 3279.3

504.9

7- 3153.8

8+ 3088.9

871.3   936.0

6+ 2217.7

BAND A

Fig. 10. Same caption as Fig. 9 but for states of negative-parity bands (band A, see text) and other negative-parity states.

4.2   U(5) dynamical symmetry approach.

The atomic nucleus ^{114}Te was not selected as exhibiting the U(5) dynamical symmetry in the systematic study of Ref. [4], because at that time experimental data were lacking[5]. The most important part of the present work is to test the vibrational character of ^{114}Te in detail. Therefore, the establishment of the odd-spin members of the quasi-γ band is important.

To establish the vibrational character of a nucleus, we will rely on the selection criteria presented in Ref. [4]. The first criterion is that the ratio $R_{4/2}$=2.09 is nearly equal to 2. The second concerns the energy spreads between the upper and lower members of the two-phonon states. For ^{114}Te the value is S=137 keV which far from the condition S < 30 keV. However, as noted in Ref. [4], except for ^{110}Pd, all vibrational nuclei exhibit large anharmonicities in the two-phonon triplet. Based on these two criteria, it seems reasonable to try to describe ^{114}Te using the U(5) dynamical symmetry. The Hamiltonian in this limit of the IBM is given by:

$$\hat{H} = \epsilon \hat{C}_1[U(5)] + \alpha \hat{C}_2[U(5)] + \beta \hat{C}_2[O(5)] + \gamma \hat{C}_2[O(3)]. \qquad (3)$$
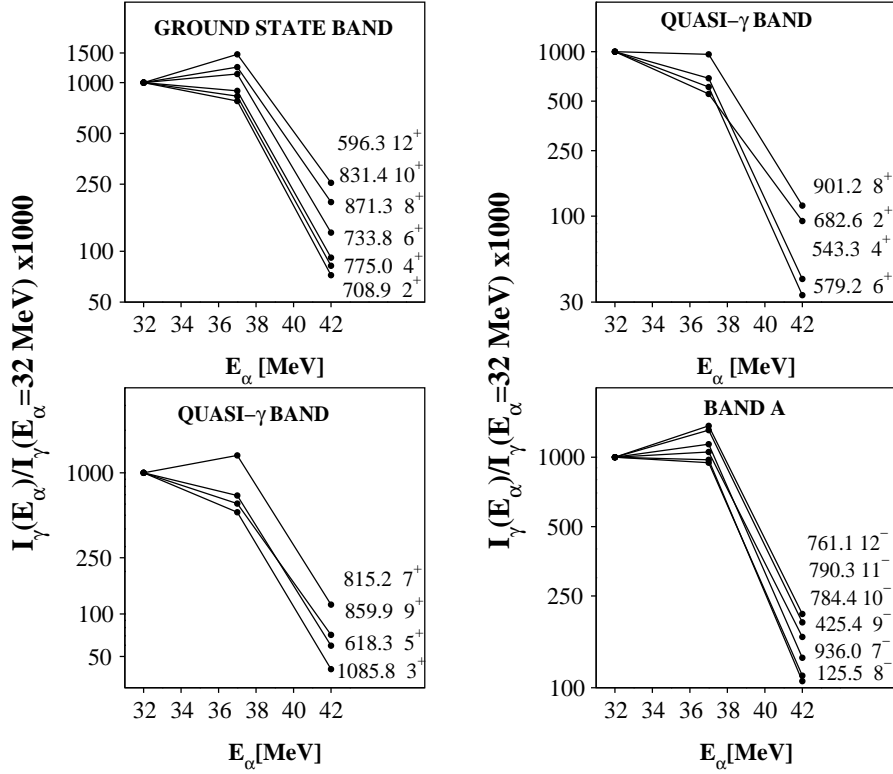
Fig. 11. Relative excitation functions of the intraband transitions.

with $\hat{C}_n(G)$ the nth order Casimir operator of the group G. The eigenvalues of the hamiltonian given by Eq. 3 lead to the third criterion for a good vibrational nucleus, namely that the level energies are well approximated by the formula:

$$E(U5) = \epsilon n_d + \alpha n_d (n_d + 4) + \beta \nu(\nu + 3) + \gamma I(I + 1), \qquad (4)$$

where n_d is the quantum number giving the number of d-bosons and ν the one giving the d-boson seniority and I the spin. The fitted parameters give for ^{114}Te the values α=-27.9 keV, ϵ=807.7 keV, β=-3.4 keV, γ=11.6 keV. The comparison between the experimental level energies and the U(5) calculation is illustrated in Fig. 12 where we also compare the predictions for higher spin states. The energies for the proposed multiphonon levels are in general well approximated. Note that the number of levels considered in the fit is still not very large. Regarding Fig. 12, we remark a good agreement between the experimental and fitted values with an acceptable deviation of 45.3 keV.

The last criterion concerns the Δn_d=$\pm$1 selection rule for electric quadrupole transition, and predicts that in a good U(5) nucleus the transitions with Δn_d $\neq \pm 1$ are hindered [4]. Only a few levels can be compared due to the absence of known lifetimes in ^{114}Te. In Table 4, the experimental B(E2) ratio values
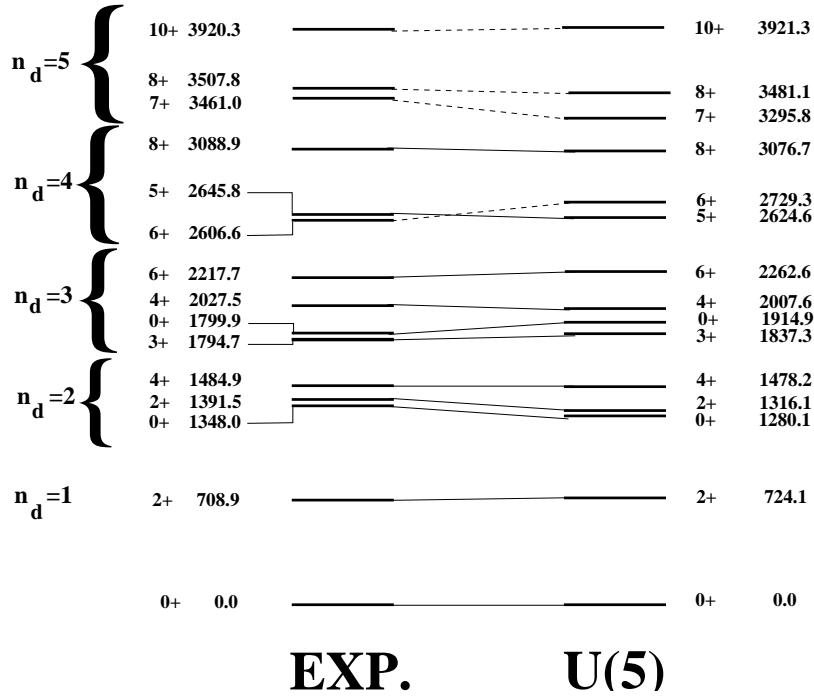
Fig. 12. Comparison between experimental and theoretical excited states calculated using the U(5) dynamical symmetry. Levels connected with solid lines were used for the fit.

for transitions depopulating the proposed multiphonon states are compared to theoretical values.

The B(E2) ratio is calculated using Equ. 5:

$$\frac{B(E2; I_i \to I_j)}{B(E2; I_i \to I_k)} = \frac{BR_{ij}}{BR_{ik}} \left(\frac{E_{ik}}{E_{ij}}\right)^5 \left(\frac{\delta_{ij}}{\delta_{ik}}\right)^2 \left(\frac{\delta_{ik}^2 + 1}{\delta_{ij}^2 + 1}\right), \tag{5}$$

where BR_{ij} (BR_{ik}) is the branching ratio of the transition, E_{ij} (E_{ik}) is the energy of the γ ray depopulating the level of interest and δ_{ij}, respectively δ_{ik}, is the multipole-mixing ratio. The terms depending on the multipole-mixing ratio are used only if a value is known for the transition of interest. Table 4 compares the resulting ratios to the theoretical parameter-free predictions.

The agreement is very poor and casts strong doubts on the character of the γ-band structure discussed above. In order to investigate this discrepancy, the data may be compared to two microscopic models: the broken-pair and QPN models.

Table 4

Comparison between experimental and calculated B(E2) ratios of selected levels (see text). The ratios are defined as $B(E2;I_i \to I_j)/B(E2;I_i \to I_k)$.

I_i	I_j	I_k	Exp.	Theory	
				U(5)	QPNM
4_2^+	4_1^+	2_2^+	0.04(1)	0.91	0.64
3_1^+	4_1^+	2_1^+	4810(520) or 181(20)	$+\infty$	–
3_1^+	2_2^+	2_1^+	724(200) or 27(7)	$+\infty$	–
3_1^+	4_1^+	2_2^+	7(2)	0.4	–
6_2^+	4_1^+	4_2^+	0.5(1)	0	0.96
6_2^+	4_2^+	6_1^+	0.45(11)	2.14	18.5
6_2^+	4_1^+	6_1^+	0.29(1)	0	17.7
8_2^+	6_2^+	6_1^+	15(4)	$+\infty$	3.2
10_1^+	8_2^+	8_1^+	21(4)	0	10.2

4.3   Comparison to Broken Pair and Quasiparticle Phonon Nuclear Models

Using a broken-pair model calculation for ^{114}Te, Akkermans [12] obtained excitation energies for the two lowest one-broken-pair states at 1.51 and 2.33 MeV for 4^+, and at 2.38 and 2.97 MeV for 6^+.

The energies of these non-collective states are very close to the calculated collective two- and three-phonon states. The broken-pair states show, however, a non-collective decay pattern i.e. one violating the phonon-selection rules. As for the U(5) dynamical symmetry calculation, there is a good agreement between the experimental and calculated level energies. The non-collective decay pattern observed in this work has already been discussed for other Tellurium isotopes and more particularly for ^{118}Te and ^{120}Te [21] and could be explained by the presence of a broken-pair component in the states of interest. But for the non-collective 8^+ and 10^+ states, the one-broken-pair calculation is not in accordance. Indeed the excitation energies for these states give 4.64 and 4.81 MeV for 8^+, and 4.67 and 4.83 MeV for 10^+ which are completely in disagreement with the experimental observation.
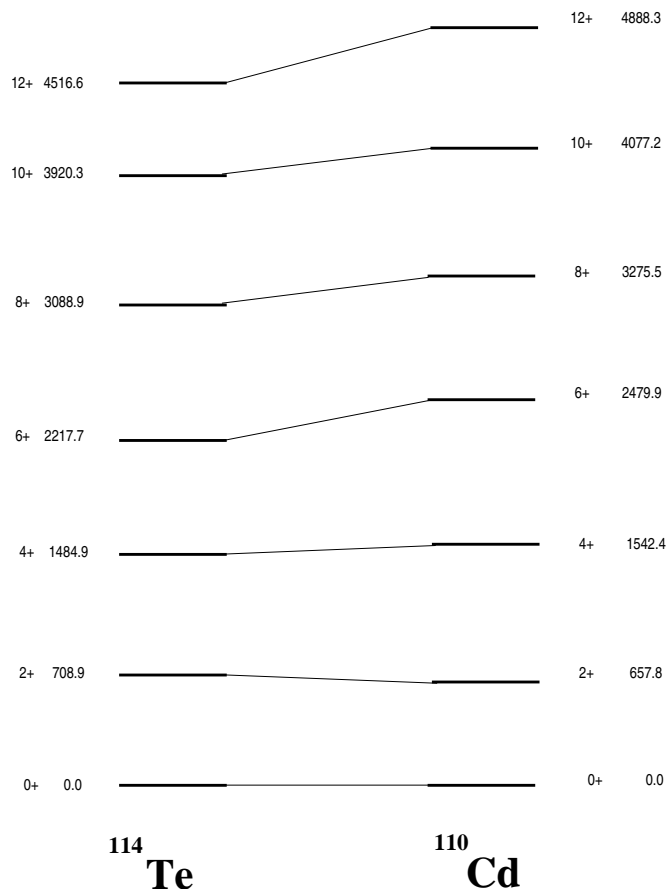
Fig. 13. Comparison between normal yrast states in ^{110}Cd and ^{114}Te nuclei.

Recently, the QPNM has been applied to the theoretical description of ^{114}Te. Using this description, Grinberg et al. [22] obtained excitation energies of 3.35 and 3.45 MeV for the two lowest 8^+ states and of 3.58 MeV for the first 10^+. As for the U(5) dynamical symmetry there is also a good agreement for the excitation energies. In Table 4, the B(E2) ratios available from the QPNM calculationare compared to the U(5) limit and the experimental ratios. A close inspection of Table 4 shows also poor agreement between theoretical and experimental values, expect for the 10_1^+ state.

4.4   Intruder analog description.

One of the aims of this work was to test the intruder-analog description which relates states formed by particle-like bosons to those formed by hole-like bosons [2]. In the case of ^{114}Te, the normal configuration has two protons outside the Z=50 proton closed shell and thus has an intruder-spin projec-

tion $I_z = +\frac{1}{2}$. The corresponding member of the doublet has the intruder-spin projection $I_z = -\frac{1}{2}$ and must have two proton holes in the Z=50 proton shell. This condition is fulfilled by ^{110}Cd. Considering Fig. 13, we can see that the normal yrast states in ^{110}Cd and ^{114}Te have quite a similar structure up to the 4^+ state. For higher spins deviations occur which might indicate the influence of two quasi-particles excitations as discussed above. The comparison of the $I = \frac{3}{2}$ multiplet is not yet possible, because we were not able to observe a 0^+ corresponding to the band head of an intruder band structure.

5   Conclusion

The atomic nucleus ^{114}Te was studied by the (α,2nγ) reaction. This study allowed the determination of 50 levels and the placement of 74 transitions belonging to ^{114}Te. The use of the set of experiments presented in this work allowed the unambiguous determination of the spins and parities of nearly all observed levels populated by the (α,2n) reaction. The aim of this work was to elucidate the structure of ^{114}Te and test the validity of the intruder-spin invariance. No evidence for the existence of intruder states in ^{114}Te was found. We have shown that, based on energies alone, ^{114}Te mimics a nucleus exhibiting the U(5) dynamical symmetry and have proposed multiphonon states up to 5 d-bosons. This nucleus fulfills well almost all the criteria determined in Ref. [4]. But an enigma remains concerning the interpretation of the B(E2) ratios in the framework of the IBM. As we have shown also the QPNM is also unable to reproduce the B(E2) ratios. A possible explanation could be the presence of a broken-pair component for these states. The knowledge of lifetimes of excited states in ^{114}Te would certainly clarify the situation and make an unambiguous characterization of the excited states possible.

6   Acknowledgements

References

[1] K. Heyde, P. Van Isaker, M. Waroquier and G. Wenes, Phys. Rev. **C25**, 3160 (1982).

[2] K. Heyde, C. De Coster, J. Jolie and J.L. Wood, Phys. Rev. **C46** 541, (1992).

[3] H. Lehmann, J. Jolie, C. De Coster, B. Decroix, K. Heyde, and J.L. Wood, Nucl. Phys. **A621**, 767 (1997).

[4] J. Kern, P.E. Garrett, J. Jolie, H. Lehmann, Nucl. Phys. **A593**, 21 (1995).

[5] J. Kern, Private Communication.

[6] J. Blachot, G. Marguier, Nucl. Data Sheets **75**, 739 (1995).

[7] T. Lonnroth, A. Virtanen, J. Hattula , Phys. Scr. **34**, 682 (1986).

[8] B.E. Zimmerman, Thesis, Univ. Maryland (1992).

[9] C.B. Moon, J.U. Kwon, S. J. Chae, J.C. Kim, S.H. Bhatti, C.S. Lee, T. Komatsubara, J. Mukai, T. Hayakawa, H. Kimura, J. Lu, M. Matsuda, T. Wanabe, and K. Furuno, Phys. Rev. **C51**, 2222 (1995).

[10] V.P. Janzen, Thesis, McMaster Univ. (1985).

[11] F. Iachello and A. Arima, *The Interacting Boson Model* (Cambridge University Press, Cambridge, 1987).

[12] J.N.L. Akkermans, Thesis, Vrije Universiteit, Amsterdam (1981).

[13] V.G. Soloviev, *Theory of Atomic Nuclei: Quasiparticles and Phonons* (IOP, Bristol, 1992).

[14] V.A. Ionescu, J. Kern, C. Nordmann, S. Olbrich and Ch. Rhême, Nucl. Instr. Meth. **163** 395, (1979).

[15] I. Thorslund, D.B. Fossan, D.R. LaFosse, H. Schnare, K. Hauschild, I.M. Hibbert, S.M. Mullins, E.S. Paul, I. Ragnarsson, J.M. Sears, P. Vaska, and R. Wadsworth, Phys. Rev. **C52**, R2839, (1995).

[16] O.D. Kovrigin, S. Arynov, K.V. Kovalchuk, and Yu. A. Lysikov, Bull. Russ. Acad. Sci. Phys. **57**, 23 (1993).

[17] N. Warr, S. Drissi, P.E. Garrett, J. Jolie, J. Kern, S.J. Mannanal, J.L. Schenker and J.P. Vorlet, Nucl. Phys. **A620**, 127 (1997).

[18] P. Taras and B. Haas, Nucl. Instr. Meth **123**, 73 (1975) .

[19] V.A. Ionescu, J. Kern, C. Nordmann, S. Olbrich and W. Reichart, Nucl. Instr. Meth. **190** 19, (1981).

[20] J. Kern, A. Bruder, S. Drissi, V.A. Ionescu,and D. Kusnezov, Nucl. Phys. **A512**, 1 (1990).

[21] J.J. Van Ruyven, W.H.A. Hesselink, J. Akkermans, P. Van Nes and H. Verheul, Nucl. Phys. **A380**, 125 (1982).

[22] M. Grinberg, Ch. Protochristov, W. Andrejscheff, G. Lo Bianco, G. Falconi, Phys. Rev. **C61**, 024317.

Part III

CONCLUSION

Conclusion.

The study of nuclear structure has been a field of intense work during the last decades. A significant progress has been made in our understanding of the atomic nucleus and in the development of nuclear models. Nevertheless in the field of the low-energy nuclear structure physics a lot of work is still to be done. Concerning this thesis we can give the following conclusions for the two studied nuclei and what can still be done:

^{110}Cd

^{110}Cd has been studied using DSAM/INS technique. The obtained lifetimes have allowed us to characterize low-lying states and more particularly the intruder and 3-phonon states. We have shown that ^{110}Cd is not only well described by the Interacting Boson Model but that it is also a good example for the U(5)-O(6) model.

Moreover, we have partially answered to Iachello's question concerning the surviving of symmetries [21] using the inelastic neutron scattering reaction. It was, however, not possible to populate states with spins greater than seven. Consequently, a clear characterization of higher-multiphonon states is lacking although few lifetimes have already been extracted [17, 20].

In the future, it will be very useful to measure lifetimes of the negative parity states in order to characterize the proposed octupole-quadrupole coupled states [19]. Moreover, it is necessary to obtain lifetimes for proposed higher multiphonon states in order to have a complete answer to the question of the survival of symmetries.

^{114}Te

^{114}Te has been investigated using in-beam spectroscopy with the $(\alpha,2n)$ reaction. This study has allowed the determination of 50 levels, with 16 new ones, and the placement of 74 transitions belonging to ^{114}Te. The first aim of this study was to test the validity of the intruder-spin invariance. However, we were not able to find the intruder configuration in the low-lying states of this nucleus despite the fact that a high-spin study has found a positive parity intruder band [28]. No connection with the lower part of the level scheme was possible.

We have also explained the observed structure of ^{114}Te using a U(5) dynamical symmetry. We could so propose multiphonon states up to 5d-bosons. But the absence of known lifetimes do not permit us to clearly characterize the structure of this nucleus. An effort has to be made to measure lifetimes in ^{114}Te. The presence of a proposed intruder band in ^{114}Te by a high spin study [28] imposes that also shape coexistence structures has to exist at low energy. However, no clear evidence of this intruder band has been found in the present work. A study of ^{114}Te with another reaction could be useful for example ^{114}I decay study in order to clarify the existence or not of the low-lying states not observed in this work.

List of publication.

- **The double γ vibration in ^{164}Dy**, F. Corminboeuf, J. Jolie, H. Lehmann, K. Föhl, F. Hoyler, H.G. Börner, C. Doll, P.E. Garrett, Phys. Rev. **C56**, R1201 (1997).

- **Lifetimes of the lowest $2^+_{K^\pi=0^+}$ levels in ^{168}Er and ^{164}Dy**, H. Lehmann, J. Jolie, F. Corminboeuf, H.G. Börner, C. Doll, M. Jentschel, R.F. Casten, N.V. Zamfir, Phys. Rev. **C57**, 569 (1998).

- **On the Importance of the SU(3) Description for the Interpretation of the First Excited $K^\pi=0^+$ Band in Deformed Nuclei**, H. Lehmann, H.G. Borner, R.F. Casten, F. Corminboeuf, C. Doll, M. Jentschel, J. Jolie, N.V. Zamfir, J. Phys. (London) **G25**, 827 (1999).

- **Study of the Vibrational Nucleus ^{100}Ru by the ^{98}Mo(α,2nγ) and ^{99}Ru(n,γ) Reactions**, L. Genilloud, H.G. Borner, F. Corminboeuf, Ch. Doll, S. Drissi, M. Jentschel, J. Jolie, J. Kern, H. Lehmann, N. Warr , Nucl. Phys. **A662**, 3 (2000); Erratum Nucl. Phys. **A669**, 407 (2000).

- **Characterization of Three-Phonon States in ^{110}Cd**, F. Corminboeuf, T.B. Brown, L. Genilloud, C.D. Hannant, J. Jolie, J. Kern, N. Warr, S.W. Yates, Phys. Rev. Lett. **84**, 4060 (2000).

- **Study of the double-γ vibration in ^{164}Dy using cold neutron capture**, F. Corminboeuf, L. Genilloud, J. Jolie, J. Kern, J.-L. Schenker, in Proceedings of the 10th Int. Symp. on Capt. Gamma-Ray Spectroscopy and related topics, Editor Stephen Wender, 603 (2000).

- **Lifetime measurements of three-phonon states in ^{110}Cd**, F. Corminboeuf, T.B. Brown, L. Genilloud, C.D. Hannant, J. Jolie, J. Kern, N. Warr, S.W. Yates, in Proceedings of the 10th Int. Symp. on Capt. Gamma-Ray Spectroscopy and related topics, Editor Stephen Wender,606 (2000).

- **Collectivity of the "three-phonon" region in ^{100}Ru**, L. Genilloud, T.B. Brown, F. Corminboeuf, P.E. Garrett, C.D. Hannant, J. Jolie, J. Kern, N. Warr, S.W. Yates, in Proceedings of the 10th Int. Symp. on Capt. Gamma-Ray Spectroscopy and related topics, Editor Stephen Wender, 651 (2000).

- **Structures and lifetimes of states ^{110}Cd**, F. Corminboeuf, T.B. Brown, L. Genilloud, C.D. Hannant, J. Jolie, J. Kern, N. Warr, S.W. Yates, Accepted for publication in Phys. Rev. C

- **Characterization of the "three-phonon" region of** ^{100}**Ru**, L. Genilloud, T.B. Brown, F. Corminboeuf, P.E. Garrett, C.D. Hannant, J. Jolie, J. Kern, N. Warr, S.W. Yates, Accepted for publication in Nucl. Phys. A.

- **Nuclear Structure of** ^{196}**Au - more evidence on its supersymmetric structure**, J. Gröger, J. Jolie, R. Krücken, C.W. Beausang, M. Caprio, R.F. Casten, J. Cederkall, J.R. Cooper, F. Corminboeuf, L. Genilloud, G. Graw, M. de Huu, A.I. Levon, A. Metz, J.R. Novak, N. Warr, T. Wendel, Accepted for publication to Phys. Rev. C.

- **Study of** ^{114}**Te by the** ^{112}**Sn(α,2nγ) reaction**, F. Corminboeuf, S. Drissi, L. Genilloud, J. Jolie, J. Kern, H. Lehmann, N. Warr, Submitted for publication in Nucl. Phys. A.

Curriculum vitae.

Name	:	CORMINBOEUF
Forename	:	Frédéric
Date of birth	:	07th May 1973
Place of birth	:	Estavayer-Le-Lac
Nationality	:	Swiss
Originating from	:	Ménières (FR)
Marital Status	:	Married, one child

1979–1983	:	Primary School in Romont (FR)
1983–1985	:	Primary School in Villarsiviriaux (FR)

1985–1989	:	Secondary School at Cycle d'Orientation de Romont (FR)

1988–1989	:	First year of Maturity at Cycle d'Orientation de Romont (FR)
1989–1992	:	2nd to 4th year of Maturity at Collège St–Michel de Fribourg

1992–1997	:	Diploma in experimental physics at Université de Fribourg
1996–1997	:	Diploma in the Research Group of Nuclear and Atomic Physics of Prof. Dr. J. Kern, entitled : "Etude de la structure du ^{164}Dy par la méthode GRID" under the direction of P.D. Dr. J. Jolie.

1997–2000	:	Assistant/Ph.D. student in the Department of Physics of Université de Fribourg

Remerciements.

Je voudrais remercier ici toutes les personnes qui m'ont aidé à réaliser ce travail de thèse

Je tiens en premier à remercier mes parents qui m'ont permis de mener à bien mes études. Merci aussi pour leur soutien moral et financier durant toutes ces années.

Un grand merci au Prof. Dr. Jan Jolie, directeur de ce travail de thèse, qui grâce à son expérience, ses compétences et son enthousiasme a su me proposer un sujet au combien intéressant et motivant.

Merci à tous les membres anciens et actuels du groupe PAN pour l'ambiance de travail agréable et pour l'amitié qu'ils m'ont témoignée.

Merci également aux collaborateurs de l'Université de Kentucky pour m'avoir accueilli dans leur groupe de recherche et permis d'obtenir de précieuses données sur le ^{110}Cd. Un merci tout particulier au Dr. Nigel Warr et au Prof. S.W. Yates pour leur aide et leur soutien durant mes séjours.

Finalement, je remercie mon épouse, Stéphanie, et mon fils, Hugo, pour avoir courageusement et patiemment supporté mes absences lors d'expériences à l'extérieur de l'Université de Fribourg.

Je salue la mémoire du Prof. Dr. J. Kern et je le remercie de m'avoir accueilli et permis d'effectuer mon travail de thèse dans son groupe de recherche.

A vous tous et à tous ceux que j'aurais oublié de mentionner, je tiens à vous dire

MERCI.